8-2021

Combination of Oncolytic Adenoviruses, T-cell Activation, and Blockade of IDO Metabolic Circuitry for the Treatment of Glioma

Teresa Nguyen

Combination of Oncolytic Adenoviruses, T-cell Activation, and Blockade of IDO Metabolic Circuitry for the Treatment of Glioma

by

Teresa Tuệ-Minh Nguyen, B.S.

APPROVED:

_____
Juan Fueyo, M.D., F.A.A.N., Supervisory Professor

_____
Chantale Bernatchez, Ph.D.

_____
Krishna Bhat, Ph.D.

_____
Joya Chandra, Ph.D.

_____
Jason Huse, M.D./Ph.D.

_____
Ji Young Yoo, Ph.D.

APPROVED:

_____

Dean, The University of Texas

MD Anderson Cancer Center UTHealth Graduate School of Biomedical Sciences

Combination of Oncolytic Adenoviruses, T-cell Activation, and Blockade of IDO Metabolic Circuitry for the Treatment of Glioma

A

DISSERTATION

Presented to the Faculty of

The University of Texas

MD Anderson Cancer Center UTHealth

Graduate School of Biomedical Sciences

in Partial Fulfillment of the Requirements for the Degree of

DOCTOR OF PHILOSOPHY

by

Teresa Tuệ-Minh Nguyen, B.S.

Houston, Texas

May 2021

Dedication

To my mother, my father, my sisters, my nieces, and my nephew.

Acknowledgements

This dissertation was a result of five years of intense learning, hard work, determination, perseverance, and commitment of many people who I have met or worked with directly. To them, I owe my success in my development as a researcher.

First, I would like to thank my mentor, Dr. Juan Fueyo, and my co-mentor, Dr. Candelaria Gomez-Manzano. Thank you for being exceptional role models in both science and life. Thank you for the continual mentorship, support, guidance, and opportunities that were necessary for me to grow as a scientist. I learned so much from the both of you, not only about how to rigorously take on the scientific process, but also how to think critically, write, and speak publicly. Thank you for believing in me throughout my time as a student in your labs. I am grateful of your active roles in helping me accomplish all my goals. You have always made me feel valued, heard, and supported. Your kindness and understanding of the personal obstacles of life is also something I will never forget. You have made my graduate studies a memorable one.

I would also like to thank past and present members of my examining and advisory committee: Dr. Chantale Bernatchez, Dr. Joya Chandra, Dr. Krishna Bhat, Dr. Ji Young Yoo, Dr. Jason Huse, Dr. Scott Kopetz, Dr. Jonathan Kurie, Dr. William Plunkett, Dr. Russel Broaddus, and Dr. Amy Heimberger. Thank you for your precious time and valued advice in driving my work forwards.

Thank you to Dr. Derek Wainwright for your kind collaboration with us all the way from Northwestern University; your expertise and generosity elevated this project.

Thank you to my previous undergraduate mentors at the University of Colorado Anschutz Medical Campus, Dr. Marileila Varella-Garcia, Dr. Lynn Heasley, and Dr. Raphael Nemenoff. Thank you for giving me a chance to work with you in your labs. I pursued a career in biomedical

research because my experiences in your labs made me fall in love with answering fascinating questions by doing experiments.

I am grateful for all my current and past lab colleagues. I am thankful every day that I get to work with some of smartest people I have ever met. Thank you: Dr. Hong (Helen) Jiang, Dr. Sumit Gupta, Dr. Sagar Sohoni, Dr. Belayat Hossain, Dr. Shifat Rehnuma, Dr. Yisel Rivera-Molina, Dr. Francisco Puerta-Martinez, Dr. Yanhua Yi, future Dr. Dong Ho Shin, Xuejun Fan, future Dr. Ashley Ossimetha, Lauren McElwee, and Maira Rodriguez. Truly, I could not have done this without you. To Yisel and Fransisco, you were the first people I met upon joining the lab and made me feel instantly welcomed; thank you for sticking by me, even on my 1:00 am days trying to optimize protocols. To Dong Ho and Sagar, thank you for assisting in numerous days of long animal experiments, late lunches, editing papers, and constant trouble shooting. To Fan, thank you for making my life in the lab smooth and easy. To Sumit, thanks for the free medical advice; I will miss seeing you randomly in the lab at 10:00 pm. To Helen, Belayat, and Shifat, thank you for your showing me so much intellectual guidance and kindness throughout my studies. To Ashley, thank you for teaching me how to be a better leader. To Lauren and Maira, thank you for taking care of my grants and assisting in tasks that allowed me to focus on my experiments. I am so grateful that you were the people I worked closely to in the last 5 years.

Importantly, I would like to thank the countless mice I have had the pleasure of working with. Without this sacrifice, my work and countless other significant discoveries would not have been possible. Thank you for being the ideal scientific model that aids in the improvement of public health.

Thank you to all my family and friends who have supported me throughout these years. I give special thanks to Salena who was there to celebrate all my successes, feed me on bad days, and make Houston feel like home. Thank you to my four wonderful sisters, Judy, Xuan, TT, and

Bernie for never doubting in my abilities and always being there for me in good times and in bad. To Bernie, thank you being there for me every day and making the conscious effort to understand what I do, it means the world to me. Thank you to my adorable nieces, Ava, Audrey, and Ellie, and nephew, Makai for reminding me to slow down, live in the moment, and enjoy life; seeing new pictures or videos of you would always make my day better. To my parents, thank you so much for undoubtedly believing I could succeed. Thank you for all that you did to get me to this point in my life. You have worked so hard and sacrificed so much, and I live every day hoping that I can show you the same amount of love and support. To my late grandpa, Ông Ngoại, and late grandma, Bà Ngoại, thank you for being there for me as a kid; thank you, on behalf of my parents, my sisters, my nieces, my nephews, and cousins, for immigrating from Vietnam to America and allowing us the opportunity to live-out our own American dream. I owe this monumental opportunity to you. To my other late grandpa, Ông Nội, and my other grandma, Bà Nội, thank you for your unconditional love and making me proud to be a Vietnamese-American scientist.

Combination of Oncolytic Adenoviruses, T-cell Activation, and Blockade of IDO Metabolic Circuitry for the Treatment of Glioma

Teresa Tuệ-Minh Nguyen, B.S.

Supervisory Professor: Juan Fueyo, M.D., F.A.A.N.

Glioblastoma is the most common malignant primary brain tumor in adults; the current aggressive treatment results in a 5% five-year survival rate. More effective therapies should be developed. One promising alternative is oncolytic adenovirus, Delta-24-RGD, which elicits cancer cell lysis and immunogenic cell death. In fact, Delta-24-RGD produced complete responses in 20% of recurrent glioblastoma patients through immune mechanisms that activate anti-tumor cytotoxic properties of T-cells. This cytolytic effect can further be enhanced by adding immune agonists, namely OX40L, which engages the OX40 receptor to co-stimulate activated T cells for enhanced proliferation. Hence, we produced the next generation of Delta-24-RGD, called Delta-24-RGDOX, which expresses OX40L. Our previous publications exhibited enhanced immune-activating responses and improved survival in glioma-bearing mice treated with Delta-24-RGDOX compared to Delta-24-RGD. Nevertheless, maximal survival of glioma-bearing mice is unattainable, suggesting the presence of sustained immunosuppression within the glioma microenvironment. For example, indoleamine-2,3-dioxygenase (IDO) is upregulated in glioblastoma, correlates with poor prognoses, and is a main source of immunosuppression. IDO is an IFN inducible enzyme that catabolizes tryptophan resulting in diminished proliferation or apoptosis of surrounding effector T cells. Furthermore, kynurenine (Kyn), a tryptophan metabolite, induces T-cell differentiation into Tregs. Excess Kyn also activates carcinogenic transcription factor, aryl hydrocarbon receptor (AhR), which further mediates lymphocyte dysfunction and immunosuppression. Relating to our studies, the immune stimulating effect of Delta-24-RGDOX triggers IFN production contributing to a positive IDO-Kyn-AhR feedback

loop. Additionally, IDO-mediated tryptophan depletion hinders viral replication. Therefore, we hypothesized that combining Delta-24-RGDOX with IDO inhibitors will improve therapeutic outcomes and enhance antitumor immune responses of murine glioblastoma. Here, we showed that Delta-24-RGDOX activated the IDO-Kyn-AhR cascade in glioma cells. Furthermore, we demonstrated enhanced therapeutic effectiveness of combined IDO inhibitor and Delta-24-RGDOX treatment compared to single agents, which was validated in immunocompetent IDO-KO mice. The combination treatment efficacy required $CD4^+$ T cell activation and associated with increased activation of T cells and decreased Tregs and MDSCs. This microenvironment remodeling correlated with complete tumor elimination. Altogether, Delta-24-RGDOX activates the IDO-Kyn-AhR cascade, identifying new targets, which when inhibited have the potential to enhance anti-glioma effects of oncolytic-viruses by reversing tumor immunosuppression.

Table of Contents

List of Tables

List of Figures

Chapter 1: Background and Significance

I. Glioblastoma

Brain tumors or gliomas can be divided into four grades based on its histology. The grade of gliomas increases proportionally to levels of differentiation or anaplasia and aggressiveness (1). The highest grade (IV) of glioma is known as glioblastoma and is the most common malignant primary brain tumor in adults. Glioblastoma is characterized by high mitotic activity with microvascular proliferation, necrosis, and displays anaplasia. These criteria result in tumors that that are very aggressive and are considered malignant. Glioblastoma accounts for 15% of all brain malignancies, and accounts for the majority of primary malignant brain tumor cases at 48% (2). With the aggressive conventional treatment of maximal surgery, radiation, and adjuvant chemotherapy, such as temozolomide, the 5-year survival rate remains around 5% and the median survival is approximately 15 months (3). Recurrence often occurs within 6-12 months because the tumors are molecularly heterogeneous and the blood-brain barrier is an obstacle for therapeutic penetration (4). In addition, brain tumors can often employ mechanisms of immunosuppression, discussed below, which allow for further tumor progression. At present, patients with recurrent glioblastoma can be treated with bevacizumab which targets vascular endothelial growth factor (VEGF), and is often used in combination with Lomustine, a DNA alkylating chemotherapy (5). Other FDA approved treatments for recurrent glioblastoma includes alkylating agent, Gliadel (6), and Novocure, a device that can be worn as a helmet, and uses electric fields, called *Tumor Treating Fields (7)*, to treat the solid tumor. Despite the advances made in this field in the past decades, the survival rates and mortality statistics have remained the same. The need for more effective therapies to treat both primary and secondary glioblastomas is apparent.

II. Immunosuppressive Environment of Glioma

Glioblastoma employs various immunosuppressive mechanisms, leading to its maintenance and progression. Glioblastoma elicits immunosuppression through secretion of cytokines, employment of immune checkpoints, and modulation of different cell types in the tumor microenvironment. These mechanisms are often dependent on each other, creating an immune microenvironment that is favorable for tumor growth.

Glioblastoma cells secrete immunosuppressive cytokines including, transforming growth factor beta (TGF-β), interleukin (IL)-10, and IL-1, all of which are important in the prevention of autoimmune diseases (8). Glioblastoma also secretes colony stimulating factor 1 (CSF-1) (9), which elicits the immunosuppressive M2 phenotype in tumor associated macrophages and thus leads to a glioma-enhancing environment (10). Adding to the immunosuppression is the secretion of granulocyte-macrophage-CSF, important for granulocyte and macrophage function, which can induce the activation of myeloid derived suppressor cells (MDSCs) (11).

Inhibition of immune activating cells is another method employed by glioblastoma for maintenance of immunosuppression. For example, differentiated dendritic cells are inhibited by the secretion of VEGF. Dendritic cells are important antigen presenting cells that present antigens in the context of major histocompatibility complex (MHC), which is required for T-cell activation (12). Additionally, natural killer cells are inhibited by the secretion of regeneration and tolerance factor (RTF) (13).

Studies have shown that the expression of immune checkpoint regulators are increased on glioblastoma cell surfaces and surrounding T cells. Cytotoxic T-Lymphocyte-associated protein 4 (CTLA-4) is a substantial negative regulator of the immune system and has been seen to be associated with many cancers, particularly melanoma (14). The activation of CTLA-4 normally functions to regulate over-activity of the host immune system. In the context of cancer,

the expression and activation of CTLA-4 will keep the cancer microenvironment suppressed, allowing for unchecked tumor growth. Activation of T cells requires two basic signals: 1) the recognition of the antigen presented in the context of MHC by the T-cell receptor and 2) a co-stimulation signal. This secondary co-stimulation signal includes the interaction of a CD28 family receptor of the T cell and a ligand of the B7 family of the target cell, such as a tumor cell or antigen presenting cell. However, the signal conferred by CTLA-4, a member of the CD28 receptor family, and a B7 protein renders an inactive co-stimulation signal, and will not implement T-cell responses. Thus, CTLA-4 suppresses T-cell responses against tumor cells allowing tumor growth (15). Programmed death ligand 1 (PD-L1) is also expressed on glioblastoma cells and can interact with the negative regulating receptor, programmed death 1 (PD-1), which is expressed on T-cells, to suppress its activity (16).

Regulatory T-cell (Treg) activation also aids in immunosuppression of glioblastoma. Glioblastoma produces the chemokine C-C ligand 2, which triggers and traffics Tregs to the tumor site (17). Additionally, Tregs can be activated through the metabolism of tryptophan (Trp) by the enzyme, indoleamine-2,3-dioxygenase (IDO) (18).

Signal transducer and activator of transcription 3 (STAT3) is ubiquitously expressed in glioblastoma cells (19). Blockade of STAT3 can upregulate immune activating cytokines, including IL-6; the presence of hypoxia enhances this pathway, which is a hallmark of many cancers, including glioblastoma (20). As such, under hypoxic conditions, VEGF signaling increases, adding to the immunosuppressive and tumorigenic nature of glioblastoma (21).

The mechanisms that glioblastoma cells engage to produce an immunosuppressive environment are complex. Understanding these mechanisms will allow for new immuno-therapeutic approaches.

III. The IDO Pathway

As mentioned above, IDO is a contributing factor to the immune suppression visible in glioblastoma patients. IDO was originally discovered in the placenta of pregnant mice, as a mechanism of immune tolerance against their fetuses during gestation (22). In the context of cancer, the catabolism of Trp to kynurenine (Kyn) results in various immunosuppressive pathways allowing the tumor to progress. Of relevance, studies have shown that patients with high expression of IDO have a poorer prognosis and a diagnosis associated with higher grade brain tumors, including glioblastoma (23). While three enzymes, Tryptophan-2,3-dioxygenase (TDO), IDO, and Indoleamine-2,3-dioxygenase 2 (IDO2), regulate the conversion of Trp into downstream Kyn, TDO is expressed in the liver and neurons and thus its pharmacological targeting may induce unacceptable toxicity (24), and IDO2, for which expression pattern there are fewer reports, has a significantly lower enzymatic activity than IDO (25, 26). Hence, most studies targeting the IDO pathway do not explore IDO2 or TDO.

IDO can be expressed by tumor cells, dendritic cells, and stromal cells. The enzyme can be activated via engagement of type I and II interferons, oncogenic ligand-receptor signaling complexes, pathogen associated molecular patterns, PD-1/PD-L1 signaling, or B7 co-stimulation signals. Immunosuppressive properties of TGF-β have also been implicated in activation of IDO (27). IDO-mediated tumor-associated immunosuppression is explained by the local depletion of Trp and, consequently, the excess of Kyn in the tumor microenvironment (23, 27-31). Downstream Kyn accumulation contributes to the conversion of naive $CD4^+$ T cells into immunosuppressive FOXP3-expressing regulatory T cells by virtue of the interaction between Kyn and the aryl hydrocarbon receptor (AhR) (32, 33). In addition, T effector cells that sense Trp deprivation via the IDO pathway can activate stress kinase signals via GCN2 (general control nonderepressible 2), resulting in phosphorylation of eIF2 (Eukaryotic Initiation Factor 2),

which is a key translation regulator that delays translation and stimulates the integrated stress response pathway, resulting in cell cycle arrest or apoptosis of these effector T cells (27, 34, 35). Moreover, this integrated stress response pathway can lead to transcription and expression of various inflammatory cytokines, such as IL-6 (36), which has been shown to be essential in both IDO-mediated MDSC formation and tumor growth (37). The deprivation of Trp can also be sensed by amino acid sensing kinase GLK1, which can control mammalian target of rapamycin complex 1 (mTORC) responses in T effector cells; in environments of low tryptophan, mTORC1 signaling is inhibited, which in turn, blocks the phosphorylation of ribosomal kinase S6K, which is involved the process of translation (27, 38). In summary, the activation of IDO employs various mechanisms of immunosuppression.

Although brain tumors can be targeted by different types of anti-cancer therapies, any anti-tumor effects can be counteracted by IDO-mediated metabolic and immune suppression mechanisms to maintain the deep immunosuppressive environment in the core of gliomas. Further studies have shown how the inhibition of IDO, which may, in itself, be insufficient to reverse the tumor immunosuppression, but dramatically improves the responses of other common cancer therapies, most likely due to the conversion by conventional therapies of non-immunogenic "cold" tumors to immunogenic "hot" tumors, exposing the targets necessary for efficacy of IDO inhibition (27, 39-41).

IV. The AhR pathway

The deep immunosuppression caused by IDO can be further enhanced by the activation of downstream receptor, AhR. The production of Kyn by an active IDO enzyme can bind AhR, resulting in both the expression and activation of IDO, generating a highly immunosuppressive IDO-Kyn-AhR positive feedback loop. In fact, the IDO-Kyn-AhR circuit is a key player in the

immunosuppression of the microenvironment of gliomas and other tumors (28, 29). Reports have shown that the levels of IDO, Kyn, and AhR are increased in gliomas. This is important because the activation of IDO and AhR in the tumor microenvironment cooperate to suppress tumor-specific responses, promoting glioma immune evasion and tumor progression (32, 33). For example, agonists of AhR, including Kyn, can directly aid in the differentiation of naïve $CD4^+$ T cells to the immunosuppressive regulatory T cell via elicitation of the immunosuppressive cytokines, IL-10, TGF-β, and VEGFA (29).

When AhR is bound to its activating ligand, such as Kyn, it undergoes a conformational change that allows it to move into the nucleus to dimerize with its translocator partner, ARNT, which in turn binds to dioxin responsive elements that lead to the transcription of its target genes including enzymes from the cytochrome P450 family, like CYP1A1, CYP1A2, and CYP1B1 (42). These enzymes have been implicated in the metabolism and bioactivation of carcinogens, including polycyclic aromatic hydrocarbons, which occur naturally in coal, crude oil, and gasoline (43). Interestingly, increased CYP1B1 mRNA expression is correlated with a poor glioblastoma prognosis (44).

The activation of AhR also leads to the transcription of certain histone deacetylases including, HDAC1, which have been implicated in tumorigenesis (45). Furthermore, AhR can induce an inflammatory signal via IL-6 through dioxin responsive elements. This inflammatory signal can recruit different inflammatory mediators and growth factors to the tumor cell, allowing it to undergo growth and proliferation; in addition, these mediators and growth factors can also elicit $CD4^+$ T cell differentiation into the Treg cell via the same immunosuppressive cytokines (IL-10, TGF-β, and VEGFA) utilized by Kyn (29). Activation of the IDO-Kyn-AhR cascade also activates immunosuppressive macrophages; more specifically, AhR has been reported to drive expression of ectonucleotidase, CD39, in tumor associated macrophages, which can cause the

dysfunction of cytotoxic $CD8^+$ T cells by producing adenosine which cooperates with CD73, which has recently been reported to be involved in T-cell co-signaling (46).

The mechanisms of immunosuppression employed by the IDO-Kyn-AhR cascade are implicated in glioblastoma; this pathway provides several druggable targets that can aid in improved prognoses of patients with glioblastoma.

V. Targeting the IDO Pathway

IDO has been reported to be overexpressed in various cancers including those of the cervix, kidney, lung, colon, (47) and brain (23). Moreover, IDO has been reported to protect mouse tumors from immune rejection (18). Naturally, this has led to pre-clinical studies targeting IDO as a treatment for cancer. There have been many reports of the use of IDO inhibitors providing a therapeutic benefit in various mouse models of cancer when combined with cancer vaccines, immune checkpoint inhibitors, or chemotherapy (18, 48-51). Of relevance, Wainwright and colleagues showed a durable therapeutic effect of using a triple therapy that blocked IDO, CTLA-4, and PD-L1 in a murine glioblastoma model (52). These numerous studies led to the development of several IDO inhibitors to be used in the clinic (53).

Currently, two classes of IDO inhibitors are being used. The first class includes Trp-mimetics, including Indoximod (1-methyl-D-tryptophan) and 1MT (1-methyl-D, L-tryptophan). Although the mechanism of Indoximod and 1MT are not fully understood, the negative regulation of mTORC signaling in T effector cells caused by tryptophan depletion of IDO activation can be restored with these drugs (54). As such, Indoximod is currently being tested in phase II clinical trials in combination with cancer vaccines, chemotherapies, or immune checkpoint inhibitors in various cancer types including leukemia, melanoma, pancreatic, breast, and other solid tumors (53). A phase I/II study of the use of adenovirus-p53 transduced dendritic cell vaccine combined

with Indoximod in patients with metastatic solid tumors showed that patients tolerated a maximum dose of 1600 mg BID with no severe toxicities; determinations of efficacy are warranted by future trials.

The second class of IDO inhibitors are direct IDO enzyme inhibitors including, Epacadostat, Navoximod, and BMS-986205, which can shut off any downstream targets of IDO activation including both the Kyn pathway and the amino acid deprivation stress pathways (27). The most advanced direct IDO enzyme inhibitor is Epacadostat, which showed encouraging results in patients with advanced melanoma when treated in combination with PD-1 blocking antibody, pembrolizumab, in phase I/II trials (55). This prompted the start of a large phase III trial (ECHO-301/KN-252) testing this combination in patients with advanced melanoma. The trial was later closed when initial results from the study showed no therapeutic benefit when comparing the combination to pembrolizumab alone (56). Intrinsically, this has somewhat dampened the interest to use IDO inhibitors in the clinic. However, the failure of this drug in the phase III setting may be attributable to dosing issues or inappropriate patient selection. More investigations that can elucidate which patients will most likely benefit from IDO blockade is essential. Additionally, the reported poor prognoses in cancer patients with high IDO expression along with the supporting pre-clinical evidence demonstrating the anti-cancer effects by targeting IDO with other anti-cancer drugs warrant further investigation and the continuation of targeting IDO in cancer.

Other novel IDO enzyme inhibitors are also being investigated in pre-clinical models. For example, Ladomersky and colleagues demonstrated that the use of triple therapy of CNS-penetrating IDO enzyme inhibitor, BGB-5777, combined with a PD-1 monoclonal antibody and radiotherapy was more therapeutically beneficial then single agents or any dual therapy combination in a mouse model of glioblastoma (39). The same group was able to validate these

results using the clinical grade version of BGB-5777, called BGB-7204 (57), which has been used in some studies of this dissertation.

VI. Viral Infection and IDO

There have been reports of increased IDO expression and activity during human immunodeficiency virus (HIV), influenza, hepatitis B virus (HBV), or hepatitis C virus (HCV) infection (58). This induction of the IDO pathway by these viruses is generated by both type I and type II interferons. Furthermore, the IDO activation in response to these viral infections results in immunosuppression.

HIV

There have been several reports linking the IDO pathway to HIV-infected patients. These patients show increased serum levels of both IFNγ and Kyn (59). Elevated IDO mRNA levels have also been seen in the peripheral blood mononuclear cells (PBMCs) of patients infected with HIV (60). One study found that HIV infection of PBMCs *in vitro* leads to secretion of type I interferons, IFNα and IFNβ, which was associated with IDO expression and activity (61). In these same cultures, the use of Trp-mimetic, 1MT, led to the increase of $CD4^+$ and $CD8^+$ T cell proliferation (60, 61), indicating the immunosuppression aided by IDO. Similarly, IDO enzyme activity was associated in the antigen presenting cells of HIV-infected patients to reduce anti-viral T cell responses via regulatory T cells (62).

Influenza

Studies have shown that mouse influenza can induce IDO expression in mouse lung tissue and nearby lymph nodes (63, 64). Similar to HIV, the mouse influenza virus, X31, induced IFNγ secretion in the lymph nodes leading to increased IDO production in surrounding non-

hematopoietic cells (64). The treatment of influenza infected mice with 1MT also increased the number of functionally active $CD4^+$ T cells and virus-specific memory $CD8^+$ T cells (65) and enhanced Th1 responses via IFNγ secretion by $CD4^+$ and $CD8^+$ T cells (66), indicating the immune suppression caused by IDO under influenza virus infection.

HBV and HCV

IDO has also been implicated in patients with HBV and HCV chronic infections (67). These patients also had high systemic Kyn/Trp ratios in their blood compared to healthy controls (68). *In vitro* studies demonstrated that PBMC monocytes from HCV patients led to differentiation of IDO-positive dendritic cells that induced regulatory T cells by LPS or IFNγ more potently compared to healthy controls (67), again indicating the immunosuppression caused by IDO.

Adenovirus

Like the viruses mentioned above, IFN activation is triggered by sensing of adenoviral DNA in the cell. For example, the immune responses by adenoviruses include elicitation of IFNα via MyD88 signaling of TLR9 (69). Furthermore, IFNβ induction by the adenovirus is required for viral functions including entry, endosomal escape, and release of the viral DNA into the cytoplasm (70). While type I IFNs, IFNα and IFNβ, are secreted by adenovirus-infected cells, IFNγ is produced by T cells and NK cells and plays an important role in cell-mediated immunity against adenoviruses (71). IFNγ induces an antiviral state so that adenoviral replication is inhibited. However, E1A gene products can suppress transcription of IFNγ (72). These contrasting effects of IFNγ by adenoviruses and the T cells or NK cells may represent an example evolutionary reaction between virus and host. As mentioned above, these IFN responses associated with adenoviral infection are also directly related to the expression and activation of IDO. In fact, one report showed that stimulation of dendritic cells with IFNα significantly

upregulated IDO expression (73). In this dissertation, we show that modified oncolytic adenoviruses increase the expression and activation of IDO in various human and mouse models of cancer, including glioblastoma. Furthermore, we demonstrate that these modified oncolytic adenoviruses also activate the downstream pathway of IDO, AhR.

VII. Adenovirus Structure and Life Cycle

The structure of the adenovirus is conferred by its genome, which is comprised of about ~ 36 kb of linear double stranded DNA. Adenoviruses are classified as non-enveloped and are about 95 nm in size (157 MDa). They have an icosahedral shaped capsid composed of 240 copies of the hexon protein (II) and 12 penton (III) capsomeres with fiber proteins (IV) attached. Minor capsid proteins include protein IIIa, VI, VIII, and IX, which stabilize the viral capsid structure and are involved in endosomal escape and transcriptional activation. Core proteins include the terminal proteins, V, VII, and mu, all of which interact with the viral DNA to condense it (74).

To start infection, the knob domain of the fiber protein binds to the coxsackie adenovirus receptor (CAR) or the CD46 receptor to stimulate internalization via clathrin-coated pits. The fibers shed allowing the endosome to internalize the uncoated virus. Acidification of the endosome disassembles the viral capsid further, leading to the release of internal proteins into the endosome. Then, activated viral proteases cleave protein VI, which lyses the endosome to facilitate viral escape. The partially uncoated virus consequently moves to the nuclear pores via microtubules with the help of protein VII (75).

After this infection into the nucleus, E1A transcription occurs and stimulates the transcription of all early viral genes, which affects the transcription profile of the host cell. E1B-55K then inhibits p53-induced apoptosis and E1B-19K binds to the BCL-2 family protein complex BAK-BAX, preventing the formation of mitochondrial pores. After E1A activation,

transcription of the E3 gene occurs, which encodes for several proteins that inhibit the host innate and acquired immune response to viral infection. The E4 region has 7 open-reading frames, which stimulate the production of cellular translational factors, inhibits the cellular DNA double-strand break response, forms a complex with E1B-55K to inhibit p53, and recruits the cellular transcription factors to the E2 promoter. The transcription of the E2 region occurs last, and codes for adenoviral DNA polymerase, ssDNA binding protein, and the preterminal protein, all of which are required for viral replication (76).

After completion of viral replication, the synthesis of major capsid proteins occurs in the cytoplasm. Hexon, fiber, and penton assemble into multimeres in the cytoplasm and transport to the nucleus. With the support of the L1 52/55k protein, the Iva2 protein facilitates DNA packaging of the virion. DNA packaging is associated with core protein precursors, including protein VI, VII, VIII and mu. The viral protease cleaves these precursors to produce mature viral particles (77). The E3-11.6 kDa protein promotes release of these viral particles. These viral particles interact with the MAD2B gene to promote cell lysis and the consequent infection of surrounding cells to perpetuate its life cycle (78).

VIII. Delta-24 and Delta-24-RGD

The easy manipulation of the adenovirus makes it a good candidate for oncolytic viral therapy. Adenoviruses can be easily modified for attenuation, specificity, and cytotoxicity against tumor cells. In 2000, our group developed tumor selective adenovirus, Delta-24, which relies on the retinoblastoma (RB) pathway dysregulation, that is present in ~80% of glioblastomas, for viral replication (79, 80). For adenoviral replication to occur, E1A must bind Rb to release it from E2F, resulting in cell cycle entry through activation of the E2 promoter (81). Delta-24 contains a 24 base pair deletion of the E1A gene producing a mutant E1A, making it unable to bind Rb. This

deletion confers specificity to cancer cells since the binding of E1A to Rb will not occur in normal cells due to a defective E1A protein manifested by the 24bp deletion; thus, replication of the virus will be inhibited in normal cells. Contrastingly, the Rb pathway is dysregulated in glioblastoma cells, which allows the cancer cells proliferate uncontrollably; the viral life cycle of Delta-24 can take advantage of this and will be able to replicate (82).

Infection and internalization depend on viral binding to the coxsackie adenovirus receptor or the CD46 receptor (83). However, glioma cells do not normally express these receptors. Thus, to increase the tropism of the adenoviruses to glioblastoma cells, the RGD motif was added at the carboxyl end of the fiber protein of Delta-24 to produce the next generation virus called Delta-24-RGD (84). The RGD motif can bind to RGD-related integrins, such as the αvβ3 and αvβ5 integrins (85), of which are highly expressed on glioblastoma cells (86).

Once infection of cancer cells occur, Delta-24-RGD can cause oncolytic lysis through autophagy and immunogenic cell death. *In vitro* and *in vivo* studies show an increase in autophagy mediators (87), which is thought to be associated with inhibition of the AKT/TOR pathway (88). The effect of autophagy made by the adenovirus may be thought of as an innate immune response because of viral clearance. Moreover, the immune response is increased by proteasome activity, which generates tumor associated antigens that can be presented in the context of MHC to cytotoxic $CD8^+$ T-Cells (89).

Our group recently published results from a Phase I clinical trial testing Delta-24-RGD in patients with recurrent glioblastoma. This trial resulted in 20% of patients living past three years. Furthermore, the patients who responded portrayed radiographic signs of inflammation, or a pseudoprogression, followed by a response. Moreover, the clinical trials indicate that part of the oncolytic virus-mediated anti-glioma effect was due to an anti-tumor immune response as indicated by the obvious infiltration of immune cells seen in the H&E staining from patient

biopsies after treatment with Delta-24-RGD. Moreover, these same biopsies of the glioblastoma in the patients' post-virus treatment showed infiltration of $CD8^+$ and T-bet T cells, indicating the elicitation of a Th1 immune response. Importantly, further histological staining indicated that the virus was cleared within a month of infection. These responses indicate that the anti-viral response triggered an immune response against the virus and the tumor (90).

One trial (NCT02798406) is currently testing therapeutic efficacy of the combination therapy of Delta-24-RGD with pembrolizumab, the PD-1 monoclonal antibody, in glioblastoma patients. The anti-tumor response will be coupled with the inhibition of immunosuppression aided by PD-1 for a robust immune response against the tumor.

IX. Delta-24-RGDOX

To increase the immune response of Delta-24-RGD, our group developed the next generation virus, called Delta-24-RGDOX. Delta-24-RGDOX is similar to Delta-24-RGD, in that it contains the 24 bp deletion in the E1A gene and the addition of the RGD motif, as previously mentioned. Unlike Delta-24-RGD, Delta-24-RGDOX also contains the OX40-ligand (OX40L) expression cassette, allowing for expression of this immune agonist on infected cancer cells (91). OX40L is part of the tumor necrosis factor receptor/tumor necrosis factor family and is expressed on activated $CD4^+$ and $CD8^+$ T cells, serving as costimulatory signals to promote the proliferation and clonal expansion of effector and memory T cells (92, 93). Thus, the expression of OX40L on cancer cells transforms the cancer cells into an ad-hoc antigen presenting cell, thus enhancing the proliferation of activated T cell clones that can recognize cancer antigen.

Preclinical studies, performed in our lab, indicate that Delta-24-RGDOX is more therapeutically effective than Delta-24-RGD in a glioblastoma immunocompetent murine model. Furthermore, when tested in an immune deficient model, the therapeutic efficacy of both Delta-

24-RGD and Delta-24-RGDOX is completely eradicated. Additionally, we observed that Delta-24-RGDOX provides a more robust anti-viral and anti-tumor immune response compared to Delta-24-RGD as indicated by functional co-culture experiments utilizing the brain infiltrating lymphocytes from these glioblastoma bearing virally treated mice. Moreover, Delta-24-RGDOX elicited a more immunogenic tumor microenvironment compared to Delta-24-RGD as indicated by an increase in $CD3^+$, $CD4^+$, and $CD8^+$ T cells (91). Our studies also showed that Delta-24-RGDOX increased expression of both MHC1 and MHCII expression on infected cancer cells, indicating that these tumor cells can act as antigen presenting cells (94). Interestingly, Delta-24-RGDOX also increases expression of PD-L1 and PD-1 expression within the microenvironment. In fact, the combination of Delta-24-RGDOX and PD-L1 antibodies is more effective in treating murine glioma than Delta-24-RGDOX alone. This indicates that despite the cytotoxic T cell responses, immune suppression can still be present in Delta-24-RGDOX treated tumors (91). PD-L1 engagement has been implicated in IDO activation, which adds to our speculation that Delta-24-RGDOX can elicit mechanisms of immunosuppression. As such, Delta-24-RGDOX has shown to be a good candidate for various combination treatments, including IDO inhibitors.

Glioma is a non-metastatic localized disease, which allows the intra-tumoral injection within the brain, which will not cause any potential systemic infection. The ease in manipulation of adenovirus led to the construction of the non-pathogenic Delta-24-RGDOX, which has an increased tropism to glioma cells and elicits a stronger anti-tumor immune response compared to its predecessor. The non-lymphocytic nature of the brain increases the chance of viral infectivity, and thus oncolysis. In addition, Delta-24-RGDOX can elicit an immune response, which can start off as a response for viral clearance and transform into immunity against the tumor. This observation, which is also common among other oncolytic viruses (95-98), has led to the paradigm shift that oncolytic virotherapy should be considered a type of immunotherapy. Stated more

explicitly, Delta-24-RGDOX can elicit a positive immune response against the tumor by transforming a non-immunogenic tumor microenvironment (glioblastoma) into an immunogenic one. This perspective is leading the field to discovering combination treatments with oncolytic viruses that will synergize with current immunotherapies to increase anti-tumor immunity.

X. Current Landscape of Oncolytic Viruses as Clinical Treatments in Glioma

In addition to the adenovirus (90) family, other families of viruses have been heavily clinically studied including the herpes simplex virus type I (98-101), reovirus (102-104), Newcastle Disease virus (105-108), and poliovirus (97). The measles virus (NCT00390299), vaccina virus (NCT03294486), and the parvovirus (109) have also been tested clinically, however there are currently no reports assessing their effect on patient survival. The benefits of oncolytic virotherapy in the treatment of cancers including glioblastoma is that the viruses can elicit cancer cell death using multiple methods including oncolysis and immunogenic cell death. For example, upon viral infection, the innate and adaptive immune response can be elicited by danger- and pathogen-associated molecular patterns (110). The result is an anti-viral immune response that could also elicit an anti-tumor immune response. In fact, some common effects of treatment of glioblastoma with different oncolytic viruses includes the induced immunogenicity. Inherently, this provides a hurdle for oncolytic therapy because the increased immunogenicity is initially directed towards removing the pathogen from the host. As such, the effectiveness of oncolytic viruses depends on the balance between the anti-viral immune responses and the virus mediated anti-tumor immune responses. Despite this obstacle, there have been major strides demonstrating the therapeutic effect of these oncolytic viruses that are currently being tested in clinical trials.

Herpes Simplex Virus Type 1 (HSV1)

HSV1 belongs to the *Herpesviridae* family and is composed of dsDNA that encodes 81 viral genes. For attenuation and specificity three genes are often deleted and include, dlsptk, γ34.5, and UL39. dlsptk encodes the gene for thymidine kinase, an enzyme that aids in the generation of thymidine monophosphate, which is important in the process of DNA replication. The deletion of dlsptk is not sufficient for attenuation, as this single mutation can still cause neuropathogenicity. Thus, both copies of γ34.5 are often deleted for generation of the oncolytic HSV (111). γ34.5 encodes the gene for ICP34.5. The function of ICP34.5 is two-fold. First, ICP34.5 can recruit protein phosphatase 1 for the dephosphorylation of phosphorylated eIF2α which leads to the activation of protein synthesis. Phosphorylated eIF2A, thus, inhibits protein synthesis, which is an anti-viral defense mechanism that is mediated by host RNA-induced protein kinase R (112). Second, ICP34.5 forms a complex with proliferating cell nuclear antigen, which aids in DNA replication and repair (113). The deletion of ICP34.5 thus will decrease the ability of the HSV1 to undergo both DNA replication and translation. This modification also confers specificity because HSV1 mutants do not depend on ICP34.5 for replication in tumor cells. However, in normal cells ICP34.5 is crucial for viral replication (114-116). UL39 encodes the gene ICP6, which translates to the large subunit of ribonucleotide reductase (117, 118). Ribonucleotide reductase functions to increase the dNTP pools of cells for DNA replication. However, in cancer cells, the dNTP pools are quite abundant and thus do not depend on ribonucleotide reductase for replication (119). Thus, this mutation confers specificity because the lack of a functional ribonucleotide reductase in normal cells will not allow for the replication of the viral DNA.

Currently, there are four different oncolytic HSVs being tested in clinical trials. These include HSV1716, G207, rQNestin34.5, G47Δ, and M032. HSV1716 contains the deletion of both alleles of γ34.5. HSV1716 has been tested in four clinical trials. All these clinical trials show

the safety of this attenuated virus. Of the available data, HSV1716 show survival of patients for 14-24 months after treatment in 11 of 21 GB patients (99, 101, 120). G207 contains the deletion of both alleles of γ34.5 and a lacZ gene insertion in the ICP6 gene. G207 has been tested in three Phase I clinical trials in a total of 36 patients of malignant glioma (98, 100, 121). The trials show the safety of the attenuated virus. Although tumor decreases were seen in 11 of 36 patients, the median survival was not ameliorated compared to results from use of conventional therapy. The treatment of glioma using G207 before and after resection yielded a median survival of 6.6 months (100). The use of G207 preceding irradiation yielded a median survival of 7.5 months (98). Despite these data, some patients can benefit greatly from G207, and MRI images suggest anti-tumor activity (121). This anti-tumor effect may be attributed to the anti-tumor immune response. GB patients that receive G207, resections show increases in $CD3^+$, $CD8^+$, and $HAM56^+$ immune cells suggesting both an innate and adaptive immune response against the tumor (100). In a different patient cohort, G207 showed a 20% response rate in pediatric patients with high-grade glioma, with a median overall survival of 12.2 months, which is higher than the medial overall survival of the primary disease (122). Two other oHSVs are also in Phase I clinical trials and include rQNestin34.5, G47Δ, and M032, but the data from these open trials are unpublished. rQNestin34.5 was developed to increase replication in GB cells through the reinsertion of one copy of γ34.5 into the UL39-deleted, γ34.5-delted viral genome, which is controlled by the nestin promotor (123). G47Δ is an extension of G207 and contains the deletion of the α47 gene, which increases MHC class I expression to aid in mediation of antigen presenting for T lymphocytes (124). M032 lacks both copy of γ34.5 and expresses IL-12 to increase the antigenic stimulation response of the tumor microenvironment (125). G47Δ and M032 are relatively new to the clinic, but the pre-clinical data show that they can modulate the immune system for a greater cytotoxic immune response against the tumor (124, 125).

Reovirus

Of the *Reoviridae* family, reovirus is a non-enveloped RNA virus that can cause asymptomatic or mild intestinal infections in human beings. The reovirus is considered to be a natural oncolytic virus because it specifically replicates in cells that employ RAS activation, which include glioma cells (126). Pre-clinical studies revealed that reovirus can elicit complete regression in subcutaneous and intracranial glioma mouse models (127), and can elicit increased T-cell infiltration and Type I IFN responses (104). The clinical translation of reovirus into the clinic revealed that this virus produces no adverse effects (102, 103), and generated increased tumor leukocyte infiltration along with upregulated expression of IFN, caspase 3, and PD-L1 within the brain tumor of the treated patients (104). There are currently no reports assessing the survival of glioblastoma patients being treated with reovirus.

Newcastle Disease Virus (NDV)

Of the *Paramyxoviridae* family, NDV encapsulates negative sense, single-stranded RNA. Because NDV infects mainly avian species, there is minimal pathogenicity in human beings (128). The replication of NDV depends on deficiencies of the type I IFN response (107, 129). Furthermore, published reports described the requirement of GTPase Rac1 for the replication of NDV; GTPase Rac1 maintains glioblastoma stem properties (130, 131). Pre-clinical studies revealed that NDV provides an enhanced anti-cancer effect in type I IFN-deficient glioblastoma cells (132). Still, the use of glioblastoma mouse models showed the apoptotic and therapeutic effect of NDV either alone or in combination with temozolomide (133-136). NDV has been tested in several studies ranging from phase 0 to phase II. The use of the mesogenic strain of NDV called MTH-68/H for the treatment in human high-grade glioma resulted in survival rates lasting 5-9 years (105). Similarly, there was an increase in overall survival in patients with recurrent glioma after treatment with NDV infected dendritic cells (107). A different phase I/II study testing a

lentogenic NVD strain called OV001/HUJ revealed a 7% complete response rate in patients with recurrent glioblastoma (106).

Poliovirus

Of the *Picornaviradae* family, polioviruses encapsulate single strand RNA. Unattenuated polioviruses generate neurotoxicity. To make polioviruses clinically relevant, Gromeier and colleagues developed an unattenuated polio–rhinovirus chimera, called PVSRIPO, which replaced the internal ribosome entry site of the Sabin strain of the poliovirus vaccine with the non-virulent human rhinovirus type 2 (137). Pre-clinical studies of PVSRIPO proved its ability to infect and kill glioma cells both *in vitro,* which was associated with enhanced survival of glioma bearing mice *in vivo* (138-140). Results from an interventional study testing PVSRIPO in 61 patients with recurrent glioblastoma showed 21% of patients surviving after 36 months (97). A phase II study (NCT02986178) and a phase Ib study (NCT03043391) are currently ongoing.

XI. Hypothesis and Aims

Glioblastoma is the most common malignant primary brain tumor in adults. Conventional treatment of glioblastoma includes chemotherapy, radiotherapy, and surgery. However, upon diagnosis, and with the aggressive conventional therapies, the median survival is about 15 to 17 months (2). Alternative forms of glioma therapy are crucial. Oncolytic viruses (OV) provide a promising alternative to current treatment because it induces cell death by several cytotoxic and immune mechanisms that stem from direct lysis (141, 142). In addition, because apoptosis is not the OV's mode of killing, apoptosis-resistant glioma cells are not the basis of recurrence. Delta-24-RGD is an OV that is highly replicative and tumor specific (89, 143). Delta-24-RGD has been translated to the clinic and was tested in Phase I and II clinical trials. Recently published data from a Phase I Study show that treatment of recurrent glioblastoma with Delta-24-RGD led to

complete tumor regression in 20% of patients (90). Moreover, the clinical trials indicate that part of the OV-mediated anti-glioma effect was due to an anti-tumor immune response, as indicated by the presence of pseudoprogression and an infiltration of $CD8^+$ T cells. In this regard, pre-clinical studies of Delta-24-RGD in glioblastoma have shown that in addition to the production of pathogen associated molecular patterns, the adenovirus infection induces autophagy, a mechanism underlying antigen presentation and immunogenic cell death with production of damage associated molecular patterns (89, 143). Thus, the Delta-24-RGD infection of the cancer cells elicits an anti-viral immune response that eventually becomes an anti-tumor immune response in a small percentage of patients. Further enhancement of the immune component of oncolytic viral therapy should increase the percentage of glioblastoma patients sensitive to Delta-24-RGD. One approach to increase the cytotoxic immune response consists of the modulation of T-cell immune checkpoints (41). Based on this tenet, our group recently generated an immune-agonist armed version of Delta-24-RGD, named Delta-24-RGDOX, which express the immune co-stimulatory molecule, OX40L, a member of the tumor necrosis factor superfamily, and is a positive regulator or agonist of the immune synapsis and enhances the activation and proliferation of cytotoxic T-cells through co-stimulation (92, 93, 144). Our recently published data show that Delta-24-RGDOX has a superior anti-tumor effect compared to Delta-24-RGD in an orthotopic glioblastoma immunocompetent mouse model (91). We hypothesize that Delta-24-RGDOX will directly enhance the activity of cytotoxic T-cells against glioblastoma. We are also taking into consideration that a positive activation of lymphocytes can be halted by the immune suppressive tumor microenvironment. For example, T-cell anergy can occur when the T-cell receptor engages the MHC-antigen complex without a co-stimulatory signal, to result in a non-active T cell and subsequent tolerance of the tumor, as seen with engagement of CTLA-4 or PD-1 (145). Particularly, indoleamine-2,3-dioxgenase or IDO, has been reported to cause T-cell anergy (146).

Of importance, IDO is upregulated in high-grade glioma and correlates with a poor prognosis (18, 23). In the setting of cancer immunology, the catabolism of tryptophan by IDO is sensed by the surrounding T cells, eliciting stress responses to prompt cell cycle arrest (146, 147) and decreases in proliferation (148). Furthermore, the metabolites of tryptophan, including kynurenine, can induce apoptosis of effector T-cells and its differentiation into immunosuppressive regulatory T cells through activation of the aryl hydrocarbon receptor (AhR) (32, 33, 149-151). Activation of AhR also stimulates dioxin responsive elements that aid in transcription of carcinogenic mediators. Furthermore, AhR activates immunosuppressive macrophages, and other populations of cells causing immunosuppression (46). Of relevance to our study, IDO expression increases dramatically after virus infection and is inducible by IFNγ (63, 152), which is a direct effect of adenoviral infection. Moreover, the use of IDO inhibitors has been seen to reverse immune resistance in IDO-expressing tumors (18). Collectively, these data suggest the immunosuppression by IDO and the activity of a continual feedback loop of IDO during a viral infection, providing the rationale to target IDO in combination with the treatment of the Delta-24-RGDOX. In summary, a functional IDO can cause immunosuppression within the tumor microenvironment and thus decrease the immune effects of oncolytic viruses. Based on these observations, the central hypothesis of this study is that therapy of Delta-24-RGDOX combined with an IDO inhibitor will stimulate a cytotoxic immune response and inhibit the suppressive immune response against the tumor cells providing a potential effective novel treatment for glioblastoma. ***Figure 1*** shows the current working model of our proposed hypothesis.

To test the central hypothesis and achieve the objectives of the project, we proposed the following two specific aims:

> ***Aim 1****: Compare the therapeutic efficacy of using Delta-24-RGDOX with and without IDO inhibitors in mouse models of glioblastoma.*

***Aim 2**: Analyze the ability and effectiveness of Delta-24-RGDOX in combination with IDO inhibitors to reshape the murine glioblastoma microenvironment.*

Accomplishing the aims of this project will provide valuable information about the effects of manipulating several axes of the immune system to achieve an anti-tumor immune response and will elucidate the role of immunomodulators and IDO in T-cell anergy during active virotherapy. These results should provide the basis for the future translation of the proposed strategy to the clinical setting.

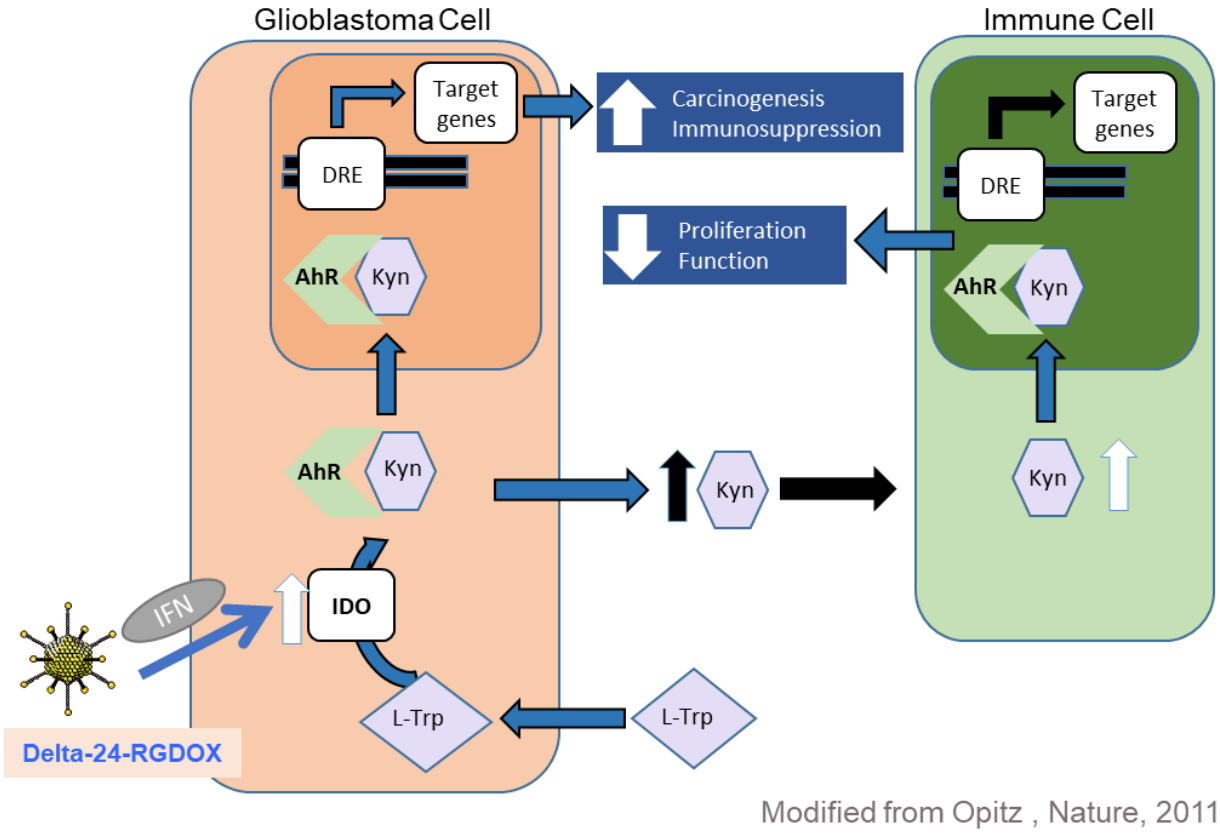

Figure 1: **The current working model of our proposed hypothesis.**

Infection of the glioblastoma cell by Delta-24-RGDOX can increase the expression and activation of IDO via IFN responses. The subsequent activation of IDO catabolizes tryptophan (L-Trp) into kynurenine (Kyn). Kyn acts as an activating ligand for the carcinogenic transcription factor, aryl hydrocarbon receptor (AhR). Activation of AhR by Kyn will translocate it to the nucleus and promote stimulation of dioxin responsive elements (DRE), which aid in transcription of target genes of the glioblastoma cell that will result in carcinogenesis and immunosuppression. Activation of the IDO-Kyn-AhR pathway in immune cells can decrease proliferation and function, limiting the immune response against cancer cells. Overall, the effect of infection of glioblastoma by Delta-24-RGDOX will produce an immunosuppressive microenvironment via the IDO-Kyn-AhR pathway, which when targeted can combat the tumor cells and lead to tumor elimination.

Chapter 2: Materials and Methods

Cell Lines

Mouse glioma cell lines, GL261, GL261-5 (GL261 isolated clone with slower *in vivo* growth kinetics than parental cells) (91), or GL261-IDO-OE (the GL261 cell line with constitutive IDO overexpression, kindly provided by Dr. Derek Wainwright of Northwestern University, Feinberg School of Medicine) were cultured in Dulbecco's modified Eagle's medium with nutrient mixture F12 (DMEM/F12). Mouse GSC-005 cells (kindly provided by Dr. Inder M Verma of the The Salk Institute for Biological Studies) were maintained in DMEM/F12 supplemented with N2 (1x, Invitrogen), fibroblast growth factor-2 (20 ng/mL, PeproTech), epidermal growth factor (20 ng/mL, Promega), and heparin (50 μg/mL, Sigma). Mouse melanoma cell line B16-F10 and mouse breast cancer cell line 4T1.2 cells expressing the luciferase gene (kindly provided by Dr. Chandra Bartholomeusz of the University of Texas MD Anderson Cancer Center) were both maintained in RPMI 1640 medium. Human HeLa and HEK293 cells were maintained in DMEM, and human A549 cells were maintained in DMEM/F12. Human neuronal or glioma stem cell (NSC or GSC) lines NSC11, GSC20, GSC7-2, GSC13, and GSC8-11 were cultured in DMEM/F12 with B27 (1x, Invitrogen), antibiotic-antimitotic (1x, ThermoFisher Scientific), basic fibroblast growth factor (20 ng/mL, Sigma), and epidermal growth factor (20 ng/mL, Sigma). Cultures, except for cultures of GSCs, were supplemented with 10% fetal bovine serum (HyClone Laboratories) and antibiotics (100 μg/mL penicillin; 100 μg/mL streptomycin) (Corning). All cells were kept at 37˚C in a humidified atmosphere containing 5% CO2.

Oncolytic Adenoviruses

Two previously constructed oncolytic adenoviruses, Delta-24-RGD (80) and Delta-24-RGDOX (91), were propagated in human lung carcinoma A549 cells. Virions were collected and purified using the Adenopure kit (Puresyn, Inc, Malvern, PA) following the manufacturer's instructions. Viral titers and replication were determined by measuring plaque-forming units per mL (pfu/mL), by conventional methods. Briefly, HEK293 (2.5×10^5) cells were incubated in 24-well plates with serial dilutions of the viral stock. Forty-eight hours later, cultures were fixed with 100% ice-cold methanol for 10 min at -20°C. Cells were stained for hexon expression using an anti-adenovirus polyclonal antibody (1 h, 37˚C) (anti-adenovirus, Millipore Sigma, AB1056), followed by secondary staining with a biotinylated anti-goat IgG (1 h, 37˚C) (Biotinylated anti-goat IgG (H+L), Vector Biolabs, BA-5000). The Vector Vectastain ABC kit (PK-4000) and ImmPACT DAB peroxidase substrate kit (SK-4105) was utilized for visualization of positive cells. Hexon-stained areas were counted under a light microscope (20× objective) in 10 individual fields per well. In wells with viral dilutions showing 5-50 positive cells/field, the viral titer was calculated using the following formula: pfu/mL = [(mean number of positive cells/field) * (fields/well)] / [volume virus (mL) * dilution factor].

IDO Inhibitors

For mice treated with IDO inhibitors, the following reagents were administered: Indoximod or 1-methyl-DL-tryptophan (1MT) (both purchased from Sigma-Aldrich) suspended in PBS containing glass balls (3mm, Thomas Scientific, #3000) and rotated overnight to help re-suspend the drug to form a uniform and smooth solution. We also used a clinical grade direct enzyme inhibitor called BGB-7204 (kindly provided by Dr. Derek Wainwright of Northwestern University, Feinberg School of Medicine), which was suspended in Ora-Plus (Oral Suspending

Vehicle from Perrigo), and whose pharmacokinetic/pharmacodynamics properties were previously described (57). For *in vitro* use of these inhibitors, DMSO was used as the diluent, and stored at -80°C in between uses.

In Vivo Studies

For glioma tumor implantations, 5×10^4 GL261-5 or GSC-005 cells/mouse or 1×10^3 B16-F10 cells/mouse were implanted into the caudate nucleus of 7- to 10-week-old male or female C57BL/6 mice by using a guide-screw system as previously described (84), and then mice were randomly assigned to experimental groups. Treatment began 7 days after tumor cell implantation. Delta-24-RGDOX adenoviruses (5×10^7, 2.5×10^7, 1.25×10^7, or 1×10^8 pfu/dose, depending on the study) were injected intratumorally on days 7, 9, and 11. For 4T1.2 breast cancer tumor implantation, 1×10^4 cells were injected into the right mammary pad of 7-to 10-week-old female BALB/c mice; intratumoral Delta-24-RGDOX injections were administered on days 10, 14, 16, 18, and 21. Indoximod (275 mg/kg), 1MT (400 mg/kg), or BGB-7204 (100mg/kg) was administered twice daily, by oral gavage, 5 days/week, for 28 days. Mice surviving 120 days were re-challenged with a new intracranial tumor injection using GL261-5 cells (5×10^4 cells/mouse) on the contralateral side of the initial tumor injection. For the CD4 depletion experiment, anti-CD4 depletion antibodies (200 µg per dose, clone GK1.5, InVivoMAb, BioXcell) and rat IgG2b isotype control (anti-keyhole limpet hemocyanin, 200 µg per dose, InVivoMAb, BioXcell) were administered intraperitoneally in mice starting on day 4 post tumor implantation and continued every fourth day until day 36. C57BL/6 IDO-KO (B6.129-Ido1^{tm1Alm}/J) mice were purchased by The Jackson Laboratory, and bred in our mouse housing facility. All experimental procedures involving mice were performed in accordance with protocols approved by the Institutional Animal

Care and Use Committee of MD Anderson Cancer Center, National Institutes of Health, and United States Department of Agriculture guidelines.

RNA-sequencing and data analysis

Total RNA was extracted from flash frozen tumor using the RNeasy Plus Mini Kit (Qiagen). Sequencing was performed by Novogene. Quality control of RNA was performed to measure quantification using Nanodrop, test RNA degradation or potential contamination using agarose gel electrophoresis, and check for RNA integrity using Agilent 2100 Bioanalyzer System. Library construction was developed from mRNA eukaryotic organisms, which was enriched using oligo(dT) beads. This eukaryotic mRNA is then fragmented randomly in fragmentation buffer, followed by cDNA synthesis using random hexamers and reverse transcriptase. After first-strand synthesis, a custom second-strand synthesis buffer (Illumina) is added with dNTPs, RNase H, and Escherichia coli polymerase I to generate the second strand by nick-translation. The final cDNA library is ready after a round of purification, terminal repair, A-tailing, ligation of sequencing adapters, size selection, and PCR enrichment. Sequencing was performed using HiSeq machines (Illumina). Key steps of RNA-seq data analysis include evaluation of quality of reads by fastqc (fastqc/0.11.8) followed by removal sequencing adapters and unpaired reads by trimmomatic (trimmomatic/0.33). (153) These trimmed FASTQ files were used to map reads to mouse genome /ENSEMBL.mus_musculus.release-75 by STAR aligner (star/2.6.0b) (154). Feature Counts extracted from resulting .bam files by subread (subread/1.6.3) (155). Estimates of unwanted variations in raw read counts across samples were determined by ‘remove unwanted variation’ on Galaxy platform (RUVs: which estimates the factors of unwanted variation using replicate samples) (156). RUV uses the empirical Bayes approach to estimate a moderated t-statistic. These estimates were used as batch factors in DESeq2 analyses to determine differentially expressed

genes in the group comparisons (157). For preparation of heatmaps, log2 normalized values for genes with significant adjusted p-value (<0.05) from DESeq2 analyses was utilized; both rows and columns were hierarchically clustered using one minus pearson correlation with average linkage. For gene ontology (GO) enrichment analysis, log2(FC) values for genes with significant adjusted p-value (<0.05) from DESeq2 PBS vs. RGDOX analyses; enrichment analyses were performed on http://www.pantherdb.org/, with false discovery rate (FDR) correction. Cutoffs for ingenuity pathway analyses (IPA), were p-value ≤0.05 and log2(FC) = ±1; activation z-score are plotted on graphs. Activation z-score of ±2 was considered significant. Expression levels of genes with significant fold change and p-values in PBS vs RGDOX analysis were overlayed onto IDO1 network (curated from IPA's knowledge base). For the prediction of immune cell compositions as inferred from RNA-seq data, we input transcripts per million (TPM) for each sample to seq-ImmuCC platform (158), the predicted percentages of various immune cell populations in each sample were plotted in excel. The gene set enrichment analyses were performed by utilizing GSEA_4.0.3 software, where whole genome expression profiles of PBS and Delta-24-RGDOX treated tumors were used as input. The Treg gene set was curated from IPA's knowledge base and the MSDC gene set was based on previous publication (159).

Viral Replication Assay

To determine the replication ability of Delta-24-RGDOX in the cell lines used in this study we performed the viral replication assay. For adherent cells, we seeded 1.5 x 10^5 cells/well in a 12 well plate, then counted the cells after letting them attach overnight to calculate the appropriate amount of Delta-24-RGDOX needed to achieve specified multiplicities of infection (MOI). Delta-24-RGDOX was diluted in PBS to achieve the certain MOI and added dropwise to the attached cells in 200 µL of serum free media for 20 min at 37˚C and shaken to disperse the virus every 5

min, after which was replaced with 1 mL of complete medium for 48 h. For non-adherent cells, infection occurred in 200 µL of serum free media for 20 min at 37˚C and shaken to disperse the virus every 5 min, after which, 800 µL of complete medium was added for 48 h. After the 48 h incubation period, cells and supernatant were collected, flash frozen and thawed 3x, then centrifuged at 500g for 5 min. The supernatant was used for viral titration in 293 cells, as explained in the "**Oncolytic Adenoviruses**" section in methods.

Viral-Induced Cytopathic Ability of Virus Assay

To determine the viral-induced cytopathic ability Delta-24-RGDOX in the cell lines used in this study, we seeded 1 x 10^4 cells/well in a 96 well plate at 75 µL. An additional 75 µL was added to the cells containing the appropriate treatment. Viral-induced cytopathic ability was measured every 24 h for up to 168 h, via levels of ATP using the ViralToxGlo Assay (Promega) according to the manufacturer's protocol.

AhR Activity Assay

To assess the activity of AhR by Delta-24-RGDOX, cells were uninfected or infected with 50 MOI of Delta-24-RGDOX and incubated for 48 h; cell supernatants were used in a commercially available Human Aryl Hydrocarbon Receptor (AhR) assay kit (INDIGO Biosciences), which uses AhR Reporter Cells that give off a luminescent signal when AhR is activated. The protocol was performed according to the manufacturer instructions.

AhR Immunofluorescence

HeLa cells were seeded in a 96-well clear bottom black sides tissue culture plate (Corning) at a density of 1 x 10^4 cells per well. Cells were uninfected (mock), treated with 150µM of Kyn,

or infected with 25 MOI of Delta-24-RGDOX in complete media for 48 h. Following treatment, immunofluorescence staining was performed by following the procedures provided by the manufacturer of the primary antibody. Briefly, cells were washed with PBS and fixed with 4% formaldehyde in PBS for 10 minutes at RT. After washing the wells three times with wash buffer (2mg/ml BSA in PBS), cells were permeabilized with 0.2% triton X-100 in wash buffer for 30 minutes at RT in moist chamber. After permeabilization, cells were washed three times with wash buffer and overlaid with primary antibody against AhR (SantaCruz, SC-74572) using a 1:100 dilution in 2mg/ml BSA in PBS overnight. After primary antibody incubation, cells were washed three times with wash buffer and incubated with FITC conjugated secondary antibody (Invitrogen, Alexa Fluor 488 Goat anti Mouse, A11001) at 1:100 dilution for 1 h at RT. Cells were washed four times with wash buffer and then stained for DAPI (1µg/ml). Cells were then overlaid with mounting medium and imaged using a Zeiss Axiovert200. Cellular and nuclear quantification of AhR intensities was performed using ImageJ software.

Quantitative Real-Time Polymerase Chain Reaction

To isolate mRNA from cultured cells, Trizol Reagent was used according to the established routine protocol; to isolate mRNA from freshly dissected tissue samples, the RNeasy Plus Mini Kit (Qiagen) was used. One microgram of total RNA was reverse-transcribed into mRNA using the High Capacity RNA-to-cDNA Kit (Applied Biosystems). Quantitative real-time polymerase chain reaction (qRT-PCR) was performed on the 7500 Fast Real-Time PCR System (Applied Biosystems) using SYBR Green PCR Master Mix (Applied Biosystems). Primers were purchased from Sigma Aldrich (human IDO, R: TGGAGGAACTGAGCAGCAT, F: TTCAGTGCTTTGACGTCCTG; mouse IDO, R: TTGCGGGGCAGCACCTTTCG, F: CCCACACTGAGCACGGACGG). The RT-PCRs were conducted in a 96 well plate and

subjected to a 10 min 95˚C holding stage followed by 40 cycles of 30 sec at 95˚C, 30 sec at 60˚C and, 45 sec of 72˚C, followed by an infinite hold at 4˚C. Relative gene expression was calculated using the $2^{-\Delta\Delta C}_t$ method by normalizing the threshold cycle (C_t) values of the gene of interest to the C_t values of the internal housekeeping gene.

Western Blots

To detect protein expression, cell lysates were prepared using RIPA lysis buffer (20mM HEPES pH 7.0, 200mM NaCl, 1mM EDTA, 1mM EGTA, 1% Triton X-100, 5mM sodium pyrophosphate, 80mM β-glycerophosphate, 50mM NaF, 0.1% SDS) plus freshly added protease inhibitor cocktail (1x, Sigma-Aldrich), proteasome inhibitor (MG-132, 1μM, Calbiochem), and phosphatase inhibitor cocktail 3 (2.5mg/ml, Sigma-Aldrich). Cell lysates were flash frozen in liquid nitrogen 3x, and centrifuged for 10 min at 4°C, 13,000 rpm. Supernatants were collected, and the concentration of protein was measured using the Bradford Protein reagent (Bio-Rad, Hercules, CA). DTT (50 mM) and NuPAGE LDS sample buffer (ThermoFisher) were added to 10-15 μg of total protein. After heated at 95°C for 5 min, samples were run on 4-20% Novex Tris-Glycine gels (Invitrogen), and then transferred to a PVDF membrane (ThermoFisher) and probed with primary antibodies overnight at 4°C (Table 1 shows antibodies and working dilutions), followed by 1hr secondary antibody staining at RT the next day. Protein bands were visualized using Western Lightning Plus-ECL, Enhanced Chemiluminescence Substrate (Perkin Elmer). Images were acquired using the ChemiDoc System (Bio-Rad).

Liquid Chromatography- Mass Spectrometry (LC-MS)

To detect IDO activity, we measured kynurenine and tryptophan levels of differently treated flash frozen brain tumors. Liquid Extraction was used for the extraction of polar

metabolites from the frozen brain tissue. Briefly, 400 µL of 80% methanol was added to the frozen tissue. Zirconia/silica beads (1mm diameter) were added to the tube. The tissue was broken down using a bead beater by pulsing the tissue for 45 seconds. The resulting solution was kept on ice for 30 min to precipitate out the proteins. 400 µL of chloroform was added and the tube pulsed in the bead beater for additional 45 sec and kept in ice for 15 min. 200 µL of water was added to induce phase separation. The tube was centrifuged and the upper aqueous phase containing the amino acids/amines was carefully transferred into another tube. 250 µL of the 500 µL aqueous phase was dried under using a vacuum. The dried tube containing the metabolites was resuspended in 40µL of buffer used for the derivatization of the amino acids/amines. 10 µL of this was taken for further derivatization and analysis by LC-MS. Standard calibration curves of known concentration of amino acids including tryptophan and kynurenine were made. Before analysis by LC-MS, 5 µM of stable isotope labeled amino acids including tryptophan and kynurenine in 10 µL are added to each sample. The concentration in the analysis sample is then calculated using linear regression on the standard concentrations by plotting area ratio (ratio of the peak area of analyte to peak area of the internal standard) and the known concentrations, followed by normalization to tumor mass.

Preparation of Single Cell Suspensions from Murine Brains and Spleens

Mouse hemispheres bearing tumors and spleens were collected. Initial suspensions were obtained by cutting the tissue or grinding the organs and filtered through 100-µm cell strainers (Fisher Scientific), then placing the cell suspension in RPMI 1640 medium (10 mL/sample). All tissues were pelleted by centrifugation (500 × g for 7 min at RT). The spleen-derived pellet was re-suspended in Red Blood Cell Lysing Buffer Hybri-Max (Sigma-Aldrich) to lyse the red blood cells, according to the manufacturer's instructions. Then, the cell suspension containing the Red

Blood Cell Lysing Buffer was brought up to 20 mL/sample with RPMI 1640 medium to stop the lysis reaction, and the cells were washed 1x in PBS. For the brain-derived pellet, 1 wash in HBSS (Corning) was performed, followed by incubation of cells in 8 pg/mL of Liberase TM (Millipore Sigma) and another wash in HBSS, then resuspended in 40% percoll (1.130 g/mL; GE Healthcare), which was overlaid on top of 80% percoll at a 1:1 ratio. The cells were centrifuged for 20 min at 500 × g at RT with an acceleration of 1 and a deceleration of zero, and the lymphocyte gradient interphase was collected and washed once with PBS. The cells from the brains and spleens were pelleted by centrifugation at 500 × g for 7 min at RT and finally re-suspended in FACS buffer (1x PBS containing 10 mM HEPES, 2 mM EDTA, and 1% fetal bovine serum).

Flow Cytometry Analysis

To analyze cell surface protein expression, using a 96-round bottom plate, single cell suspensions from murine brains and spleens were first blocked in Anti-Mouse CD16/CD32 Fc Block (eBioscience; 14-0161-85) diluted with FACS buffer and then washed once with 250 µL of cold PBS. The cells were then incubated in 100 µL of diluted viability dye (please see Table 1 for details) at 4°C in the dark for 30 min and then washed once with 250 µL of cold PBS. Then, the cells were incubated in 100 µL of primary antibody solution diluted in FACS buffer. After incubation at 4°C in the dark for 30 min, the cells were washed once with 250 µL of cold PBS. For analysis of intracellular proteins, cells were stained with the eBioscience FOXP3/Transcription Factor Staining Buffer Set (Invitrogen) following the manufacturer's instructions. The cells were finally re-suspended in 0.3 mL of FACS buffer containing 123count eBeads Counting Beads (Invtirogen), to acquire an accurate output for absolute cell count. The stained cells were then analyzed by using the BD Celesta Flow Cytometer (BD Biosciences).

FlowJo software, version 10 (FlowJo, LLC), was used for the analysis. (Table 1 shows the antibodies and working conditions used.) To control for the technique and to arrange population gates accurately, we generated fluorescence minus one (FMO) samples for each antibody using pooled spleen cells from the differently treated brain tumor bearing mice.

Analysis of Stimulation of Splenocytes in Co-Cultures with Target Cells

Co-culture set up

Indicated target cells were seeded and treated with specified treatment. Four hours later, 100 units/mL of mouse interferon gamma (IFNγ) (ProSpec Protein Specialists) were added to the cultures. Forty-eight hours after viral infection, the cells were detached with 2 mM EDTA in PBS, fixed with 1% paraformaldehyde, and cleaned with lysine (0.1 M) wash solution. A total of 2×10^4 fixed cells were seeded in 96-well round-bottom dishes. To activate immune cells, pre-fixed target cells were co-cultured with splenocytes (5×10^5/well) in RPMI 1640 medium containing 100 μg/mL penicillin (Corning), 100 μg/mL streptomycin (Corning), and 55 μM beta-mercaptoethanol (Gibco) for 48 h. Please refer to section "**Preparation of Single Cell Suspensions from Murine Brains and Spleens**" for description of how splenocytes were processed into single cells.

IFNγ or IL-2 ELISA

For analysis of stimulation of splenocytes in co-cultures with target cells, the concentration of IFNγ or interleukin-2 (IL-2) in the supernatant was assessed with a standard ELISA per the manufacturer's instructions (IFNγ or IL-2 DuoSet ELISA, R&D Systems).

Histopathological staining

Mouse brains bearing tumors were fixed in 10% buffered formalin for 24 h, transferred to 70% ethanol, and then embedded in paraffin for slide sectioning. Paraffin-embedded sections of the mouse brain tumors were deparaffinized at 60°C for 1 h and rehydrated with xylene and ethanol following conventional procedures. For hematoxylin and eosin staining, brain tumor sections were stained with Harris hematoxylin (Fisher Scientific) and Eosin-Y solution (Fisher Scientific) and mounted with Cytoseal 60 (Thermo Scientific). For the CD3 immunohistochemistry, antigens were retrieved from the brain tumor sections by exposing the slides to 10 mM citric acid (pH 6.0) inside a steamer for 30 min. Slides were then incubated in 3% hydrogen peroxide in 100% methanol for 10 min at RT to quench endogenous peroxidases. The sections were then subjected to blocking with 5% goat serum in PBS (1 h at RT), followed by incubation in primary rabbit monoclonal anti-CD3 antibody overnight (1:80, Abcam, ab16669) and incubation with a biotinylated anti-rabbit IgG secondary antibody diluted in 1% goat serum (1:200, Vector, BA-1000). The Vector Vectastain ABC kit (PK-4000) and ImmPACT and DAB Peroxidase Substrate Kit (SK-4105-Reagent 1) were utilized to visualize positive cells. Images were captured using the Aperio ScanScope slide scanner. The Aperio ScanScope slide scanner was also used to measure high grade tumor areas.

Statistical analyses

In quantitative studies, each tested group were performed at least in triplicate. All graphs and statistical tests of *in vitro* and *in vivo* studies were generated using GraphPad Prism 9. Column data graphs are presented as mean ± standard deviation. To determine statistical differences of multiple groups, we performed an ordinary one-way ANOVA. To determine statistical differences of two groups, we performed a 2-tailed Student's t-test, or the Tukey's multiple comparisons test

(which can be derived via the ordinary one-way ANOVA by selecting the option that compares every mean with every other mean). *P* values < 0.05 were considered significant.

Statistical consideration and analyses for our survival studies are based on our preliminary data, which indicated that survival in the control mice is roughly normally distributed with a median of about 38 days and a standard deviation of about 11 days. The treated mice have a standard deviation of about 22 days (since treated mice respond to varying degrees). Unless otherwise stated, we used at least 10 mice per group based on computer simulations that demonstrated roughly 91% power to detect 30 day differences in median survival between treated and control groups (using a two-sided 1% alpha). We used Kaplan-Meier estimates to graph the survival curves and performed the Log-rank Mantel-Cox test to assess for differences, where *P* values < 0.05 were considered significant.

Table 1: **List of antibodies used in hexon titration, western blot, and flow cytometry assays.**

Hexon Titration			
Antibody Name	**Company**	**Catalog Number**	**Dilution**
Goat Anti-Adenovirus Polyclonal Antibody	Millipore	AB1056	1:500
Biotinylated anti-goat IgG (H+L)	Vector Biolabs	BA-5000	1:500

Western blot				
Antibody Name	**Clone**	**Company**	**Catalog Number**	**Dilution**
Fiber: Adenovirus Type 2 Fiber Antibody (4D2)	4D2	ThermoFisher	MA5-11222	1:1000
Adenovirus-2/5 E1A Antibody	M73	Santa Cruz	sc-25	1:500
α Tubulin Antibody	B-5-1-2	Santa Cruz	sc-23948	1:2000

Flow Cytometry: Regulatory T-Cell Panel					
Marker	**Clone**	**Fluorophore**	**Company**	**Catalog Number**	**Dilution**
CD45	30-F11	APC-R700	BD Biosciences	565478	1:100
CD3e	145-2C11	PerCP-Cy5.5	BD Biosciences	551163	1:100
CD4	RM4-5	V450	BD Biosciences	560468	1:100
CD8	53-6.7	BV510	BD Biosciences	563068	1:100
CD25	PC61	APC	BD Biosciences	557192	1:100
FOXP3	FJK-16s	FITC	Invitrogen	11-5773-82	1:100
FVS780	NA	BV780	BD Biosciences	563068	1:1000

Flow Cytometry: MDSC Panel					
Marker	**Clone**	**Fluorophore**	**Company**	**Catalog Number**	**Dilution**
CD45	30-F11	APC-R700	BD Biosciences	565478	1:100
CD3e	145-2C11	PerCP-Cy5.5	BD Biosciences	551163	1:100
GR1	RB6-8C5	FITC	BD Biosciences	553126	1:100
CD11b	M1/70	APC	BD Biosciences	553312	1:100
FVS780	NA	BV780	BD Biosciences	563068	1:1000

Chapter 3: Transcriptome analyses of Delta-24-RGDOX shows activation of IDO-related genes and the triggering of immune activation and pro-inflammatory pathways.

Rationale and Expectations

A recent phase I study showed that the treatment of recurrent glioblastoma patients with Delta-24-RGD resulted in about 20% of patients living past three years (90). Furthermore, the exploratory objectives of this study showed that in addition to the anti-tumor effect of Delta-24-RGD, a robust immune response was also elicited. This was evident in the H&E sections that showed infiltration of immune cells within the tumor. Furthermore, immunohistochemical analysis also showed infiltration of T-bet associated $CD8^+$ T cells within the Delta-24-RGD infected brain tumor, suggesting the Delta-24-RGD mediated activation of a Th1 mediated immune response (90).

With the goal of improving the percentage of patients that respond to Delta-24-RGD, we developed the next generation virus called Delta-24-RGDOX, which contains the cDNA of immune agonist, OX40L (91). In addition to eliciting oncolysis, Delta-24-RGDOX can also express OX40L on the tumor cell surface (91), enhancing the co-stimulation signal of activated T cells to increase the number of clones that are activated within the tumor microenvironment (93).

The treatment of tumors with Delta-24-RGDOX should be able to stimulate both anti-viral responses and increase the immune activating arm via the OX40L-OX40 pathway. Thus, we hypothesized that Delta-24-RGDOX can dramatically reshape the microenvironment.

To test our hypothesis, we performed RNA sequencing analyses on GL261-5 mouse brain tumors that were treated with PBS or Delta-24-RGDOX. To determine global gene expression changes between the two groups, we generated a heat map of all differentially expressed genes. Furthermore, we performed enrichment analyses of gene ontology biological processes to

determine the differences between the untreated and Delta-24-RGDOX treated brain tumors. Moreover, we performed ingenuity pathway analyses to determine the top five canonical and upstream regulator pathways that were upregulated in response to Delta-24-RGDOX. Additional analyses also determined the prediction of immune cell composition within the untreated and treated brain tumors. Lastly, we explored the expression pattern of the IDO pathway.

Based on previous studies showing that Delta-24-RGDOX was more effective in generating immune responses and curing murine GL261-5 brain tumor bearing mice (91), we expected that in response to Delta-24-RGDOX, the Gl261-5 brain tumors would be dramatically different compared to untreated brain tumors in terms of their global gene expression. Furthermore, we expected that Delta-24-RGDOX would increase the immune responses, based on our hypothesis that treatment of the tumors with the adenovirus will increase the immunogenicity of the tumors (41). As such, we expected both immune activating and immune suppressing pathways, including the IDO pathway, to increase in Delta-24-RGDOX treated brain tumors.

Results

Because RNA-seq allows an unbiased cellular and molecular profiling of complex tissues in solid tumors, characterized by phenotypic alterations due the multicellular composition of the cancer cells and the tumor microenvironment, we decided to perform RNA-sequencing analyses of murine glioma tumors infected with Delta-24-RGDOX and control-treated tumors.

Delta-24-RGDOX reshapes the murine brain tumor microenvironment.

We observed that Delta-24-RGDOX treatment induced a powerful reshaping of the tumor microenvironment (***Figure 2***). In comparison with control-treated tumors, Delta-24-RGDOX-treated tumors were enriched for populations related with inflammation and Th1 and Th17 immune response, including IFNγ, TNF, and IL-17 (***Figure 3***).

Delta-24-RGDOX increases the predicted diversity and percentage of immune populations.

While transcriptional signatures related to macrophages and dendritic cells remain practically unchanged by the Delta-24-RGDOX treatment, major changes in the microenvironment promoted by the infection included the remarkable increase of the $CD8^+$ T related transcriptome ($P = 0.0031$), which were practically absent in the control treated tumors, and a trending in the upregulation of the NK transcriptional signature ($P = 0.11$). In addition, there was a significant decrease in the predicted presence of $CD4^+$ T cells ($P = 0.0127$) (***Figure 4***).

Delta-24-RGDOX induces expression of genes from the IDO pathway.

As expected, after viral infection, the tumors showed upregulation of the IDO circuitry, a pathway targeted for virus and tumors to escape the immune system. IDO-related network of genes that were upregulated after Delta-24-RGDOX treatment included TGFβ, CTLA-4, PD-1, and GATA-3 (***Figure 5***).

A

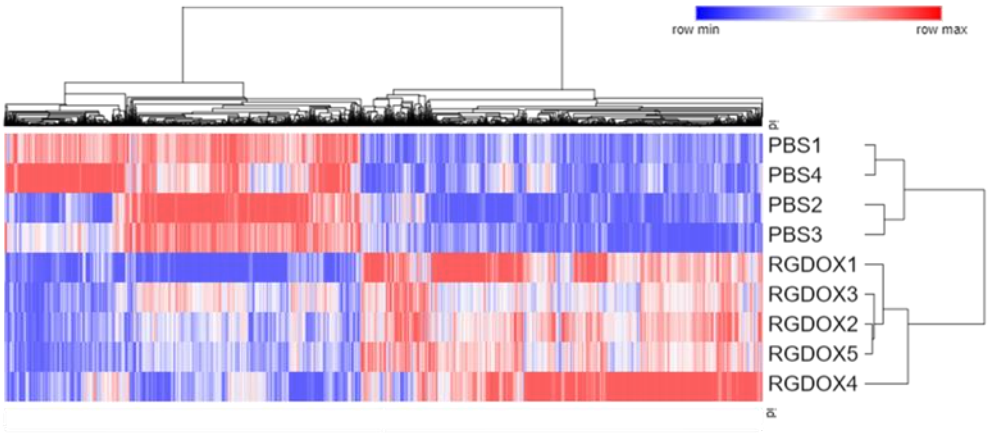

B

GO: Enrichment (PBS vs. RGDOX)

GO biological process complete	Number	overUnder*	pvalue	FDR
positive regulation of cell adhesion (GO:0045785)	207	-	0.00E+00	0.00E+00
humoral immune response (GO:0006959)	64	-	0.00E+00	0.00E+00
immune response (GO:0006955)	505	-	0.00E+00	0.00E+00
inflammatory response (GO:0006954)	219	-	0.00E+00	0.00E+00
defense response (GO:0006952)	528	-	0.00E+00	0.00E+00
nervous system development (GO:0007399)	785	+	0.00E+00	0.00E+00
mitotic cell cycle process (GO:1903047)	208	+	0.00E+00	0.00E+00
cell cycle (GO:0007049)	467	+	0.00E+00	0.00E+00
microtubule-based process (GO:0007017)	269	+	0.00E+00	0.00E+00
cell division (GO:0051301)	211	+	0.00E+00	0.00E+00
* + : PBS; - : RGDOX				

Figure 2: **Delta-24-RGDOX reshapes the brain tumor microenvironment.**

Differentially expressed genes in tumors treated with PBS versus tumors treated with Delta-24-RGDOX are utilized for clustering or GO biological process. **A**) Heatmap comparing the transcription signature of intracranial GL261-5-derived tumors treated with PBS or Delta-24-RGDOX. The log2 normalized expression levels of genes with significant adjusted *P*-value (<0.05) across samples are shown. Color scale is shown on top of the heatmap. (**B**) Gene ontology (GO) biological process enrichment in tumors treated with PBS or Delta-24-RGDOX. The five most significant (±) GO biological processes are represented. GO biological processes significantly associated with PBS treated tumors are marked as '+', whereas those in Delta-24-RGDOX are marked as '-'.

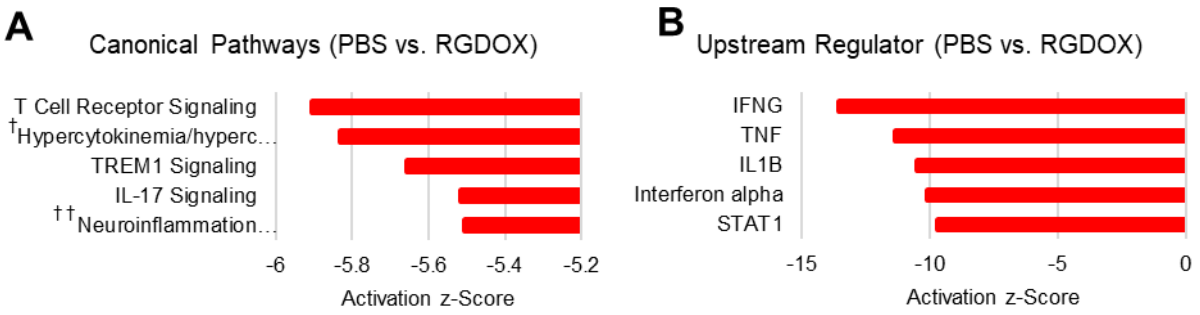

Figure 3: **Delta-24-RGDOX increases both immune-activating and immune-suppressing pathways.**

Ingenuity pathway analyses of GL261-5 brain tumors treated with PBS or Delta-24-RGDOX. (A) Five most significantly altered canonical pathways in tumors treated with PBS versus Delta-24-RGDOX. Activation z-score are plotted in the graph. (B) Five most significantly altered upstream regulators in tumors treated with PBS versus Delta-24-RGDOX. Activation z-score are plotted in the graph. The –ve z-Score represent activation in Delta-24-RGDOX. †, Hypercytokinemia/hyperchemokinemia in the Pathogenesis of Influenza; ††, Neuroinflammation Signaling Pathway.

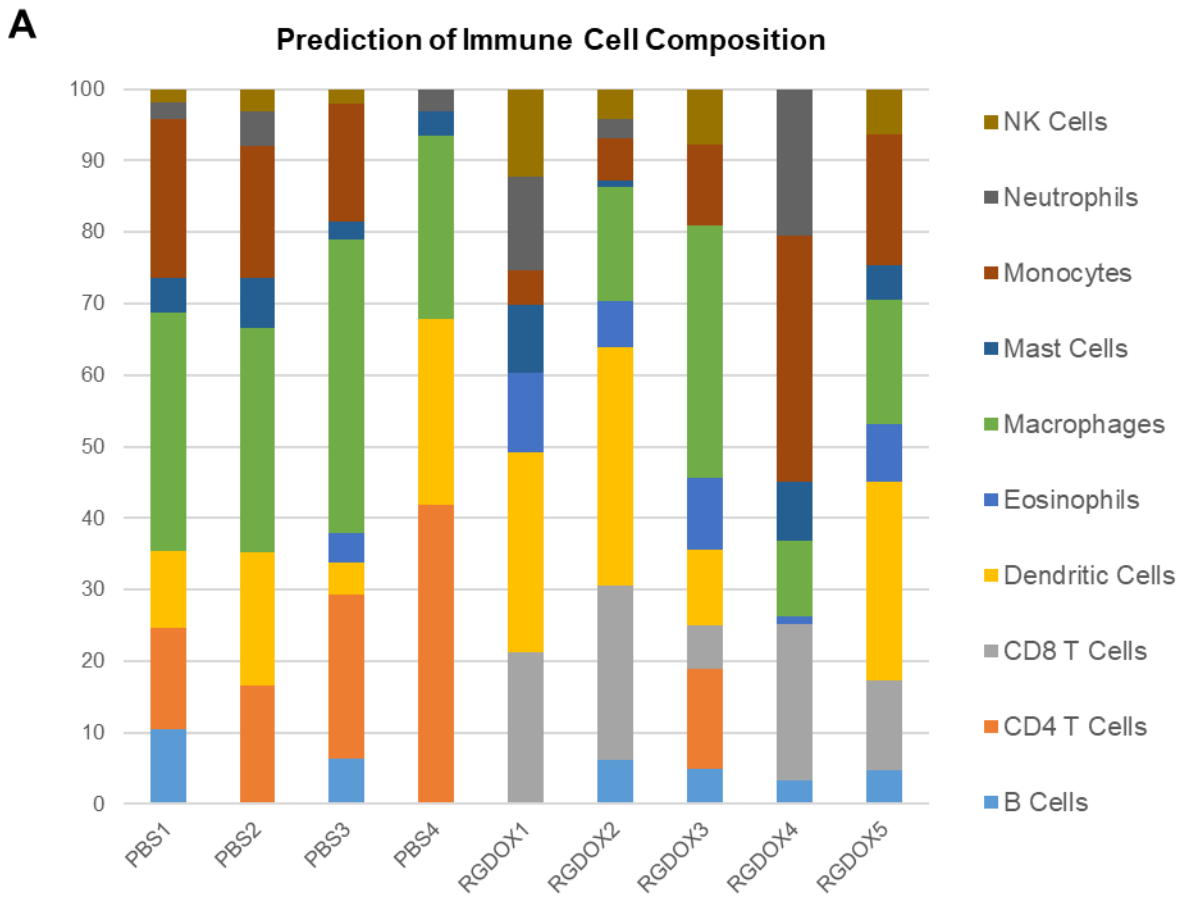

Figure 4: **Delta-24-RGDOX increases and diversifies the predicted immune cell composition within the brain tumor microenvironment.**

(A) The prediction of immune cell composition in GL261-5-derived brain tumors treated with PBS or Delta-24-RGDOX. The percentages of various immune cell populations in each sample are presented in the graph. The color code for various immune cell types is shown on the right of the graph.

A

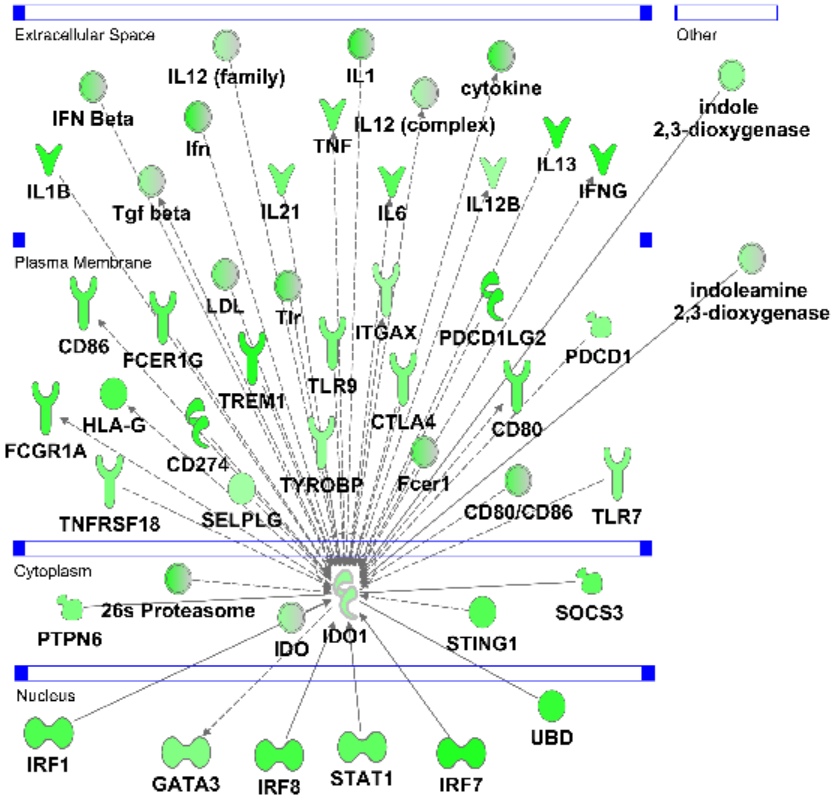

Figure 5: **Delta-24-RGDOX induces expression of genes from the IDO pathway.**

A) IDO1 network genes with significantly altered expression levels in tumor treated with PBS or Delta-24-RGDOX. The intensity of color depicts log2 fold change levels for each gene in PBS vs. Delta-24-RGDOX treated tumors.

Conclusions

Collectively, these results indicated that Delta-24-RGDOX induces a robust effect on the immune response and that there was a double-edge activation of pathways that positively and negatively regulate the immune response against virus and tumors. Among them, the infection with Delta-24-RGDOX triggered the upregulation of the IDO circuitry.

Importantly, this data shows that the treatment of these murine brain tumors increases the immunogenicity of the tumors, as indicated by the gene ontology biological processes analyses, which showed the enrichment of cancer cell cycles pathways in the PBS treated tumors and the contrasted enrichment of immune-related pathways in the Delta-24-RGDOX treated brain tumors. Furthermore, the prediction of the immune cell composition also suggests that Delta-24-RGDOX increases the diversity of various immune populations. Similarly, the ingenuity pathways analyses showed the elicitation of immune pathways. In addition to this increase of immunogenicity, it is noteworthy to mention that Delta-24-RGDOX does not only elicit immune activating pathways, but also immune suppressing pathways, including the IDO pathway.

These results confirm our hypothesis that oncolytic adenoviruses can transform “cold” tumors to “hot” tumors. This phenomenon was elegantly described by Sharma and Allison, which states that this conversion of immunogenicity can increase the likelihood of tumors to respond to immunotherapies (41). Complimentarily, the upregulation of the IDO pathway support our rationale to combine IDO inhibitors with Delta-24-RGDOX for the treatment of glioma.

Chapter 4: IFNγ or Delta-24-RGDOX infection induces IDO or AhR expression or activation in vivo and in vitro in human glioma stem cells and murine glioma cells.

Rationale and Expectations

Indoleamine-2,3-dioxygenase (IDO) is upregulated in glioblastoma and correlates with a poor prognosis (23). IDO is an enzyme that catabolizes tryptophan (Trp) into kynurenine (Kyn). The production of Kyn causes immune toxicity of the tumor microenvironment. Kyn also acts as a ligand to activate aryl hydrocarbon receptor (AhR) translocation into the nucleus, which can elicit carcinogenesis and further immune suppression (27, 29). In the context of oncolytic virotherapy, tryptophan depletion by IDO activation can hinder the generation of new virions, reducing viral spread. IDO is inducible by stimuli that are related to viral infection (58), which means that upon infection, generation of a positive IDO-Kyn-AhR pathway feedback loop can occur that aids in decreased viral activity.

Several studies have identified IDO activation during the response to external-danger stimuli, including pathogens, like viruses (27, 58, 160). Following viral infection, the main players involved in IDO activation are pathogen-associated molecular patterns, damage-associated molecular patterns, and the activation of interferons, all of which are important for the innate and adaptive responses (27). Studies have shown that human immunodeficiency virus and influenza infections induce IFNγ production (59, 66). Furthermore, one study found that HIV infection of PBMCs *in vitro* leads to secretion of type I interferons, IFNα and IFNβ (61). Importantly, these studies show that these interferons effect IDO expression and activation. Relatedly, reports have shown that in addition to generation of pathogen associated molecular patterns, adenoviral infections lead to type I and type II IFN responses, including IFNα or IFNβ, and IFNγ, respectively (69-72). Important to our studies, IDO is an IFN-inducible protein (152).

An important result of IFNα and IFNβ is its activation of the Janus family kinase-signal transducer and activator of transcription (JAK-STAT) signaling cascade. The activation of the JAK-STAT elicits host antiviral properties (161). In fact, the use of JAK1/2 inhibitor, Ruxolitinib, can enhance replication in a measles virus-resistant human derived glioblastoma cell line (162). JAK/STAT activation can also regulate IDO, and several studies have shown that inhibition of the JAK-STAT pathway led to inhibition of IDO (reviewed in (163)). Thus, not only can IDO be activated directly by IFN, but also via JAK-STAT signaling.

In summary, IDO is upregulated in glioblastoma and associates with a poor prognosis. Furthermore, viral infection elicits several stimuli that are activators of IDO including, IFNα, IFNβ, IFNγ, and JAK/STAT. This interplay between viral infection and IDO activation can generate a positive feedback loop of the IDO pathway that can: 1) hinder viral replication and 2) elicit mechanisms of immune suppression in oncolytic virus treated cancers.

We wanted to determine the effects of IFNγ and Delta-24-RGDOX in human and murine glioblastoma cancer on IDO or AhR expression and activation *in vivo* and *in vitro*. Taking into consideration the previously published literature of stimuli that lead to IDO and AhR activation, we expected the following to occur in the cancer cells:

1) IFNγ will induce IDO expression.
2) Delta-24-RGDOX will induce IDO expression.
3) Delta-24-RGDOX will activate IDO via increased Kyn/Trp levels.
4) Delta-24-RGDOX will induce AhR expression.
5) Delta-24-RGDOX will activate AhR.
6) Delta-24-RGDOX will elicit AhR translocation into nucleus.

Results

IFNγ induces IDO expression in human cancer cells.

IDO was the first known gene to be inducible by IFNγ (152). Because adenoviruses can elicit an IFNγ response *in vivo*, we wanted to determine the effects of IFNγ on IDO expression in a panel of human glioma stem cells (GSC) including NSC 11, GSC 7-2, and GSC20; we also used HeLa cells as positive control. ***Figure 6*** shows a significant increase in IDO mRNA levels in the glioma stem cells treated with IFNγ.

Delta-24-RGDOX activates the AhR pathway in human cancer cells.

IDO is an enzyme that catabolizes Trp to Kyn, which can be aided by type I interferons, IFNα and IFNβ. These IFNs can also be elicited in adenoviral infected cells. In turn, Kyn can bind to transcription factor AhR to activate it, which has been shown to cause pro-tumorigenic effects. (27, 42, 164, 165) Thus, we wanted to explore the activity of AhR in Delta-24-RGDOX infected GSCs and HeLa cells; in ***Figure 7***, we showed that there was an increase AhR activity in NSC 11, GSC 7-2, GSC20, and HeLa cells in response to Delta-24-RGDOX infection.

Delta-24-RGDOX induces Ahr expression and translocation into the nucleus.

To further explore the activation of IDO by Delta-24-RGDOX, we studied the expression of AhR in HeLa cells that were infected with Delta-24-RGDOX using immunofluorescence. ***Figure 8A*** shows that Delta-24-RGDOX infected HeLa cells show an observable increase in AhR expression within both the cytoplasm and nucleus compared to mock infected cells, indicating the translocation of AhR to the nucleus induced by Delta-24-RGDOX. Quantification of these results, as seen in ***Figure 8B-D*****,** showed increase of nuclear AhR intensity, whole cell AhR intensity, and

the frequency of AhR positive cells compared to mock treated cells. These data were complemented with HeLa cells treated with Kyn, which acted as our positive control.

IFNγ, Delta-24-RGD, or Delta-24-RGDOX induces IDO expression in vitro and in vivo in murine models of cancer.

IDO expression was also inducible by IFNγ or Delta-24-RGDOX in murine glioma cells, GL261-5 and GSC-005. When these cell lines were treated with IFNγ or Delta-24-RGDOX, IDO mRNA significantly increased compared to mock infected cells, as seen in ***Figure 9A***. To test the impact of viral infection on IDO expression *in vivo*, we treated GL261-5- bearing mice with Delta-24-RGD or Delta-24-RGDOX and collected their brain tumors 24 h after the last virus dose for analysis of IDO expression by qRT-PCR. ***Figure 9B*** shows that Delta-24-RGD increased IDO mRNA in the GL261-5 model compared to PBS treated mice, and that Delta-24-RGDOX increased IDO mRNA expression even further. Furthermore, we showed that Delta-24-RGDOX significantly increased IDO mRNA in the murine 4T1.2 breast cancer model, as seen in ***Figure 9C***, and that IDO expression decreased with the treatment of Trp-mimetic, Indoximod.

Delta-24-RGD or Delta-24-RGDOX induces IDO activation in of murine glioblastoma models.

Next, we wanted to determine IDO activity in PBS, Delta-24-RGD, or Delta-24-RGDOX treated brain tumor bearing mice by measuring the Kyn to Trp ratio by LC-MS. An active IDO will catabolize tryptophan and generate an excess of Kyn, therefore a relatively high Kyn to Trp ratio indicates IDO activity. As seen in ***Figure 10***, both the GL261-5 and GSC-005 murine brain tumor models showed that Delta-24-RGD infection increased IDO activity compared to PBS treated mice, as indicated by the increase in the Kyn to Trp ratio. The Kyn to Trp ratio further increased in the mice that were infected with Delta-24-RGDOX.

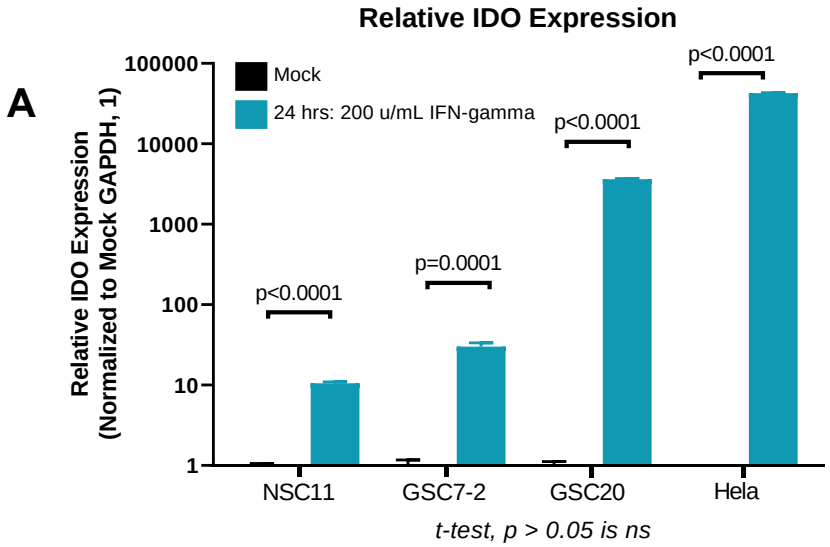

Figure 6: **IFNγ induces IDO expression in human glioma stem cells and HeLa cells.**

Cells were untreated (Mock) or treated with 200 u/mL of IFNγ for 24 hours. RNA was extracted and relative levels of IDO was measured using qRT-PCR; GAPDH or β-Actin were used as housekeeping gene controls. The column graphs show $2^{\wedge}(Ct^{GAPDH \text{ or } \beta\text{-Actin}}\text{-}Ct^{IDO})$ normalized to the Mock control.

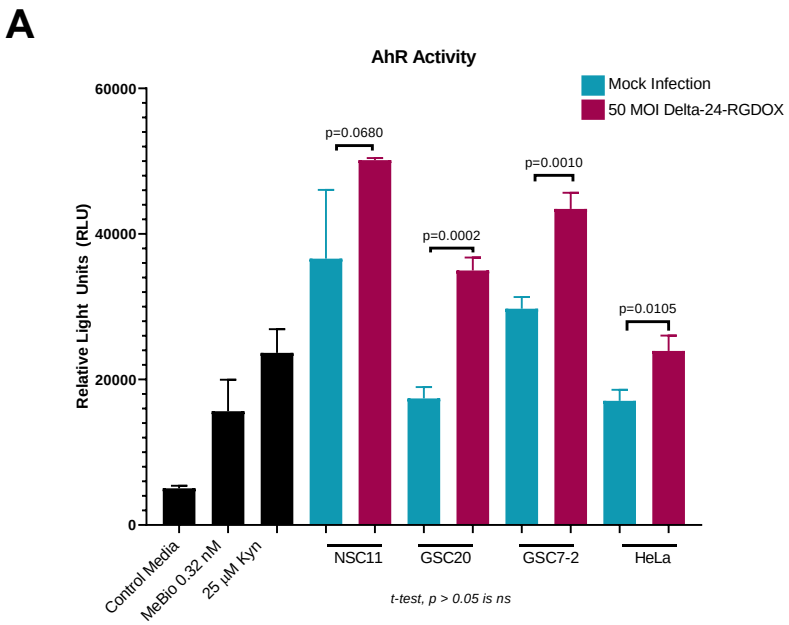

Figure 7: **Delta-24-RGDOX activates AhR in human glioma stem cells and HeLa cells.**

The figure shows AhR activity of a human GSC lines and HeLa cells in response to Delta-24-RGDOX. These cells were untreated (Mock) or infected with 50 MOI of Delta-24-RGDOX and incubated for 48 hours; the supernatants were used in a commercially available Human Aryl Hydrocarbon Receptor (AhR) assay kit (INDIGO Biosciences), which uses AhR Reporter Cells that give off a luminescent signal when AhR is activated. Controls included media (negative), media containing MeBio (positive), an AhR agonist, and media containing Kynurenine (Kyn-positive), an activator of the Ahr Pathway.

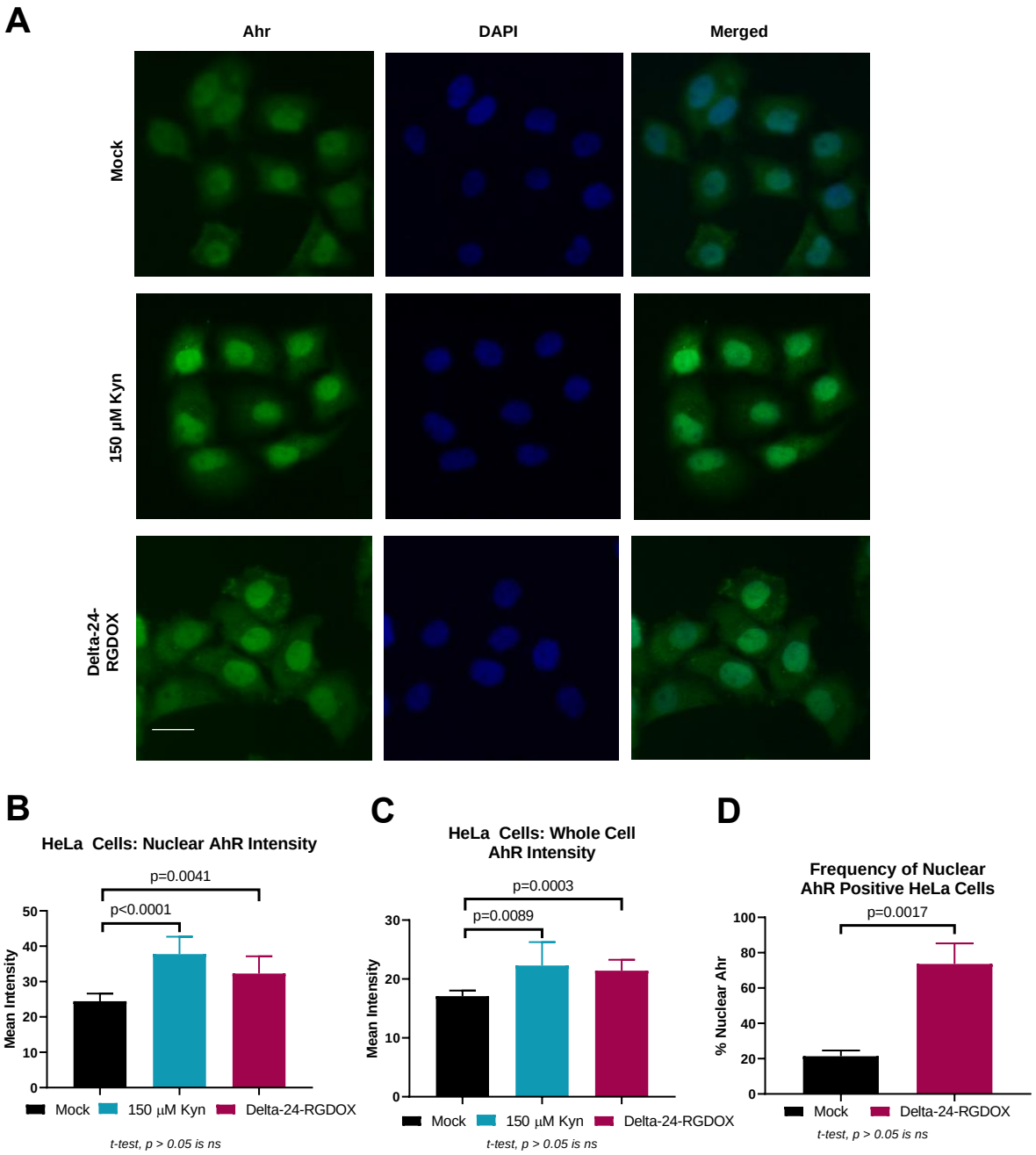

Figure 8: **Delta-24-RGDOX induces AhR expression and translocation into the nucleus.**

HeLa cells were untreated (Mock), treated with Kyn (positive control), or infected with 25 MOI of Delta-24-RGDOX, incubated for 48 hours, and then stained with AhR using immunofluorescence. The microscopy images (A) show cells stained with Ahr-FITC, DAPI, and merged FITC/DAPI. *Scale bar*, 50 µm. The column graphs represent quantification of (B) nuclear AhR intensity, (C) whole cell AhR intensity, and (D) frequency of AhR positive cells (analyzed using ImageJ software).

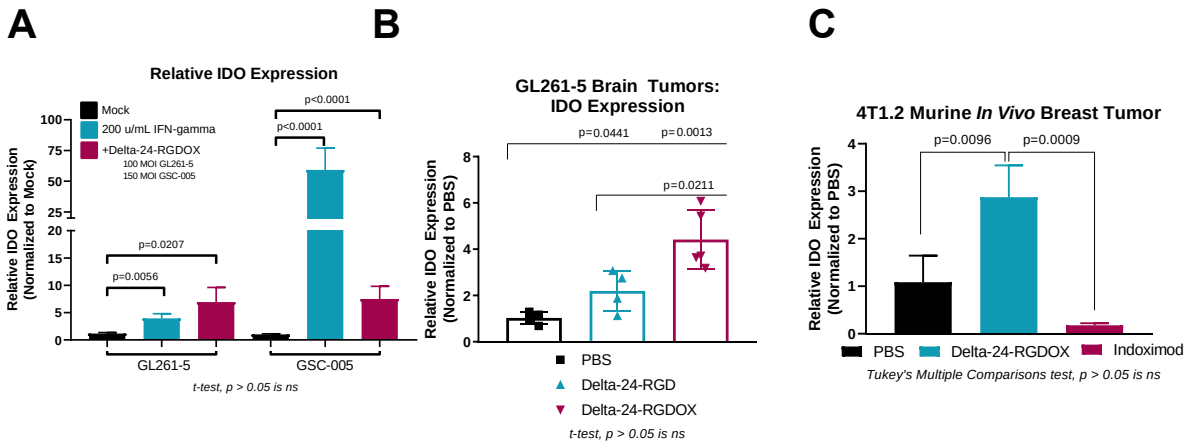

Figure 9: **IFNγ, Delta-24-RGD, or Delta-24-RGDOX induces IDO expression in cancer cells *in vivo* and *in vitro*.**

Panel (A) shows relative IDO expression murine glioma cells in response to IFNγ or Delta-24-RGDOX. Cells were untreated (Mock), treated with 200 u/mL of IFNγ, or infected with Delta-24-RGDOX for 48 hours at indicated MOIs. RNA was extracted and relative levels of IDO was measured using qRT-PCR; GAPDH or β-Actin were used as housekeeping gene controls. The column graphs show $2^{\wedge}(Ct^{GAPDH\ or\ \beta\text{-}Actin}\text{-}Ct^{IDO})$ normalized to the Mock control. Panel (B) shows relative IDO expression in GL261-5 brain tumors in response to Delta-24-RGD or Delta-24-RGDOX infection. Mice were bolted on day -7, then implanted with 5 x 10^4 GL261-5 cells on day 0; on days 7, 9, and 11, the mice were intratumorally injected with PBS, Delta-24-RGD (5 x 10^7 pfu/dose), or Delta-24-RGDOX (same dose). Mouse brain tumors were collected on day 12, cut in half and flash frozen for RNA extraction. The column graph shows relative IDO expression of the differently treated brain tumors using $2^{\wedge}(Ct^{\beta\text{-}Actin}\text{-}Ct^{IDO})$ normalized to the PBS treated mice. Panel (C) shows the relative IDO expression of 4T1.2 bearing mice treated with PBS, Delta-24-RGDOX, or Indoximod. Mice were implanted with 1 x 10^4 4T1.2 cells in the right mammary fat-pad on day 0, injected with PBS or Delta-24-RGDOX (1 x 10^8 pfu/mouse) on days 10, 14, 16, 18, and 21, or treated with Indoximod on days 10-35 (275 mg/kg, BID). The 4T1.2 breast tumors were flash frozen on day 36 and extracted for RNA and quantified for IDO mRNA using the above methods.

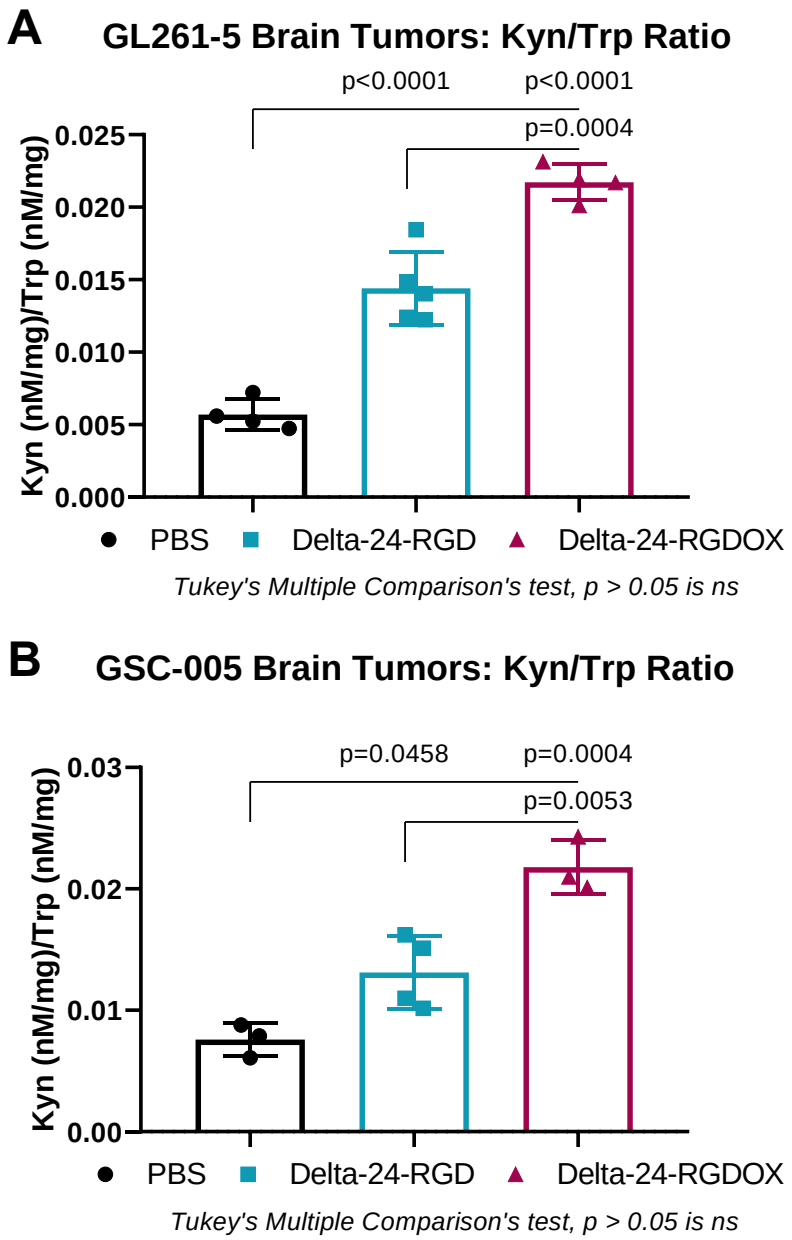

Figure 10: **Delta-24-RGD or Delta-24-RGDOX activates the IDO pathway in murine gliomas.**

Mice were bolted on day -7, then implanted with 5 x 10^4 GL261-5 or GSC-005 cells on day 0; on days 7, 9, and 11 (GL2621-5), or days 9 and 11 (GSC-005), the mice were intracranially injected with PBS, Delta-24-RGD (5 x 10^7 (GL261-5) or 1.25 x 10^7 (GSC-005) pfu/dose), or Delta-24-RGDOX (same doses). Mouse brain tumors were collected on day 12, cut in half and flash frozen for analysis of Kyn/Trp by LC-MS. The column graphs are showing (A/B) the ratio of Kyn to Trp within the tumor microenvironment of PBS, Delta-24-RGD, or Delta-24-RGDOX infected brain tumors measured by LC/MS of the (A) GL261-5 or (B) GSC-005 murine brain tumor model.

Conclusions

To support previous findings that viral infections generate different stimuli to induce expression and activation of IDO and AhR, we performed *in vitro* and *in vivo* studies testing expression and activation of both proteins induced by IFNγ or Delta-24-RGDOX.

We demonstrated that IFNγ induces expression of IDO in human glioma cells and HeLa cells. Delta-24-RGDOX induces AhR activation in these same cells. We speculate that this induction of AhR expression and activation could be due to responses by type I IFNs, IFNα and IFNβ, or JAK-STAT signaling, all of which are viral-induced stimulators of IDO. This result indirectly indicates that Delta-24-RGDOX activates IDO, since Kyn, a product of IDO enzyme activity, is an activator of AhR.

Additionally, Delta-24-RGDOX increased the expression of AhR in the cytoplasm and nucleus in HeLa cells, indicating the translocation of AhR into the nucleus by Delta-24-RGDOX. The translocation of AhR into the nucleus indicates activation, as this relocation leads to transcription of AhR target genes, which are involved in both tumorigenesis and generation of immunosuppression of surrounding immune cells (29).

Complementarily, IFNγ and Delta-24-RGDOX also induced expression of IDO in murine cancer cell lines. These data were accompanied with the increased expression and activation (via increased Kyn/Trp ratios) of IDO in Delta-24-RGD and Delta-24-RGDOX treated mouse brain tumors.

Overall, these results suggested that increased expression and activation of proteins from the IDO-Kyn-AhR cascade results from oncolytic adenoviral infection, which could hinder anti-tumor viral responses via immunosuppression. These results suggest that IDO is a proper therapeutic target and that IDO inhibitors can be combined with oncolytic adenoviruses, such as Delta-24-RGDOX to enhance the anti-glioma effect of virotherapy.

Chapter 5: Inhibition of IDO does not hinder Delta-24-RGDOX infection, replication, or viral-induced cytopathic ability in human and murine glioma cells.

Rationale and Expectations

Several studies demonstrated the role of the IDO pathway in attenuating the replication of pathogens such as cytomegalovirus, measles, herpes simplex virus, and vaccinia virus (166-169). It is important to mention that the effect of IDO was due, at least in part, to the depletion of Trp, because adding supra-physiological levels of exogenous Trp restored viral replication (170).

The depletion of Trp by an activated IDO is directly correlated to the production of the metabolite Kyn, which is an activating ligand of AhR. Emerging data have shed light on an unexpected role of the ligand-activated transcription factor AhR in transducing the function of IDO in cancer cells (30). Of interest, the AhR pathway modulates the expression of the cell cycle regulators p27 and p21 at the transcriptional level (171). These cyclin-dependent kinase inhibitors negatively regulate progression of the cell cycle by inducing G1 and G2 arrest and, thus, restricting the virus access to the S-phase machinery required for viral DNA replication (80, 172). In fact, in experiments performed by other laboratories, deletion of p27 or p21 were shown to facilitate the replication and oncolytic effect of Delta-24 (173).

Based on these observations, we hypothesized that activation of the IDO molecular pathway will attenuate the anti-glioma effect of Delta-24-RGDOX by both depleting the infected cells of the essential amino acid tryptophan and inducing AhR-mediated upregulation of the potent inhibitors of cell cycle progression, p21 and p27.

Since we have shown the expression and activation of both IDO and AhR in response to Delta-24-RGDOX *in vitro* in human and murine glioma cell lines, we expected that there would be enhancement of viral activity in the presence of an IDO inhibitor. Thus, to test our hypothesis,

we employed the cell lines, GL261-5, GSC 8-11, GSC 13, GSC 20, and GSC-005, and infected them with Delta-24-RGDOX with or without IDO inhibitor treatment using either BGB-7204 (direct IDO enzyme inhibitor) or Indoximod (Trp mimetic) and measured viral replication via a hexon titration, expression of viral proteins fiber and E1A, and viral-induced cytopathic ability via a commercially available cell viability kit. Based on data from previous publications and results from our studies from ***Chapter 4*** we expected the following:

1) In the GL261-5 cell line, we did not expect Delta-24-RGDOX to replicate, since we have shown in the past that this cell line is does not permit replication of the adenovirus (91). As such, we did not expect any changes in viral activity of Delta-24-RGDOX in GL261-5 that were also treated with an IDO inhibitor. This cell line served as our negative control.
2) Viral activity, including replication, expression of fiber, and viral-induced cytopathic ability of Delta-24-RGDOX will occur in replication-permissive cell lines, GSC-8 GSC 8-11, GSC 13, GSC 20, and GSC-005. This viral activity will be enhanced when these cell lines are also treated with an IDO inhibitor.

Results

To ascertain the effect of IDO activity on virus activity, we studied viral infection, viral replication, and viral-induced cytopathic ability of Delta-24-RGDOX in GL261-5, GSC 8-11, GSC 13, GSC 20, and GSC-005 with or without IDO inhibition using either BGB-7204 or Indoximod. BGB-7204 is a direct IDO enzyme inhibitor (provided by Dr. Derek Wainwright, Northwestern University, Feinberg School of Medicine). Indoximod is a Trp-mimetic that can provides an artificial supplement of Trp.

As we expected, mouse glioma cell line, GL261-5, our negative control, did undergo infection by Delta-24-RGDOX, as indicated by clear expression of viral infection protein, E1A, but was not capable of viral replication (***Figure 11A and 11B***, respectively). Still, after infection with a high multiplicity of infection (MOI), the GL261-5 cells endured substantial viral-induced cell death over time (***Figure 11C***). When we infected GL261-5 with Delta-24-RGDOX in the presence of an IDO inhibitor (either BGB-7204 or Indoximod), the infection, viral replication, and viral-induced cytopathic ability remained unchanged compared to Delta-24-RGDOX infection alone (***Figure 11***).

Contrary to our expectations, ***Figure 12A*** shows that Delta-24-RGDOX replication via hexon titration levels were unchanged when BGB-7204 was added to the cultures of human GSC 8-11, GSC 13, and GSC 20 glioma cells. Similarly, as seen in ***Figure 12B***, the expression of viral replication protein, fiber, was unchanged and viral infection protein, E1A, was still present when we added BGB-7204 to Delta-24-RGDOX infected cultures. Correspondingly, the viral-induced cytopathic ability was unchanged when we added BGB-7204 to Delta-24-RGDOX infected cultures, as seen in ***Figure 12C***.

Notably, the GSC-005 cell line showed enhancement of viral replication by hexon titration, fiber expression, and viral-induced cytopathic ability of Delta-24-RGDOX in the presence of BGB-7204, as seen in ***Figures 13A-C***.

These results suggest that viral function of Delta-24-RGDOX remains unchanged and can be enhanced with IDO inhibitors.

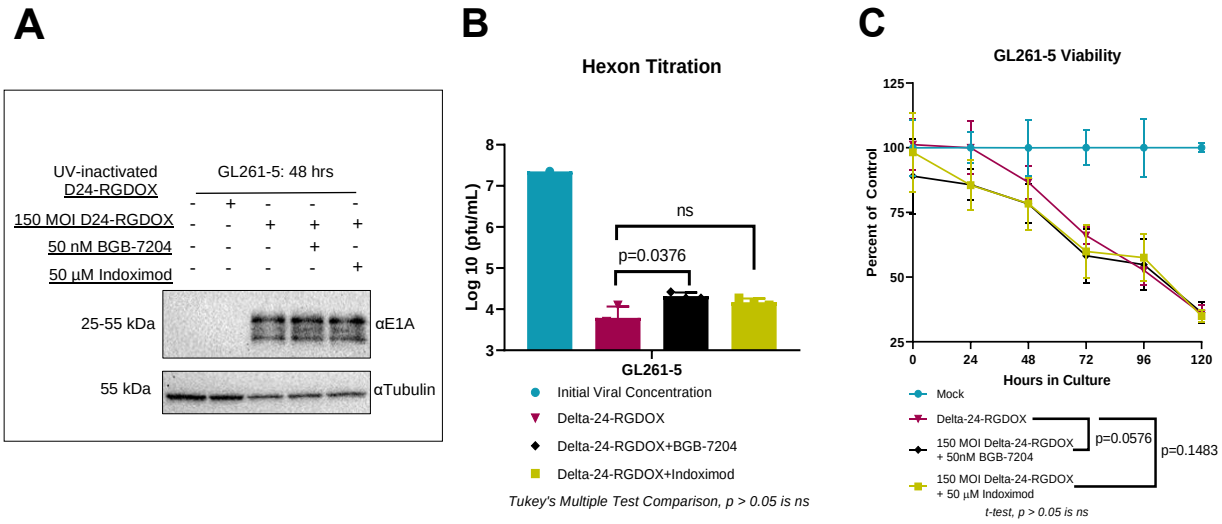

Figure 11: **Inhibiting IDO does not alter Delta-24-RGDOX infection, replication, or viral-induced cytopathic ability in murine GL261-5 glioma cells.**

GL261-5 cells were tested for Delta-24-RGDOX infection, replication, and viral-induced cytopathic ability with or without IDO inhibition. Cells were untreated (Mock), infected with UV-inactivated Delta-24-RGDOX, infected with Delta-24-RGDOX at 150 MOI, or treated with combined Delta-24-RGDOX and IDO inhibitor, BGB-7204 or Indoximod, at indicated concentrations. Panel (A) shows viral replication of Delta-24-RGDOX or combined Delta-24-RGDOX and BGB-7204 or Indoximod. The column graph shows the log concentration of the virus (pfu/mL). The cyan bar represents the initial concentration of Delta-24-RGDOX, and the subsequent bars show the concentration of Delta-24-RGDOX or combined Delta-24-RGDOX and BGB-7204 or Indoximod after infection of the cells for 48 hours, which was measured using a hexon titration assay in 293 cells. Panel (B) shows expression of viral infection protein, E1A, under different treatments. The cells were treated with the indicated treatment for 48 hours, and proteins were extracted and blotted for E1A and tubulin. Panel (C) shows viral-induced cytopathic ability of Delta-24-RGDOX or combined Delta-24-RGDOX and BGB-7204 or Indoximod. The cells were seeded in a 96 well plate and appropriately treated up to 120 hours, and viral-induced cytopathic effects was measured every 24 hours using the commercially available ViralToxGlo Assay (Promega), which quantifies cell viability via ATP levels. The graph shows the percent viability normalized to the mock infected cells.

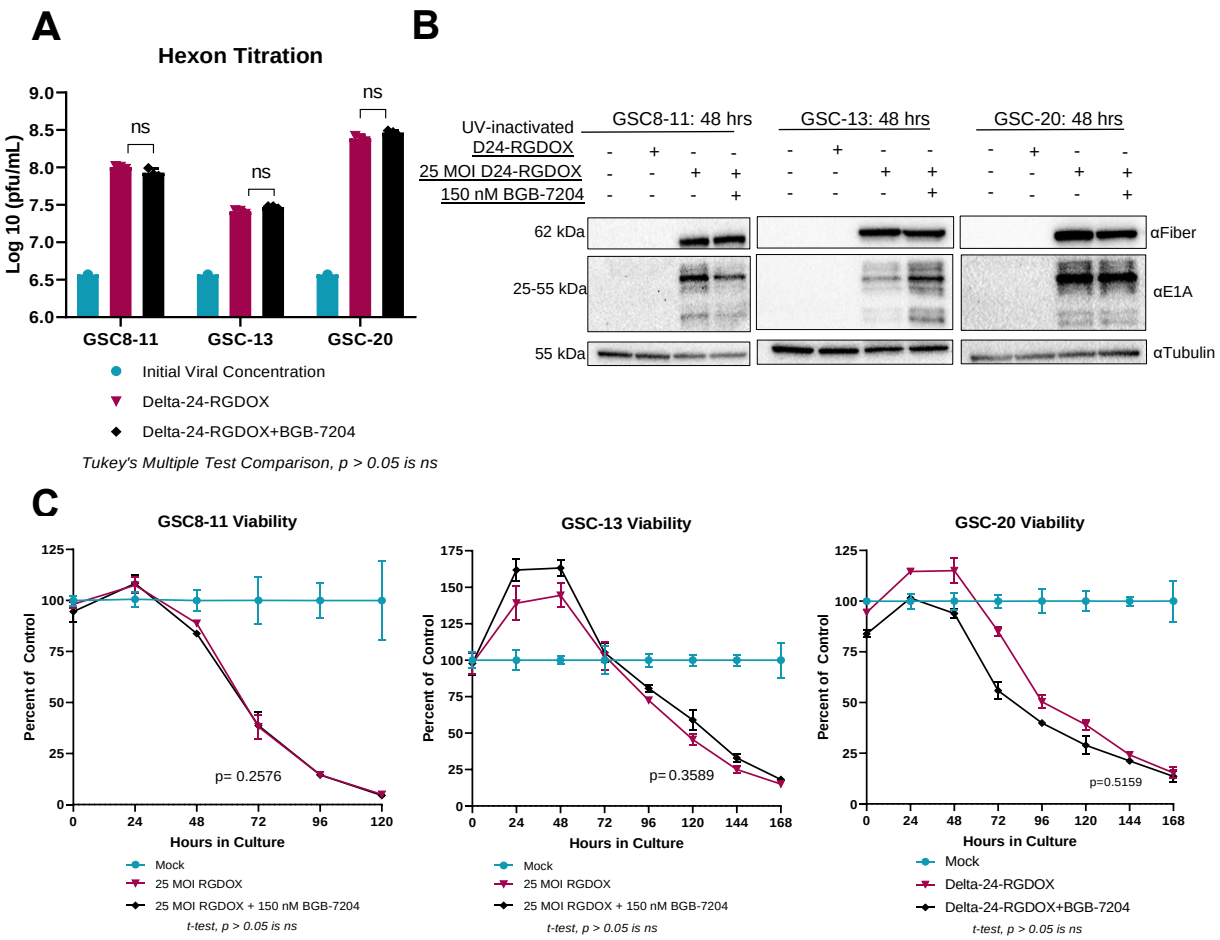

Figure 12: **Inhibiting IDO does not alter Delta-24-RGDOX infection, replication, and viral-induced cytopathic ability in human glioma stem cells.**

Patient-derived human glioma cells, GSC-11, GSC-13, and GSC-20 were tested for Delta-24-RGDOX infection, replication, and viral-induced cytopathic ability with or without IDO inhibition. Cells were untreated (Mock), infected with UV-inactivated Delta-24-RGDOX, infected with Delta-24-RGDOX at 25 MOI, or treated with combined Delta-24-RGDOX and IDO inhibitor, BGB-7204, at 150nM. Panel (A) shows viral replication of Delta-24-RGDOX or combined Delta-24-RGDOX and BGB-7204 of the indicated cell line. The column graph shows the log concentration of the virus (pfu/mL). The cyan bar represents the initial concentration of Delta-24-RGDOX, and the subsequent bars show the concentration of Delta-24-RGDOX or combined Delta-24-RGDOX and BGB-7204 after infection in the indicated cell line for 48 hours, which was measured using a hexon titration assay in 293 cells. Panels (B) shows expression of viral replication protein, fiber, and viral infection protein, E1A, in Delta-24-RGDOX or combined Delta-24-RGDOX and BGB-7204 treated cells. The cells were treated with the indicated treatment for 48 hours, and proteins were extracted and blotted for fiber, E1A, and tubulin. Panel (C) shows viral-induced cytopathic ability of Delta-24-RGDOX or combined Delta-24-RGDOX and BGB-7204 in indicated cells. The indicated cell lines were seeded in a 96 well plate and appropriately treated up to 168 hours, and viral-induced cytopathic effects was measured every 24 hours using the commercially available ViralToxGlo Assay (Promega), which quantifies cell viability via ATP levels. The graph shows the percent viability normalized to the mock infected cells.

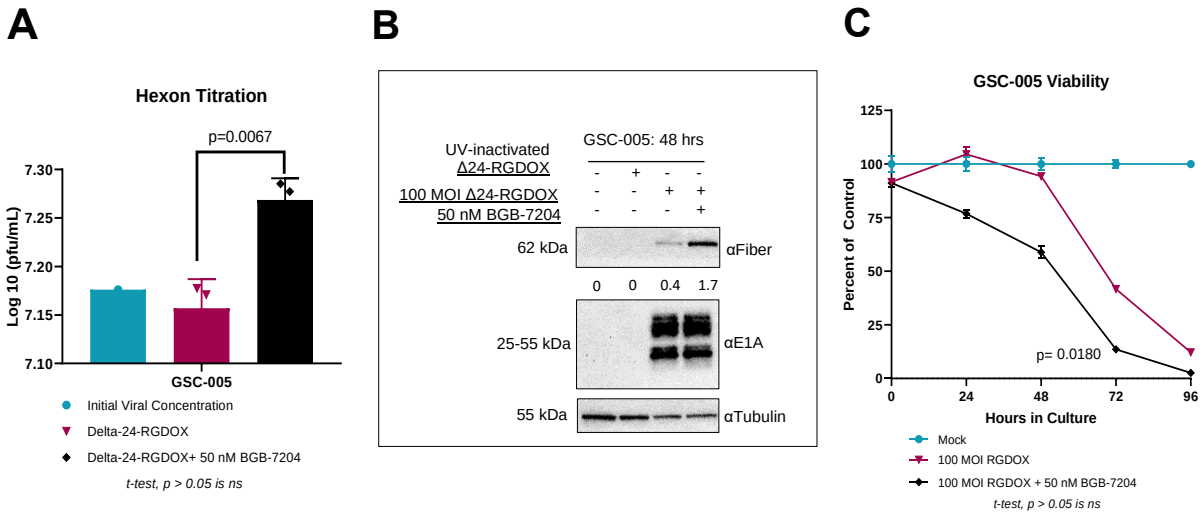

Figure 13: **Inhibiting IDO enhances Delta-24-RGDOX replication and viral-induced cytopathic ability in murine glioma stem cell line, GSC-005.**

Murine glioma cell line**,** GSC-005, was tested for Delta-24-RGDOX infection, replication, and viral-induced cytopathic ability with or without IDO inhibition. Cells were untreated (Mock), infected with UV-inactivated Delta-24-RGDOX, infected with Delta-24-RGDOX at 100 MOI, or treated with combined Delta-24-RGDOX and IDO inhibitor, BGB-7204, at 50nM. Panel (A) shows viral replication of Delta-24-RGDOX or combined Delta-24-RGDOX and BGB-7204. The column graph shows the log concentration of the virus (pfu/mL). The cyan bar represents the initial concentration of Delta-24-RGDOX, and the subsequent bars show the concentration of Delta-24-RGDOX or combined Delta-24-RGDOX and BGB-7204 after infection for 48 hours, which was measured using a hexon titration assay in 293 cells. Panel (B) shows expression of viral replication protein, fiber, and viral infection protein, E1A, in Delta-24-RGDOX or combined Delta-24-RGDOX and BGB-7204 treated cells. The cells were treated with the indicated treatment for 48 hours, and proteins were extracted and blotted for fiber, E1A, and tubulin. The ratio of fiber/tubulin were acquired by finding the ratio of pixels of fiber and tubulin using Image J software. Panel (C) shows viral-induced cytopathic ability of Delta-24-RGDOX or combined Delta-24-RGDOX and BGB-7204 of the cells. The cells were seeded in a 96 well plate and appropriately treated up to 96 hours, and viral-induced cytopathic effects was measured every 24 hours using the commercially available ViralToxGlo Assay (Promega), which quantifies cell viability via ATP levels. The graph shows the percent viability normalized to the mock infected cells.

Conclusions

In ***Chapter 4***, we established the induction of IDO or AhR expression or activation in response to Delta-24-RGDOX infection *in vitro*. As such, we initially believed that blockade of IDO *in vitro* in Delta-24-RGDOX infected human and murine glioma cells would enhance viral activity, on the basis that IDO blockade would decrease Trp depletion and reverse potential AhR inhibitory effects of cell cycle progression (171).

Interestingly, in the GSC-005 cell line, viral replication and viral-induced cell death induced by Delta-24-RGDOX increased in the presence of an IDO inhibitor. However, when we infected GSC8-11, GSC13, and GSC20 with Delta-24-RGDOX in the presence of an IDO inhibitor, we observed no changes in viral replication or viral-induced cytopathic ability compared to Delta-24-RGDOX infection alone. The results from the human glioma stem cells mirrored the result of our negative control, GL261-5. Still, it is noteworthy to mention that even with treatment with these IDO inhibitors, the viral activity is maintained, strengthening our rationale that IDO inhibitors are a good candidate to be combined with Delta-24-RGDOX.

This result is important because it shows that there are no unwanted drug interactions between the virus and the IDO inhibitors. Furthermore, these contrasting results between GSC-005 and the other cell lines underscore the complexity of viral activity in the context of the IDO-Kyn-AhR pathway.

In conclusion, treatment of murine and human glioma cells with an IDO inhibitor has no effect or a positive effect on adenovirus replication suggesting that adding IDO inhibitors with oncolytic adenoviruses will not result in detriment of the effect of virotherapy.

Chapter 6: Survival advantage in IDO-KO mice treated with Delta-24-RGDOX compared to WT mice.

Rationale and Expectations

In the previous chapters, we demonstrated that Delta-24-RGDOX infection of cancer cells induces expression and activation of IDO and AhR. This suggests that despite the anti-tumor responses we can generate using Delta-24-RGDOX, immunosuppression can still be maintained by an active IDO and AhR. We additionally showed that inhibiting IDO in cancer cell cultures infected with Delta-24-RGDOX does not alter viral replication or viral-induced cytopathic ability.

Our previous studies proved that glioma bearing mice treated with Delta-24-RGDOX survive longer than mice treated with PBS (91). To ensure that the therapeutic effect of Delta-24-RGDOX is maintained under IDO blockade, we tested the survival in glioma bearing C57BL/6 IDO-knock out (KO) (Jackson Laboratory) mice treated with PBS or Delta-24-RGDOX. Based on our *in vitro* data showing that viral activity of Delta-24-RGDOX is maintained when we inhibit IDO, we expected the following:

1) All glioma bearing IDO-KO mice treated with PBS will die.
2) Glioma bearing IDO-KO mice treated with Delta-24-RGDOX will have a longer durable survival compared to PBS-treated mice.

In addition to determining if the therapeutic efficacy of Delta-24-RGDOX is maintained in IDO-KO mice, we also wanted to ascertain whether targeting IDO in combination with Delta-24-RGDOX would provide enhanced therapeutic responses in glioma bearing mice. More specifically, to dissect any potential off-target effects of the IDO inhibitors that might mask the predominant effects on the anti-tumoral immunity induced by the proposed therapy of combined Delta-24-RGDOX and IDO inhibitor, we tested the anti-glioma effect of Delta-24-RGDOX using

IDO-KO mice. In doing so, we were also able to determine the feasibility of combining IDO inhibitors with Delta-24-RGDOX for the treatment of murine glioblastoma.

IDO is also involved in numerous immunosuppressive mechanisms, such as the differentiation of naïve $CD4^+$ T cells into the immunosuppressive regulatory T cell and the induction T effector anergy or apoptosis via Trp depletion (27). Thus, by testing the anti-glioma effect of Delta-24-RGDOX in IDO-KO mice and comparing them to wild-type (WT) mice using IDO-WT glioma models, we can generalize the IDO effects of the host immune system and its relationship to therapeutic responses. Based on these immunosuppressive mechanisms employed by IDO, the IDO-KO mice should have decreased immunosuppressive mechanisms.

We expected the following results:

1) All glioma bearing mice treated with PBS will die regardless of genotype.
2) The deficient function of IDO in IDO-KO mice will enhance the therapeutic efficacy of Delta-24-RGDOX against glioma, leading to longer and more durable survival compared to WT mice.
3) These experiments will offer strong evidence that the effects of the IDO inhibitors are justified by their effects on the respective targets.

Results

Delta-24-RGDOX prolongs survival of IDO-KO glioma bearing mice.

Our previous *in vitro* results indicated that the inhibition of IDO did not alter viral replication or viral induced cytopathic ability. To validate that inhibition of IDO still allows for an oncolytic ability *in vivo*, we monitored the survival of IDO-KO C57BL/6 mice (The Jackson Laboratory) bearing GL261-5 brain tumors after treatment with either PBS or Delta-24-RGDOX. As seen in ***Figure 14***, we demonstrated the oncolytic effect of Delta-24-RGDOX under the extreme case of IDO inhibition via the IDO KO mice, as indicated by the significant delay in median days of survival (55 vs 41.5 days, $p = 0.0006$) and presence of more long-term survivors compared to PBS treated mice (30% vs 0%, $p = 0.0006$).

Glioma bearing mice of the IDO-KO genotype survive longer than the WT genotype when treated with Delta-24-RGDOX.

We then wanted to ascertain whether the survival of glioma bearing mice can be enhanced in IDO-KO mice compared to WT mice when treated with Delta-24-RGDOX. Thus, we used WT or IDO-KO C57BL/6 mice, implanted them with GSC-005 cells, and treated them intratumorally with either PBS or Delta-24-RGDOX. As seen in ***Figure 15***, expectedly, all the PBS treated mice died, regardless of genotype ($p = 0.6967$). Interestingly, the IDO-KO mice had a longer median survival (107.5 vs 55 days, $p = 0.0028$) and more long-term survivors (20% vs 11.1%, $p = 0.0028$) compared to WT mice when treated with Delta-24-RGDOX. These data corroborate our *in vitro* data of ***Figure 13***, which showed that in the GSC-005 model, viral activity, including replication and viral-induced cytopathic ability increased in the presence of IDO inhibition by BGB-7204.

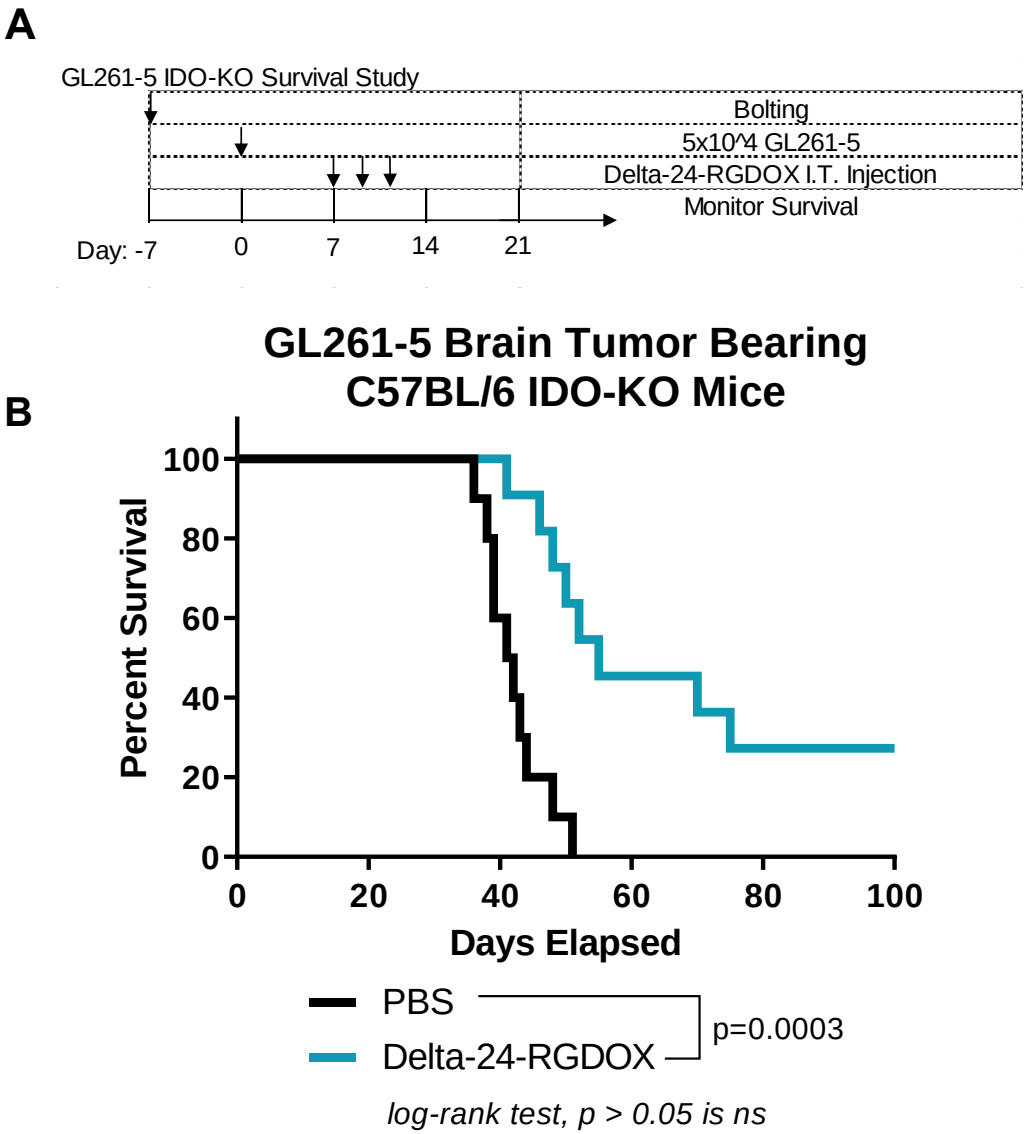

Figure 14: **Delta-24-RGDOX prolongs survival of IDO-KO glioma bearing mice.**

Panel (A) shows the treatment scheme of this survival study. IDO-KO C57BL/6 mice were bolted on day -7, followed by an implantation of $5x10^4$ GL261-5 cells on day 0. On day 7, mice were split into their respective groups, including PBS or Delta-24-RGDOX treatments. When applicable, mice received an intratumoral injection of Delta-24-RGDOX (2.5×10^7 pfu/dose) on days 7, 9, and 11. Survival was monitored over 100 days. Panel (B) shows a survival plot of IDO-KO mice bearing GL261-5 tumors treated with PBS (n=10) or Delta-24-RGDOX (n=11). I.T., intratumoral.

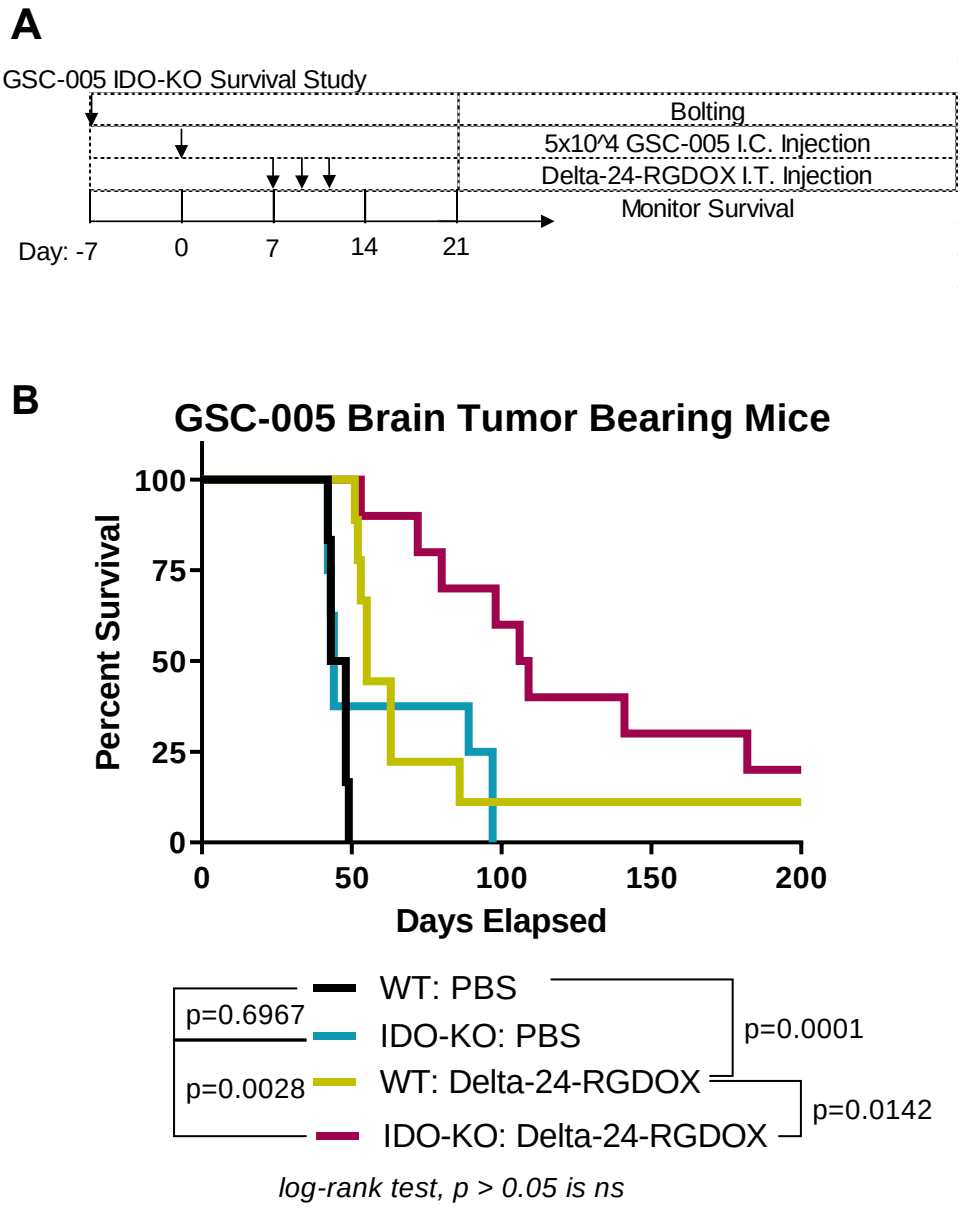

Figure 15: **Glioma bearing mice of the IDO-KO genotype survive longer than the WT genotype when treated with Delta-24-RGDOX.**

Panel (A) shows the treatment scheme of this survival study. Mice were bolted on day -7, followed by an implantation of $5x10^4$ GSC-005 cells on day 0. On day 7, mice were split into their respective groups including PBS or Delta-24-RGDOX treatments in either WT or IDO-KO C57BL/6 mice. When applicable, mice received an intratumoral injection of Delta-24-RGDOX (2.5×10^7 pfu/dose) on days 7, 9, and 11. Survival was monitored over 200 days. Panel (B) shows a survival plot of IDO-KO or WT mice bearing GSC-005 tumors treated with PBS (WT, n=6; IDO-KO, n=8) or Delta-24-RGDOX (WT, n=9; IDO-KO, n=10). I.C., intracranial. I.T., intratumoral.

Conclusions

The oncolytic and therapeutic effect of armed oncolytic adenoviruses, including Delta-24-RGDOX, in glioma-bearing mice has been proven in our lab many times (91, 94, 174). First, to ensure the therapeutic effect of Delta-24-RGDOX during on-target IDO blockade, we implanted IDO-KO mice with murine glioma cells and treated them with PBS or Delta-24-RGDOX. Here, Delta-24-RGDOX treated mice survived longer than PBS treated mice in glioma bearing IDO-KO mice, suggesting that the oncolytic ability of Delta-24-RGDOX maintains its therapeutic effects against murine glioma under IDO depletion.

Next, to strengthen our rationale to combine IDO inhibitors with Detla-24-RGDOX for the treatment of glioma, we compared the survival of IDO-KO mice to WT mice bearing gliomas that were treated with either PBS or Delta-24-RGDOX. The utilization of the IDO-KO mice provides a precise evaluation of the on-target blockade of the IDO pathway combined with Delta-24-RGDOX. This experiment revealed that the IDO-KO mice have a survival advantage over WT mice when treated with Delta-24-RGDOX. This study also suggests that the effect of IDO immunosuppression is generated from the host immune system, rather than the glioma cells, and that targeting IDO in addition to treatment with Delta-24-RGDOX would be beneficial. Additionally, this result of increased survival of the IDO-KO mice compared to the WT mice suggest that the enhanced therapeutic effect is from the on-target inhibition of IDO.

Altogether, these data demonstrate the role of IDO as a negative regulator of the Delta-24-RGDOX-mediated anti-glioma effect and supports the therapeutic use of IDO inhibition during oncolytic virotherapy in glioma.

Chapter 7: Treatment of brain tumor-bearing mice with the combination of IDO inhibitors and Delta-24-RGDOX results in a survival advantage over single agent treatments and induces anti-glioma immune memory.

Rationale and Expectations

Data from our clinical trials (175) and preclinical mechanistic studies (91, 94, 174) suggest that the Delta-24-RGD and Delta-24-RGDOX infection of cancer cells elicits an immune response against the virus that eventually shifts to an anti-tumor immune response, providing the rationale to use immunomodulators as adjuvants to enhance the anti-tumor immune component of the virotherapy.

IDO gained the interest of oncologists as a targetable pathway in different malignancies, including malignant gliomas (23, 27, 30, 39, 40, 52, 57). Several pre-clinical studies have shown that IDO inhibitors enhance the therapeutic effects of chemotherapy, cancer vaccines, or immunotherapy (18, 48-51). For that reason, clinical trials are underway to test the triple combination of IDO and PD-1 inhibitors with chemotherapy (NCT03661320) or with cancer vaccines (NCT03519256).

There is a strong rationale for combining oncolytic viruses and IDO inhibitors: a) IFNγ is the main response against adenoviruses such as Delta-24-RGDOX, and IDO is an IFNγ-responsive gene (152); b) IDO activity is a major response of the host cell against pathogens, including viral infections (166-169), and c) IDO is found overexpressed in many malignancies including glioblastoma (23) and activated in the course of viral infections (166-169). Consistent with these previously published observations, we proved in the current study that IFNγ induced IDO expression and that Delta-24-RGDOX induced expression and activation of IDO and AhR in human or murine glioma cells. Gathering all this data, we expected that the combined Delta-

24-RGDOX and IDO inhibitor treatment would enhance survival of glioma bearing mice compared to single agent treatments. More specifically, we expected the following:

1) Brain tumor-bearing mice treated with combined Delta-24-RGDOX and IDO inhibitor will have longer and more durable survival compared to glioma bearing mice treated with Delta-24-RGDOX or the IDO inhibitor alone.
2) The histopathological staining will show that the mice treated with combined Delta-24-RGDOX and IDO inhibitor will have the smallest tumor mass compared to either single agent treatment.
3) Long term survivors that were previously treated with the combined Delta-24-RGDOX and IDO inhibitor will generate immune memory against the glioma and have protection against a secondary glioma implantation.

Results

Delta-24-RGDOX combined with Trp-mimetic, 1MT or Indoximod, leads to smaller tumor mass, provides a greater survival advantage, and induces a more robust anti-tumor immunity than single agents in the treatment of solid tumors.

To determine the therapeutic efficacy of Delta-24-RGDOX combined with IDO inhibitors, we performed a survival study using the immunocompetent GL261-5 C57BL/6 mouse model. As shown in ***Figure 16A***, a metal bolt was placed into the right skull directly above the caudate nucleus of each mouse under anesthesia, and 7 days later, 5×10^4 GL261-5 cells were implanted through the metal bolt. Starting on day 7 after tumor implantation, mice were split into 4 treatment groups: 1) intracranial (I.C.) PBS and PBS by oral gavage, 2) I.C. PBS and 1MT or indoximod by oral gavage, 3) I.C. Delta-24-RGDOX and PBS by oral gavage, and 4) I.C. Delta-24-RGDOX and 1MT or indoximod by oral gavage. Mice treated with Delta-24-RGDOX were infected on days 7, 9, and 11 at a dose of 5×10^7 pfu/mouse. Mice treated with 1MT or indoximod were treated twice daily, 5 days/week, for 28 days, starting 7 days after tumor implant. As shown in ***Figure 16B***, the control mice and mice treated with 1MT alone had similar survival patterns, with median survival times of 38.5 and 37.5 days, respectively ($p > 0.9999$). As expected, the mice treated with Delta-24-RGDOX alone had significantly prolonged survival, with a median survival time of 46.5 days and 20% of the mice surviving for at least 120 days (vs. control, $p=0.02$; vs. Delta-24-RGDOX plus 1MT, $p=0.01$). Interestingly, mice treated with the combination of Delta-24-RGDOX and 1MT had the longest survival, with a median survival time of 108.5 days and 50% of the mice surviving for at least 120 days (vs. control, $p<0.0001$; vs. Delta-RGDOX alone, $p=0.01$). Furthermore, in mice treated with the combination of Delta-24-RGDOX and Indoximod, hematoxylin-eosin staining revealed an observable and substantial tumor regression on day 15 and complete eradication by day 24 (***Figure 17A***), which was associated with the lowest surface

areas of high-grade cellularity (Delta-24-RGDOX vs Delta-24-RGDOX and Indoximod, 2.10 x 10^6 vs. 0.44 x 10^6, p= 0.0298) (***Figure 17B***). H&E images of individual mice are seen in ***Figure 18***. To confirm that the anti-tumor effect was immune mediated, the long-term survivors in the group treated with Delta-24-RGDOX plus 1MT were re-challenged with the same glioblastoma cell line and observed for survival. Importantly, all the mice previously treated with Delta-24-RGDOX plus 1MT survived for at least 100 days, while all the untreated mice died by day 51 (p=0.0018) (***Figure 16C***). These data demonstrated the generation of memory against the tumor by the combination of Delta-24-RGDOX and 1MT.

We also observed an enhanced survival effect using the B16-F10 intracranial melanoma model, in which 14% of mice treated with Delta-24-RGDOX and Indoximod survived for at least 26 days, compared to zero survivors in the Delta-24-RGDOX only treated group (p = 0.0140, ***Figure 19***).

These results indicated that the combination of Delta-24-RGDOX and Trp-mimetics was therapeutically superior to either treatment alone in mouse models of aggressive intracranial brain tumors.

Delta-24-RGDOX combined with the direct IDO enzyme inhibitor, BGB-7204, leads to lower tumor mass and provides a greater survival advantage compared to single agents in murine glioblastoma.

Because 1MT and Indoximod are Trp-mimetics, they are not considered direct IDO enzyme inhibitors. Thus, we also tested the therapeutic effect of Delta-24-RGDOX in the context of direct IDO enzyme inhibition using BGB-7204 (provided by Dr. Derek Wainwright). BGB-7204 is a novel pre-clinical direct IDO enzyme inhibitor that has shown therapeutic efficacy when combined with radiation and anti-PD-1 monoclonal antibodies in murine models of glioma (57).

We tested the antitumor effects in GSC-005 glioma bearing mice and submitted them to four different treatment groups included treatment groups: 1) I.C. PBS and vehicle by oral gavage (control), 2) I.C. PBS and BGB-7204 by oral gavage 3) I.C. Delta-24-RGDOX and vehicle by oral gavage, and 3) I.C. Delta-24-RGDOX and BGB-7204 by oral gavage. Mice treated with Delta-24-RGDOX were infected on days 9 and 11 at a dose of 2.5×10^7 pfu/mouse. Mice treated with BGB-7204 were treated twice daily, 5 days/week, for 28 days starting on day 7. In mice treated with the combination of Delta-24-RGDOX and BGB-7204, hematoxylin-eosin staining revealed complete eradication by day 24 (***Figure 20A***), which associated with the lowest surface areas of high-grade cellularity compared to all other treatment groups (Delta-24-RGDOX vs Delta-24-RGDOX and BGB-7204, 7.64×10^5 vs. 0.42×10^5, $p = 0.0261$) (***Figure 20B***). H&E images of individual mice are seen in ***Figure 21***. These results indicated that the combination of Delta-24-RGDOX and an IDO inhibitor was reproducible in a third murine glioma model, and that the combination is therapeutically superior to either treatment alone.

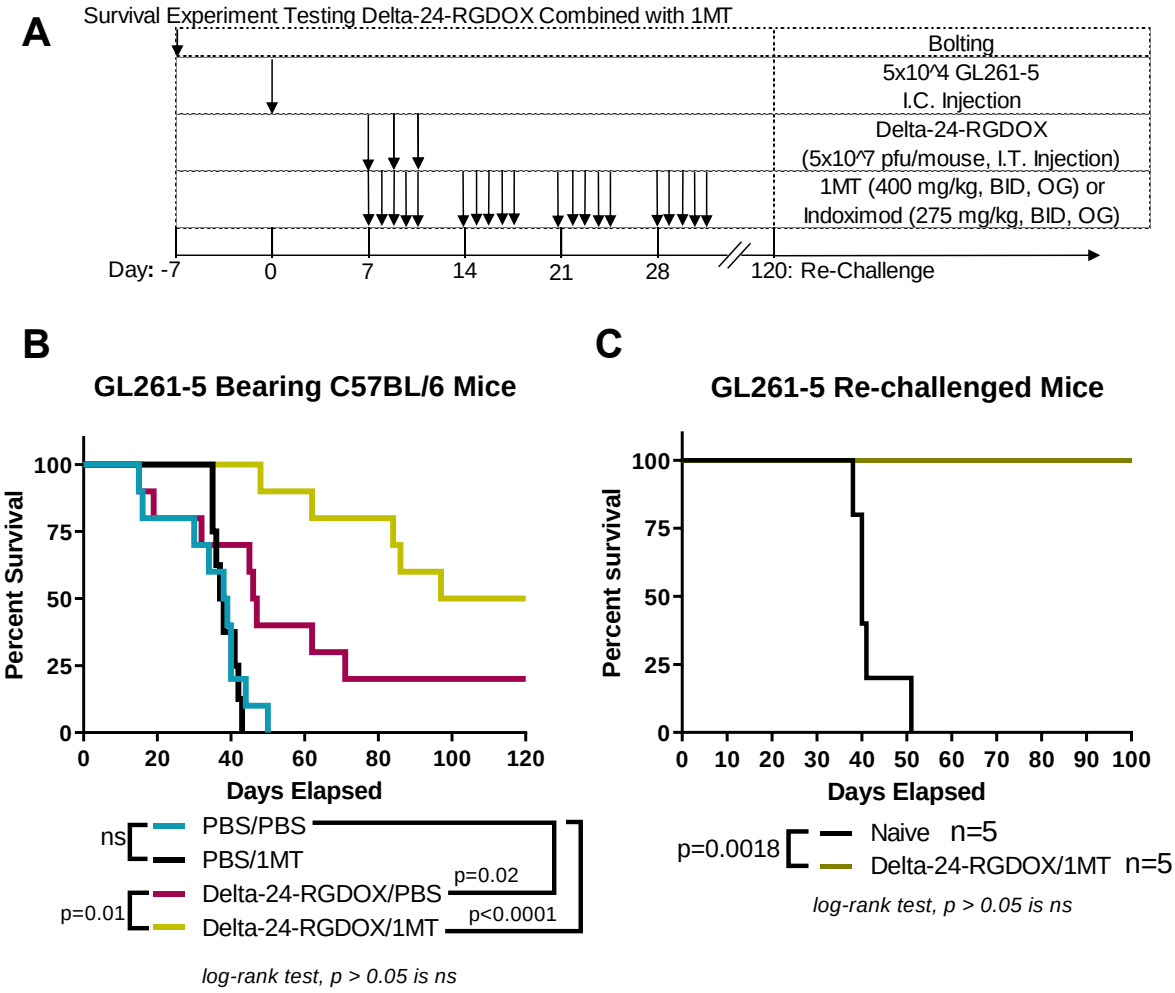

Figure 16: **Combined Delta-24-RGDOX and 1MT provides a survival advantage over either treatment alone and induces anti-glioma memory in a murine immunocompetent glioma model.**

(A) Mice were bolted on day -7, followed by injection of $5x10^4$ GL261-5 cells on day 0. On day 7, mice were split up into four treatment groups including PBS (control), 1MT, Delta-24-RGDOX, or combined 1MT and Delta-24-RGDOX. Mice received Delta-24-RGDOX ($5x10^7$ pfu/mouse) on days 7, 9, and 11. 1MT treatment started on day 7 and lasted until day 35. Panel (B) shows a survival plot of C57BL/6 mice bearing GL261-5 tumors treated with PBS, 1MT, Delta-24-RGDOX, or combined 1MT and Delta-24-RGDOX (n=10). Mice surviving 120 days from the combined Delta-24-RGDOX and 1MT treatment group were re-challenged with the same cell line on the contralateral hemisphere and observed for survival. Panel (C) shows a survival plot of combined 1MT and Delta-24-RGDOX treated mice re-challenged with the same cell line on the contralateral brain hemisphere compared to control naïve mice (n=5). I.C., intracranial. I.T., intratumoral. OG, oral gavage. BID, *bis in die*, twice daily.

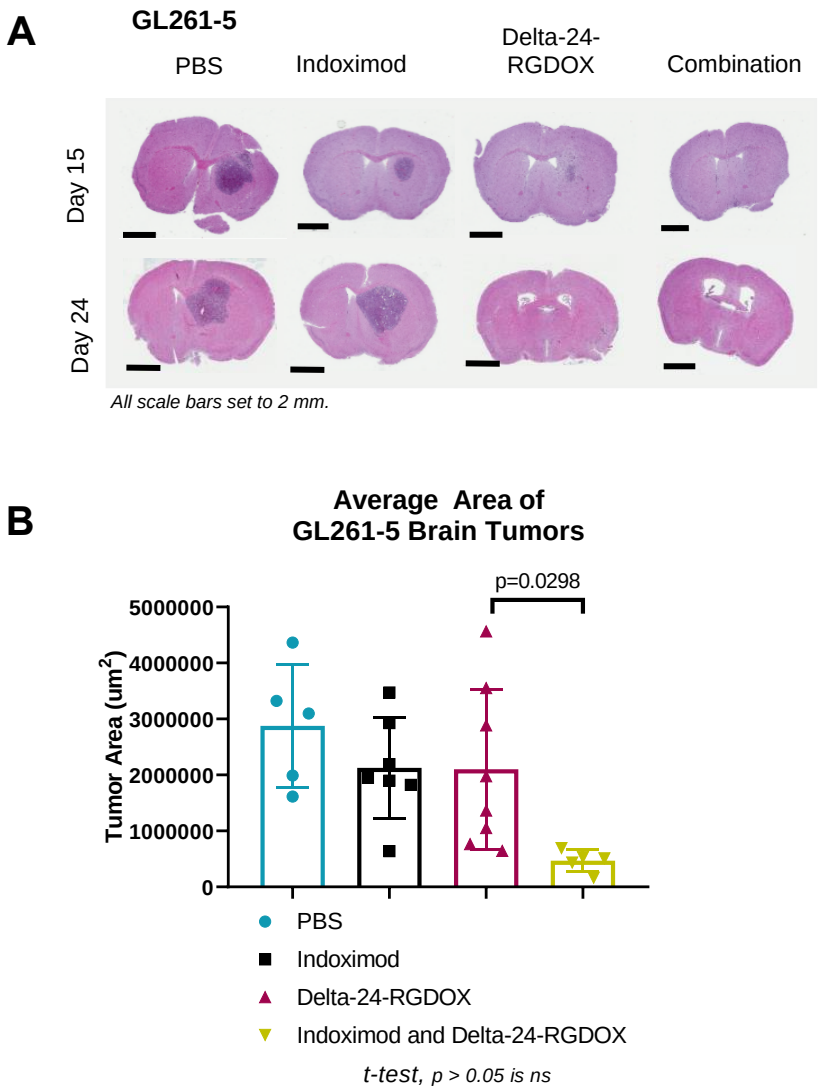

Figure 17: **Combined Delta-24-RGDOX and Indoximod leads to tumor regression in a murine immunocompetent glioma model.**

Following the same treatment schedule as in ***Figure 16***, mice were sacrificed 15 and 24 days after tumor implantation, brains were collected in formalin for embedding, sectioning, and H&E staining. Panel (A) shows representative H&E staining images of GL261-5 bearing mouse brains treated with PBS, Indoximod, Delta-24-RGDOX, or combined Indoximod and Delta-24-RGDOX 15- and 24-days post tumor implantation. Panel (B) shows the average tumor areas in differently treated mice on day 15 of GL261-5 bearing C57BL/6 mouse brains. Aperio ImageScope software was used to acquire images and to measure areas of high-grade cellularity (μm^2). Column graph values represent mean ± SD (n=5+).

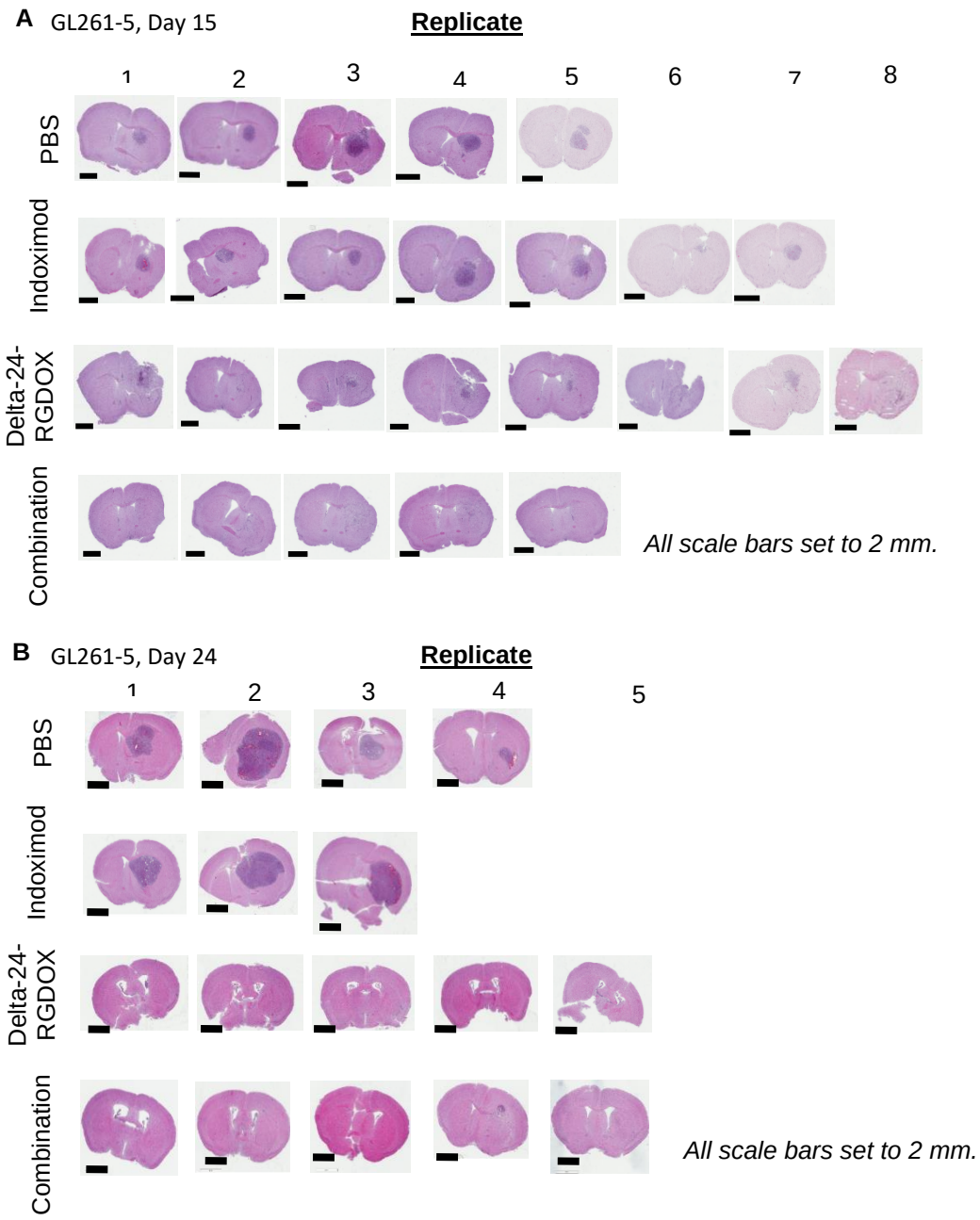

Figure 18: **Combined Delta-24-RGDOX and Indoximod treatment induces tumor regression in GL261-5 bearing mice.**

Following the same treatment schedule as in ***Figure 16,*** mice were sacrificed on (A) day 15 or (B) day 24, and brains were collected in 10% buffered formalin and transferred to 70% ethanol after 24 hours. Brain tumor coronal sections were embedded in paraffin and sectioned in 5µm slices using a microtome and affixed onto positively charged glass slides. Slides were subjected to hematoxylin and eosin staining via conventional methods. Slides were scanned using the Aperio ImageScope-Pathology Slide Viewing Software.

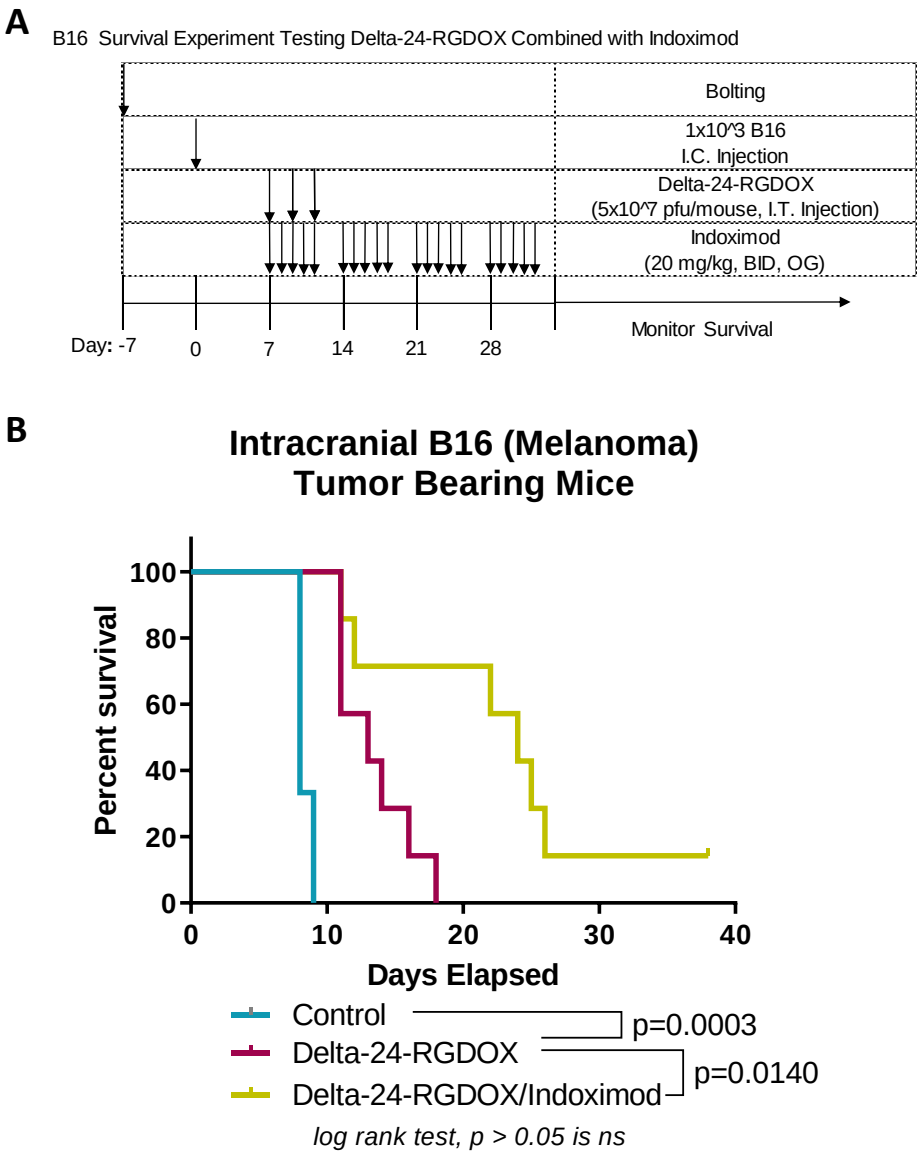

Figure 19: **Combined Delta-24-RGDOX and Indoximod treatment shows a survival advantage in B16-melanoma brain tumor bearing mice.**

Panel (A) shows the treatment schedule, where mice were bolted on day -7, followed by injection of $1x10^3$ B16 cells on day 0. On day 7, mice were split up into three treatment groups including PBS (control, n=6), Delta-24-RGDOX (n=7), or combined Delta-24-RGDOX and Indoximod (n=7). Mice received Delta-24-RGDOX ($5x10^7$ pfu/mouse) on days 7, 9, and 11 (when applicable). Indoximod treatment started on day 7 and lasted an additional 28 days (when applicable). Panel (B) shows a survival plot of the differently treated C57BL/6 mice bearing B16 brain tumors. I.C., intracranial, I.T., intratumoral. OG, oral gavage. BID, *bis in die*, twice daily.

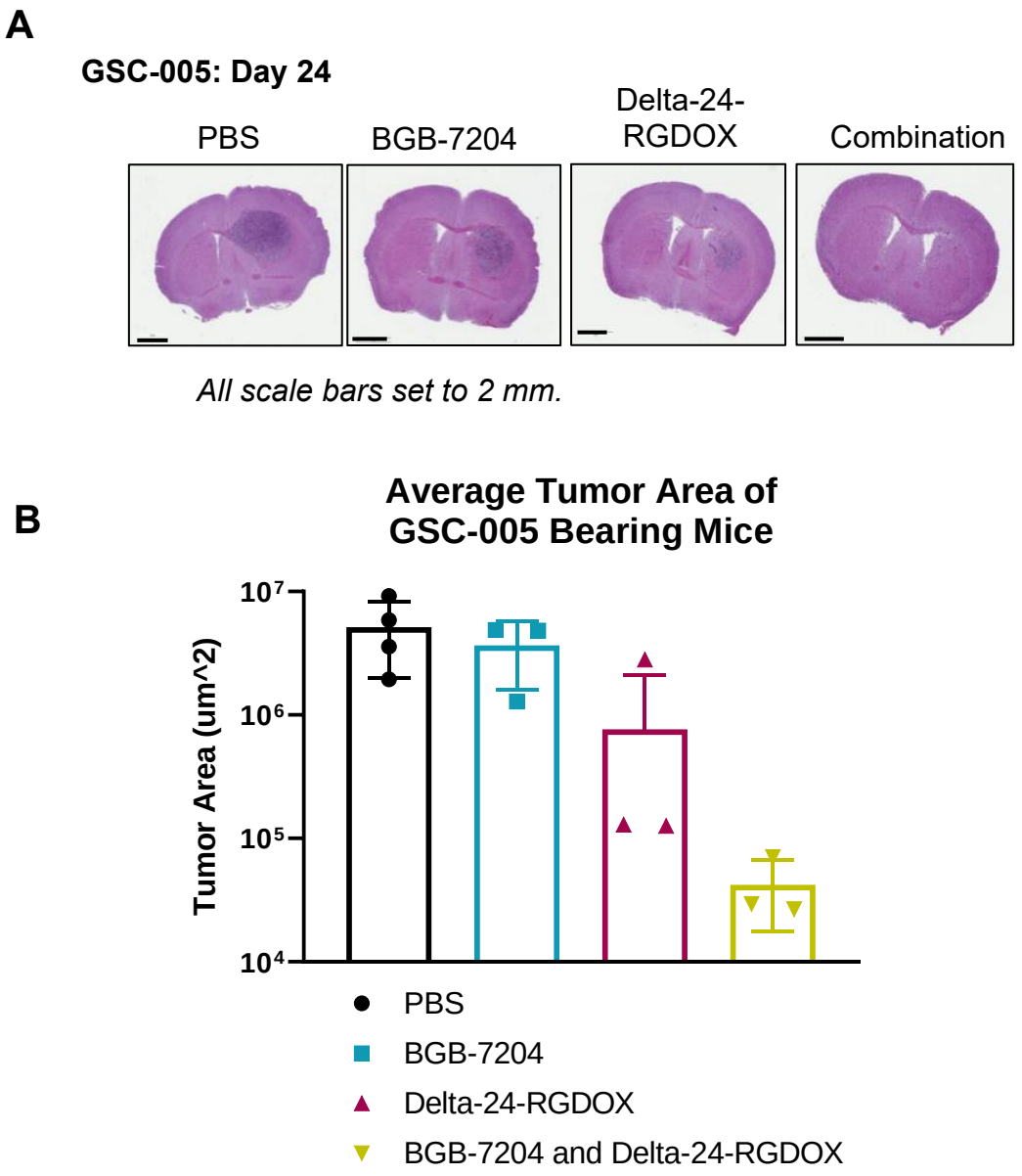

Figure 20: **Combined Delta-24-RGDOX and BGB-7204 treatment results in the smallest tumor mass compared to single agent treatments in GSC-005 brain tumor bearing mice.**

Mice were bolted on day -7, implanted with the $5x10^4$ GSC-005 cells on day 0, injected with Delta-24-RGDOX ($2.5x10^7$ pfu/mouse in 5µL) or PBS on days 9, and 11, and treated with 100 mg/kg BID per mouse of BGB-7204 on days 7-24. Panel (A) shows representative H&E staining images of coronal mouse sections on day 24. Panel (B) shows average tumor areas in differently treated mice on day 24 of these GSC-005 bearing C57BL/6 mouse brains. The methods described in ***Figure 17*** were used. Column graph values represent mean ± SD (n=3+).

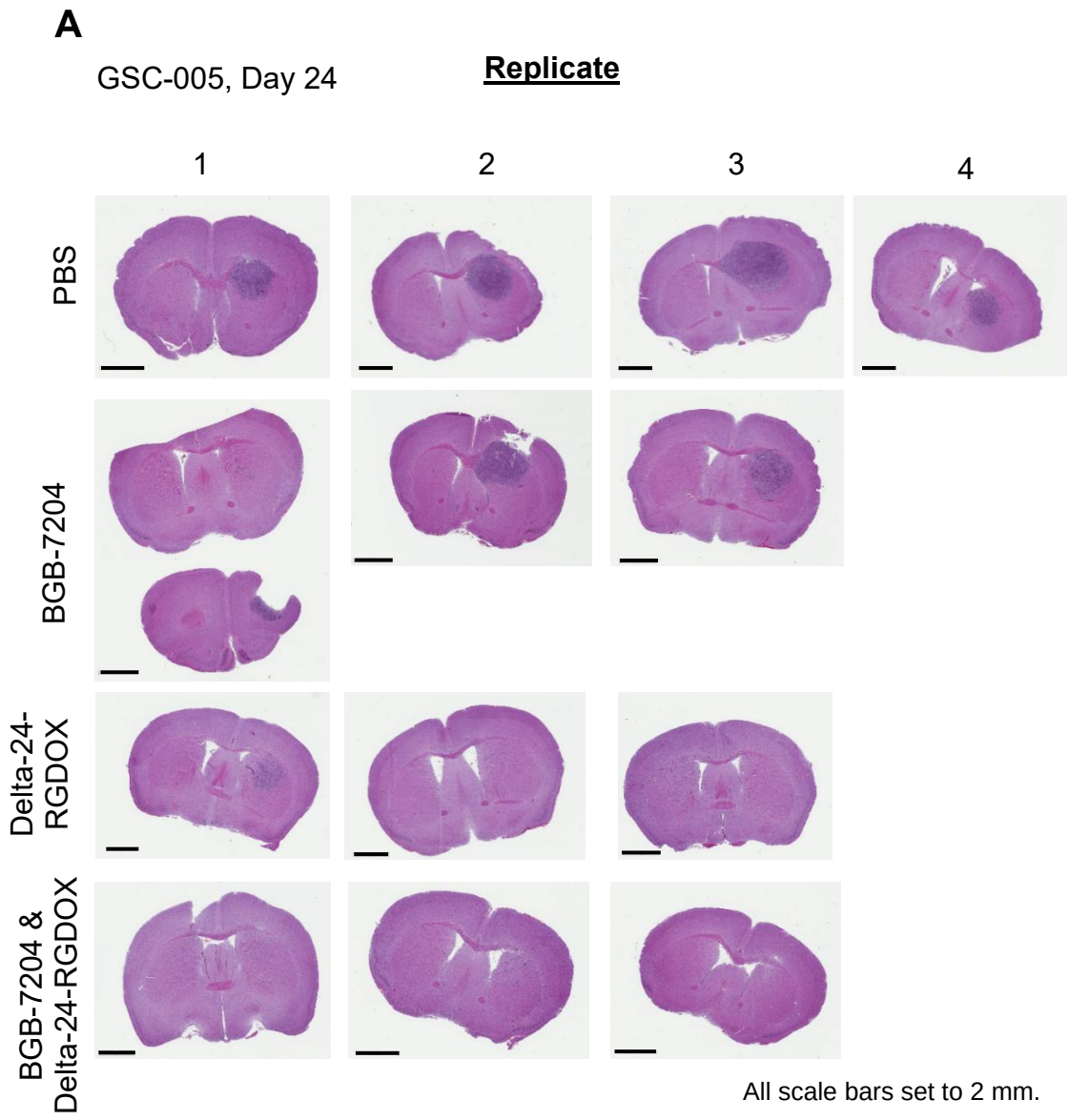

Figure 21: **Combined BGB-7204 and Delta-24-RGDOX treatment induces tumor regression in GSC-005 tumor bearing mice.**

The figure shows H&E images of mouse brain coronal sections of C57BL/6 GSC-005 bearing mice. Mice were bolted on day -7, implanted with the $5x10^4$ GSC-005 cells on day 0, injected with Delta-24-RGDOX ($2.5x10^7$ pfu/mouse in 5µL) or PBS on days 9, and 11, and treated with 100 mg/kg BID per mouse of BGB-7204 on days 7-24. Mice were sacrificed on day 24, and brains were collected in 10% buffered formalin and transferred to 70% ethanol after 24 hours. Brain tumor coronal sections were embedded in paraffin and sectioned in 5µm slices using a microtome and affixed onto positively charged glass slides. Slides were subjected to hematoxylin and eosin staining via conventional methods. Slides were scanned using the Aperio ImageScope-Pathology Slide Viewing Software.

Conclusions

In the current study, we have provided data to support our rationale to combine IDO inhibitors and Delta-24-RGDOX for the treatment of murine glioma including: 1) Delta-24-RGDOX increases IDO expression and activation and 2) the on-target blockade of IDO enhances the therapeutic efficacy of Delta-24-RGDOX. These data along with previous publications describing the immunosuppressive mechanisms caused by IDO (24, 27) supported our studies in determining the efficacy of the combination of IDO inhibitors with Delta-24-RGDOX for the treatment of murine glioma.

To assess the combination of Delta-24-RGDOX combined with IDO inhibitors, we used several murine tumor models that were syngeneic to the immunocompetent C57BL/6 mouse, including murine gliomas, GL261-5 and GSC-005, and murine melanoma, B16. The survival and histopathology of the tumor-bearing brains of these mice were studied following treatments with PBS, IDO inhibitor alone, Delta-24-RGDOX alone, or the combination of Delta-24-RGDOX and IDO inhibitor. The IDO inhibitors used included Trp-mimetics, 1MT and Indoximod, and direct IDO enzyme inhibitor, BGB-7204. These studies resulted in the following conclusions:

1) Mice bearing intracranial tumors including the immunocompetent GL261-5, GSC-005, and the B16 (melanoma) models benefit from Delta-24-RGDOX treatment; when IDO inhibitors are combined with Delta-24-RGDOX, the therapeutic effect increases.
2) The enhanced therapeutic effect of the combination treatment was evident with both Trp-mimetics (1MT or Indoximod) and direct IDO enzyme inhibitors (BGB-7204).
3) The enhanced therapeutic effect was indicated by more survival and greater decreases in the tumor mass in brain tumor bearing mice treated with combined Delta-24-RGDOX and IDO inhibitor treatment compared to mice treated with Delta-24-RGDOX alone or IDO inhibitor alone.

4) The minimal therapeutic effect of treatment by the IDO inhibitor alone indicated that IDO inhibitors may be effective when combined with another agent.
5) The rejection of a second tumor implantation in mice previously treated with the combination of Delta-24-RGDOX and IDO inhibitors suggests induction of an anti-glioma immune memory response.
6) There were no obvious signs of general toxicity by the mice, including hunched posture, diarrhea, or weight loss, by the combination treatment.

These results strengthen our rationale to translate this proposed treatment strategy into the clinic.

Chapter 8: The therapeutic efficacy of the combination of IDO inhibitor and Delta-24-RGDOX treatment requires CD4$^+$ helper T Cells.

Rationale and Expectations

Thus far, we can postulate that Delta-24-RGDOX induces both tumor-promoting and anti-tumor immune responses, as evident by 1) the RNA-sequencing data, 2) the induction of IDO expression and activation by Delta-24-RGDOX in glioma bearing mice, 3) the greater survival effect in Delta-24-RGDOX treated mice compared to PBS treated mice bearing gliomas, and 4) the enhanced therapeutic responses in glioma bearing mice by the combined Delta-24-RGDOX and IDO inhibitor treatment compared to treatment with Delta-24-RGDOX alone. We can further speculate that the enhanced therapeutic efficacy of the combination compared to single agent treatments is due to the generation of an immune memory against glioma antigens as indicated by our previous survival study that showed 100% survival in re-challenged mice that were previously treated with the combination therapy.

To further evaluate to which extent the immune component, particularly the role of T-helper cells, is responsible for the anti-cancer effect, we depleted CD4$^+$ T cells in immunocompetent GL261-5 glioma bearing mice treated with Delta-24-RGDOX or the combination Delta-24-RGDOX and IDO inhibitor. The depletion of specific CD4$^+$ T cells can be achieved by serial intraperitoneal injections of CD4 neutralizing antibodies (BioXCell-InVivoMAb anti-mouse CD4, clone GK1.5) in mice.

OX40 is a costimulatory receptor that is primarily activated on CD4$^+$ T cells and is heavily involved in regulation of CD4$^+$ and CD8$^+$ T cell proliferation, differentiation, and survival (92, 93, 176, 177). These OX40 activation mechanisms are supported by our previous studies that demonstrated a significant survival effect of Delta-24-RGDOX using the immunocompetent

GL261-5 glioma model; by contrast, when GL261-5 glioma cells were implanted in athymic immunodeficient mice and treated with Delta-24-RGDOX, 100% of the mice died, indicating the dependence of Delta-24-RGDOX on the immune system for therapeutic efficacy (91).

Patterns of survival in mice receiving treatment of Delta-24-RGDOX alone or together with the administration of an IDO inhibitors plus the CD4 neutralizing antibody should provide mechanistic data about the role of $CD4^+$ T cells on oncolytic virotherapy.

Based on the current literature and our previous findings, we expected the following:

1) Glioma bearing mice treated with Delta-24-RGDOX and the CD4 neutralizing antibody will have a similar survival pattern to the control treated mice.
2) Glioma bearing mice treated with the combination of Delta-24-RGDOX, the IDO inhibitor, and the CD4 neutralizing antibody will have a similar survival pattern to the control treated mice.
3) Glioma bearing mice treated with the combination of Delta-24-RGDOX, the IDO inhibitor, and a control antibody will survive longer than the groups treated with the CD4 neutralizing antibody.
4) $CD4^+$ T cell immune responses against the virus and tumor is required for an antitumor effect in glioma bearing mice treated with Delta-24-RGDOX or combined Delta-24-RGDOX and IDO inhibitor treatment.

Results

To understand the effects of the helper T cell population on the efficacy of combined Delta-24-RGDOX and IDO inhibitor treatment in murine glioblastoma, we performed a survival experiment using the GL261-5 C57BL/6 mouse model. The methodology is described in ***Figure 22A***, where mice were bolted 7 days prior to an intracranial 5 x 10^4 GL261-5 cell injection followed by three doses of Delta-24-RGDOX (5 x 10^7 pfu/mouse) on days 7, 9, and 11. Treatment groups included 1) control (PBS) + IgG, 2) Delta-24-RGDOX + anti-CD4 (for depletion of helper T cells), 3) Delta-24-RGDOX + Indoximod + anti-CD4, and 4) Delta-24-RGDOX + Indoximod + IgG. ***Figure 23*** shows validation of $CD4^+$ T cell depletion.

As expected, the control group had a median survival of 40 days (***Figure 22B)***. Interestingly, the mice treated with the CD4 depletion antibody and Delta-24-RGDOX or combined Delta-24-RGDOX and Indoximod had a median survival of 33 or 36 days, respectively, which mirrored the control group treated with PBS + IgG (PBS + IgG vs Delta-24-RGDOX + anti-CD4, $p = 0.0732$; vs. Delta-24-RGDOX + Indoximod + anti-CD4, $p = 0.5989$). This indicates the dependency of Delta-24-RGDOX and/or Indoximod on the T helper $CD4^+$ population for the therapeutic and long-term survival effect. Mice treated Delta-24-RGDOX + Indoximod + IgG had a 100% survival after 100 days, confirming the therapeutic efficacy of combined Delta-24-RGDOX with a Trp-mimetic (Indoximod) in this brain tumor model (Delta-24-RGDOX + Indoximod + anti-CD4 vs. Delta-24-RGDOX + Indoximod + IgG, $p < 0.0001$).

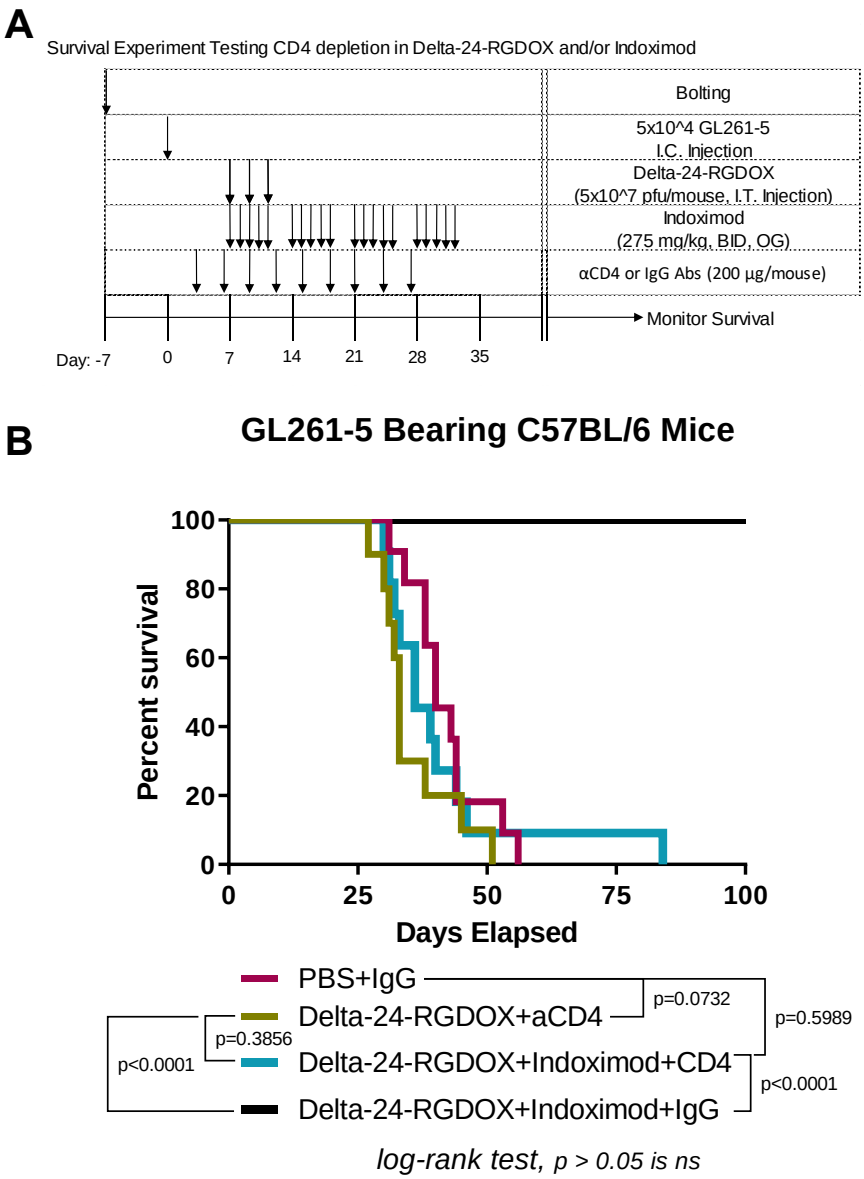

Figure 22: **Therapeutic efficacy of combined IDO inhibition and Delta-24-RGDOX treatment requires CD4$^+$ helper T cells.**

Panel (A) shows the treatment schedule, where mice were bolted on day -7, followed by intracranial injections of 5x10^4 GL261-5 cells on day 0. On day 7, mice were split up into four treatment groups including 1) PBS (control) plus IgG control antibody (BioXCell-InVivoMAb rat IgG2b isotype control, anti-keyhole limpet hemocyanin), 2) Delta-24-RGDOX plus CD4 neutralizing antibody (BioXCell-InVivoMAb anti-mouse CD4 (clone GK1.5)), 3) Delta-24-RGDOX and Indoximod plus CD4 neutralizing antibody, and 4) Delta-24-RGDOX and Indoximod plus IgG control antibody. Mice received Delta-24-RGDOX (5x10^7 pfu/mouse) on days 7, 9, and 11. Indoximod treatment started on day 7 and lasted an additional 28 days. Neutralizing or control antibodies were administered, intraperitoneally, every fourth day for nine rounds. Panel (B) shows the survival of differently treated mice. I.C., intracranial. I.T., intratumoral. OG, oral gavage. BID, *bis in die*, twice daily.

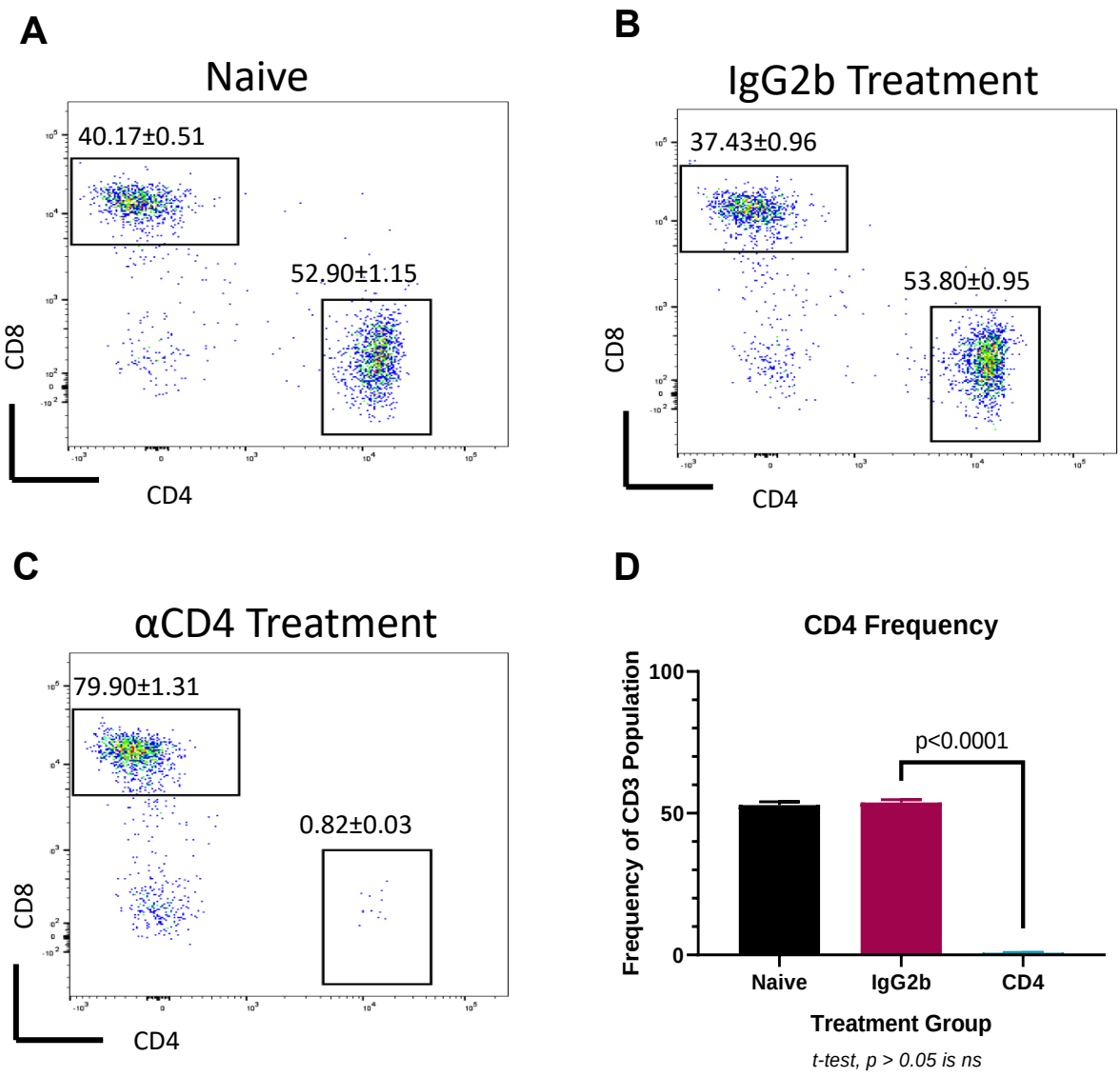

Figure 23: **CD4 neutralizing antibodies deplete CD4 populations *in vivo*.**

This figure supplements the survival study of GL261-5 bearing mice treated with Delta-24-RGDOX and/or Indoximod with or without CD4 depletion antibodies, seen in ***Figure 22***. Mice were treated with CD4 neutralizing antibodies (αCD4: BioXCell-InVivoMAb anti-mouse CD4 (clone GK1.5)) or an unreactive IgG (IgG2b: BioXCell-InVivoMAb rat IgG2b isotype control, anti-keyhole limpet hemocyanin) to serve as a control. On day 38 post-tumor implant, one mouse from each treatment was sacrificed. Spleens were collected and processed into single cells and stained for CD3, CD4, and CD8, then analyzed using flow cytometry. Flow cytometry plots show CD4 and CD8 populations of the (A) naïve, (B) IgG2b, or (C) anti-CD4 treated mice. D) The column graph shows the frequency of the CD4 population in the indicated treatment group.

Conclusions

Our previous studies underscore the importance of the host immune system to elicit the antitumor effects of Delta-24-RGDOX in glioma bearing mice (91). To further study the role of $CD4^+$ T helper cells during Delta-24-RGDOX or combined Delta-24-RGDOX and IDO inhibitor treatment, we conducted a survival study of glioma bearing mice with these respective treatments with or without depletion of the $CD4^+$ T helper cell population.

Our results indicate that we successfully depleted the $CD4^+$ T cell population allowing us to accurately determine the role of $CD4^+$ T helper cells on the therapeutic efficacy of Delta-24-RGDOX or combined Delta-24-RGDOX and Indoximod treatment in an immunocompetent murine glioma model. As such, we can make the following conclusions:

1) The therapeutic efficacy and antitumor effect of Delta-24-RGDOX or combined Delta-24-RGDOX and IDO inhibitor treatment requires $CD4^+$ T cell activity of the host.
2) The superior survival effects of combined Delta-24-RGDOX with Trp-mimetic, Indoximod in the GL261-5 glioma model is reproducible.

The 100% death of glioma bearing mice caused by the depletion of the $CD4^+$ T helper population is congruent with the outcomes of the enhanced OX40 receptor pathway activation elicited by Delta-24-RGDOX. More specifically, the OX40 receptor is a T cell activator with major effects on CD4+ T cells (144, 177).

Chapter 9: The combination of Delta-24-RGDOX and IDO inhibitors increases the amount of intratumoral T cells and decreases the count of immune tolerant populations.

Rationale and Expectations

The IDO pathway metabolite, Kyn, activates AhR in several populations of immune-related cells, shaping the pro-tumorigenic functions of the tumor microenvironment (27, 42, 164, 165). Depletion of Trp, and the subsequent excess of Kyn in the tumor microenvironment results in suppression of T-cell function and induction of T-cell apoptosis (35). Kyn-mediated activation of AhR promotes FOXP3+ regulatory T cell differentiation (32, 33). In addition, the IDO-Kyn-AhR cascade has been linked to Th17 differentiation (178, 179) of T helper cells, whose suppressive function has been associated with tumor immunosuppression (180). The activation of the IDO pathway also elicits integrated stress responses via Trp depletion leading to IL-6 cytokine signaling, which is essential for MDSC formation (36, 37).

The IDO-Kyn-AhR molecular cascade may further influence the tumor microenvironment in the context of virotherapy because it is involved in the host immune response against viruses. In agreement with this data, the IDO-Kyn-AhR pathway is an important environmental modulator that contributes to the prevalence and severity of viral infections (181). Therefore, we were interested in ascertaining the extent to which the infection of gliomas by Delta-24-RGDOX prompts activation of the IDO-Kyn-AhR pathway in the tumor microenvironment. In fact, we were able to show the increased induction of IDO expression and activation *in vivo* in Delta-24-RGDOX treated brain tumors compared to PBS-treated, seen in ***Figures 9 and 10***.

The IDO-Kyn-AhR activation after oncolytic virus administration may further contribute to increased tumor immunosuppression and, in turn, facilitate the glioma's ability to evade the T-cell immune response elicited by virotherapy. In agreement with this, we observed an enhanced

therapeutic efficacy of combined Delta-24-RGDOX and IDO inhibitor treatment compared to Delta-24-RGDOX treatment alone in murine glioma, as discussed in ***Chapters 7 and 8***. Consequently, we expected that adding an IDO inhibitor to Delta-24-RGDOX would increase general T cell populations ($CD3^+$, $CD4^+$, and $CD8^+$ T cells) and decrease immunosuppressive populations, such as Tregs or MDSCs, within the tumor microenvironment. More specifically, we expected the following:

1) Delta-24-RGDOX treatment will increase the immunogenicity of murine gliomas. Particularly, Delta-24-RGDOX will increase both anti-tumor and pro-tumorigenic immune populations, including $CD4^+$ T helper cells, cytotoxic $CD8^+$ T cells, regulatory T cells, and myeloid derived suppressor cells.
2) IDO inhibitors will enhance the infiltration of $CD4^+$ T helper cells and cytotoxic $CD8^+$ T cells generated by Delta-24-RGDOX in murine glioma.
3) IDO inhibitors will decrease the infiltration of immune tolerant populations (Tregs and MDSCs) generated by Delta-24-RGDOX in glioma.

Results

The combination of Delta-24-RGDOX with IDO inhibitors increases the frequency of intratumoral T cells.

To further understand the mechanism underlying the anti-cancer effect of the combination of Delta-24-RGDOX and IDO inhibitors, we examined phenotypic changes of lymphocyte populations within the tumor from the GL261-5 or GSC-005 bearing mice treated with 1) PBS, 2) IDO inhibitor alone, 3) Delta-24-RGDOX alone, or 4) combined IDO inhibitor and Delta-24-RGDOX. After treating the mice with indicated treatment for 17 days, we isolated brain-infiltrating lymphocytes and stained them to identify tumor-infiltrating $CD3^+$ cells, T-helper $CD4^+$ cells, and cytotoxic $CD8^+$ T lymphocytes by flow cytometry. As expected, Delta-24-RGDOX treatment resulted in an increase in tumor-infiltrating $CD3^+$, T-helper $CD4^+$ cells, and cytotoxic $CD8^+$ T lymphocytes per hemisphere after 17 days of treatment (***Figures 24A and 27***) compared to PBS or IDO inhibitor treated mice in both the GL261-5 and GSC-005 model. Of interest, the combination of Delta-24-RGDOX and IDO inhibitor treatment led to highest absolute count per hemisphere in the $CD3^+$, $CD4^+$, and $CD8^+$ populations compared to all other groups (***Figures 24A and 27***; $p < 0.05$, all populations). This pattern was also confirmed in $CD3^+$ immunohistochemistry, where the highest amounts of $CD3^+$ staining density occur in mouse tumors treated with combined Delta-24-RGDOX and IDO inhibitor treatment (***Figure 24B***). Representative images of the $CD3^+$ IHC for both models of individual mice are seen in ***Figures 25 and 26***.

The combination of Delta-24-RGDOX with IDO inhibitors decreases the frequency of immune tolerant populations.

Furthermore, to determine the tolerant immune effects within the tumor microenvironment produced by the combination of Delta-24-RGDOX and Indoximod, we used flow cytometry to analyze the populations of regulatory T cells ($CD4^+$, $FOXP3^+$, $CD25^+$) and myeloid-derived suppressor cells ($CD45^+$, $GR1^+$, $CD11b^+$) of GL261-5 brain tumors after 17 days of treatment or 24 days after the tumor implant. RNA sequencing analyses revealed that GL261-5 tumors treated with Delta-24-RGDOX harbored enrichment of Treg and MDSC gene sets (***Figure 28A and 28C***). This result was validated by the flow cytometry assays, which showed that the mice treated with Delta-24-RGDOX alone had more Tregs and MDSCs per hemisphere than PBS-treated or Indoximod-treated mice had ***(Figure 28B and 28D)***. Notably, the mice treated with the combination of Delta-24-RGDOX and Indoximod had fewer Tregs and MDSCs than the mice treated with Delta-24-RGDOX only had ($p < 0.0001$, both populations). These data indicate the decrease in immune-tolerant populations when Delta-24-RGDOX was combined with IDO inhibitors.

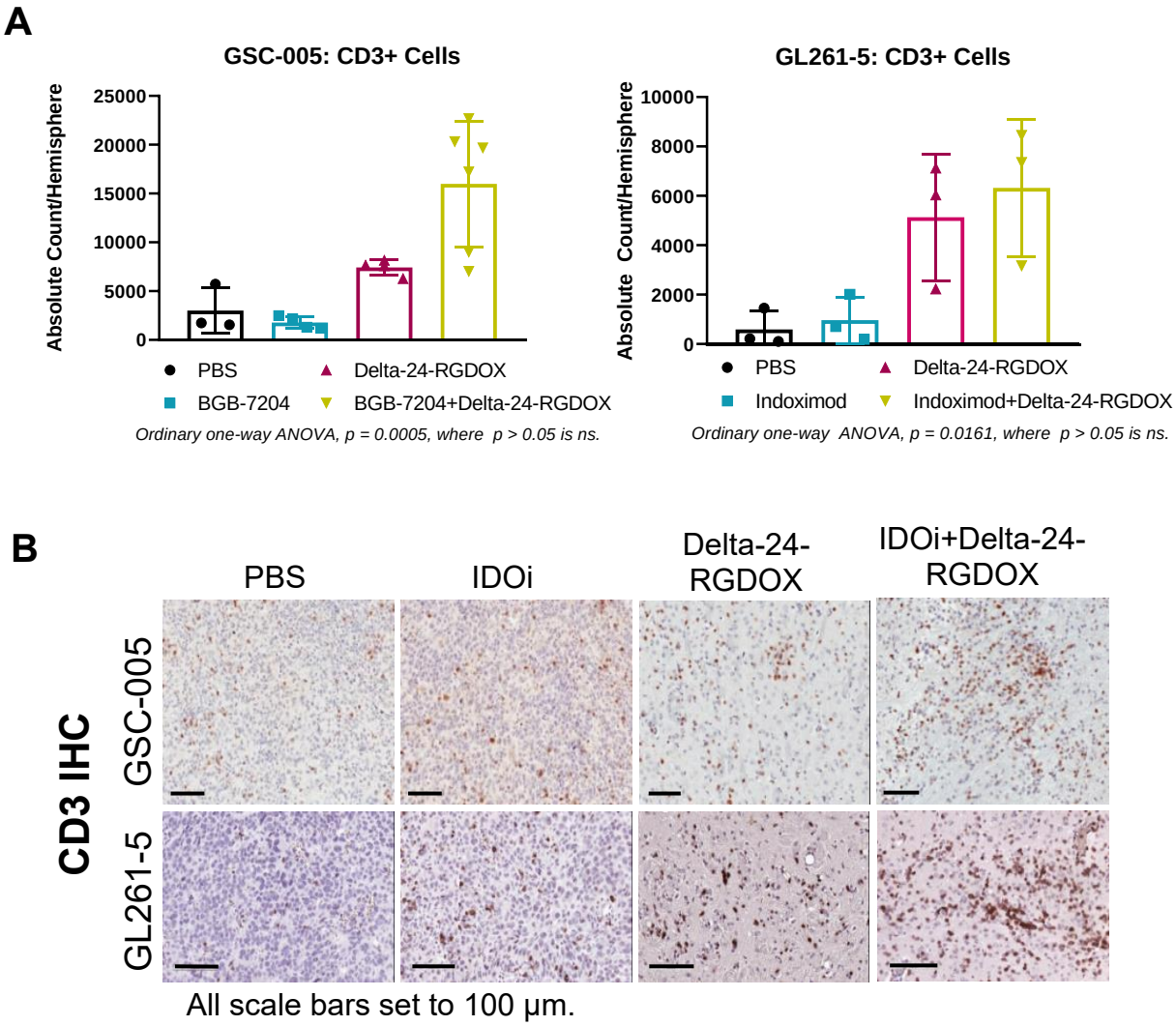

Figure 24: **The combination of Delta-24-RGDOX with IDO inhibitors increases the absolute count per hemisphere of intratumoral T cells in murine glioma.**

Mice were bolted on day -7, then implanted with 5 x 10^4 GSC-005 or GL261-5 cells on day 0; on days 9 and 11 (GSC-005) or days 7, 9, and 11 (GL261-5), the mice were intracranially injected with PBS, Delta-24-RGDOX (2.5 x 10^7 (GSC-005) or 5 x 10^7 (GL261-5) pfu/dose). IDO inhibitors (IDOi: Indoximod, 275 mg/kg or BGB-7204, 100 mg/kg, BID) were administered from days 7 to 24. On day 7, mice were split up into four treatment groups including PBS (control), IDOi, Delta-24-RGDOX, or combined IDOi and Delta-24-RGDOX. We sacrificed the mice on day 24. The brain tumor bearing mouse brains were collected and processed into single cells and enriched for immune cells using a percoll gradient. Immune cells were stained for CD3, then analyzed using flow cytometry. Panel (A) shows column graphs of absolute count of cells/hemisphere for the $CD3^+$ T cell population. Panel (B) shows representative images of brain tumor sections of the differently treated mice stained for CD3 by immunohistochemistry. Images were acquired using the Aperio ImageScope-Pathology Slide Viewing Software.

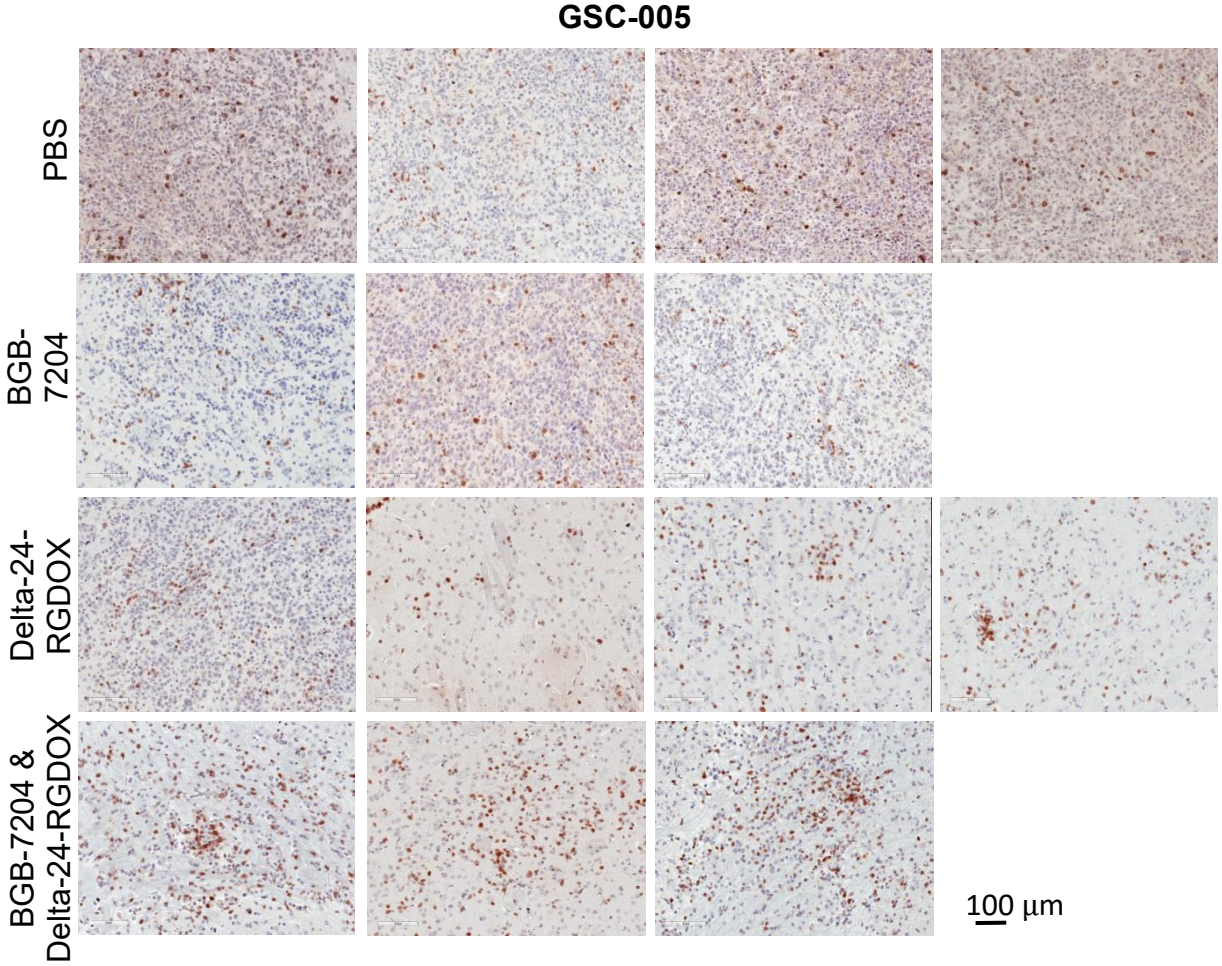

Figure 25: **BGB-7204 enhances CD3$^+$ T cell infiltration of Delta-24-RGDOX infected GSC-005 brain tumors.**

Representative images of CD3 immunohistochemistry of individual mice in the different treatment groups of GSC-005 brain tumor bearing mice. Mice were bolted on day -7, implanted with the $5x10^4$ GSC-005 cells on day 0, injected with Delta-24-RGDOX ($2.5x10^7$ pfu/mouse in 5µL) or PBS on days 9 and 11, and/or treated with 100 mg/kg per mouse of BGB-7204 on days 7-24. Mice were sacrificed on day 24, and brains were collected and fixed in 10% buffered formalin and transferred to 70% ethanol after 24 hours. Brain tumor coronal sections were embedded in paraffin and sectioned in 5µm slices onto positively charged glass microscope slides using a microtome. Slides were stained for anti-CD3 using immunohistochemistry. Slides were scanned and images were acquired using the Aperio ImageScope-Pathology Slide Viewing Software.

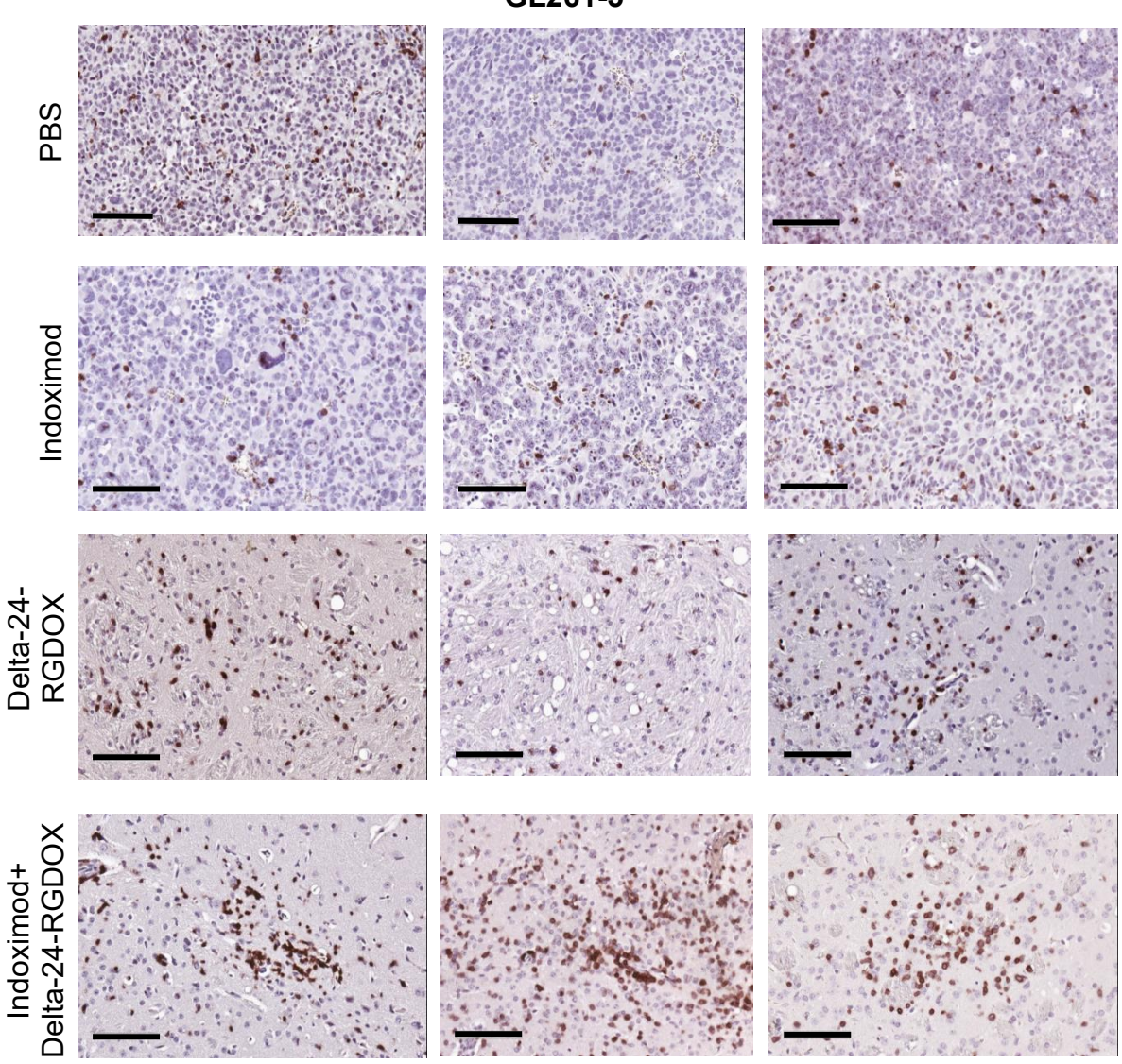

All scale bars set to 100 μm.

Figure 26: **Indoximod enhances CD3$^+$ T cell infiltration of Delta-24-RGDOX infected GL261-5 brain tumors.**

Representative images of CD3 immunohistochemistry of individual mice in the different treatment groups of GL261-5 brain tumor bearing mice. Mice were bolted on day -7, implanted with the $5x10^4$ GL261-5 cells on day 0, injected with Delta-24-RGDOX ($5x10^7$ pfu/mouse in 5μL) or PBS on days 7, 9, and 11, and/or treated with 275 mg/kg per mouse of Indoximod on days 7-24. Mice were sacrificed on day 24, and brains were collected and fixed in 10% buffered formalin and transferred to 70% ethanol after 24 hours. Brain tumor coronal sections were embedded in paraffin and sectioned in 5μm slices onto positively charged glass microscope slides using a microtome. Slides were stained for anti-CD3 using immunohistochemistry. Slides were scanned and images were acquired using the Aperio ImageScope-Pathology Slide Viewing Software.

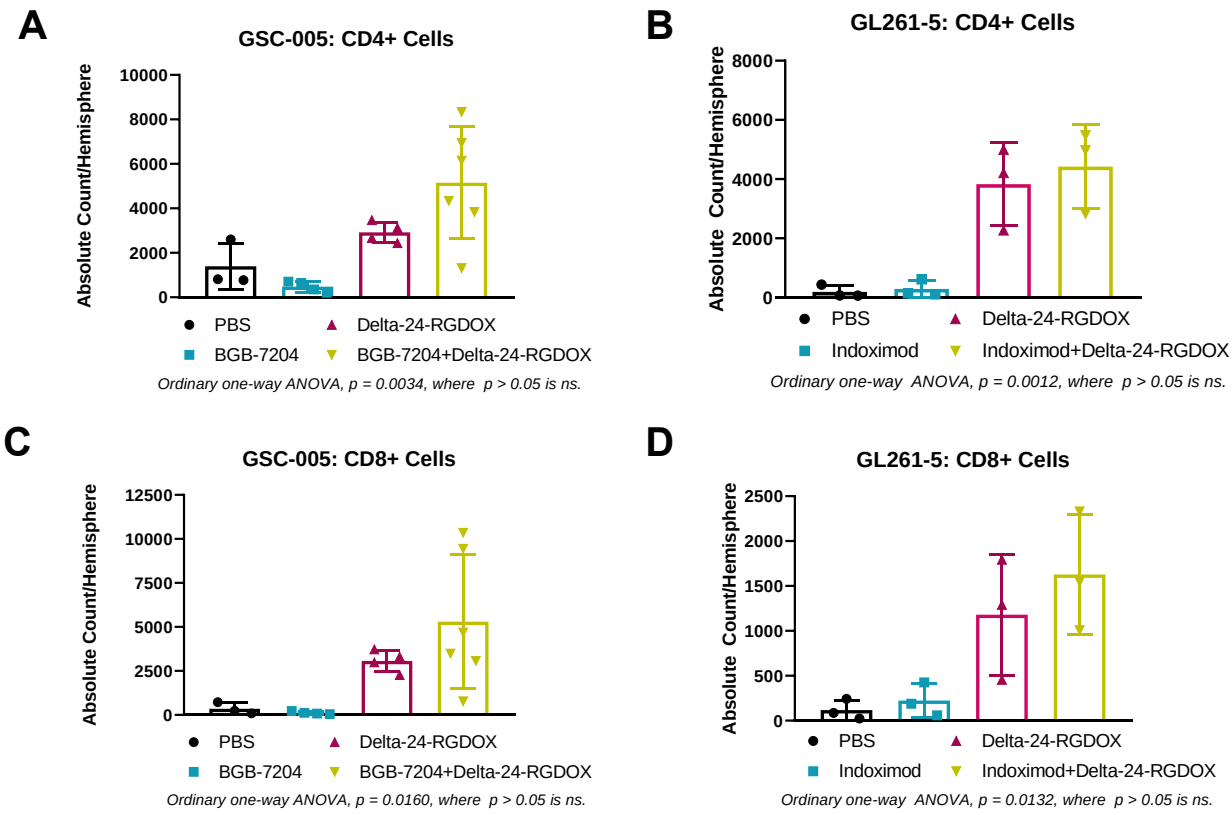

Figure 27: **IDO inhibitors increase the frequency of intratumoral $CD4^+$ and $CD8^+$ T cell populations generated by Delta-24-RGDOX infection in murine gliomas.**

Following the same treatment scheme as in ***Figure 24***, the mouse brain tumors were collected and processed into single cells and enriched for immune cells using a percoll gradient. Immune cells were stained for CD45, CD3, CD4, and CD8, then analyzed using flow cytometry. Column graphs show absolute count of cells per hemisphere for the (A/B) $CD4^+$ and (C/D) $CD8^+$ populations within the brain tumor microenvironment of the differently treated mice of the (A/C) GSC-005 or (B/D) GL261-5 murine glioma model.

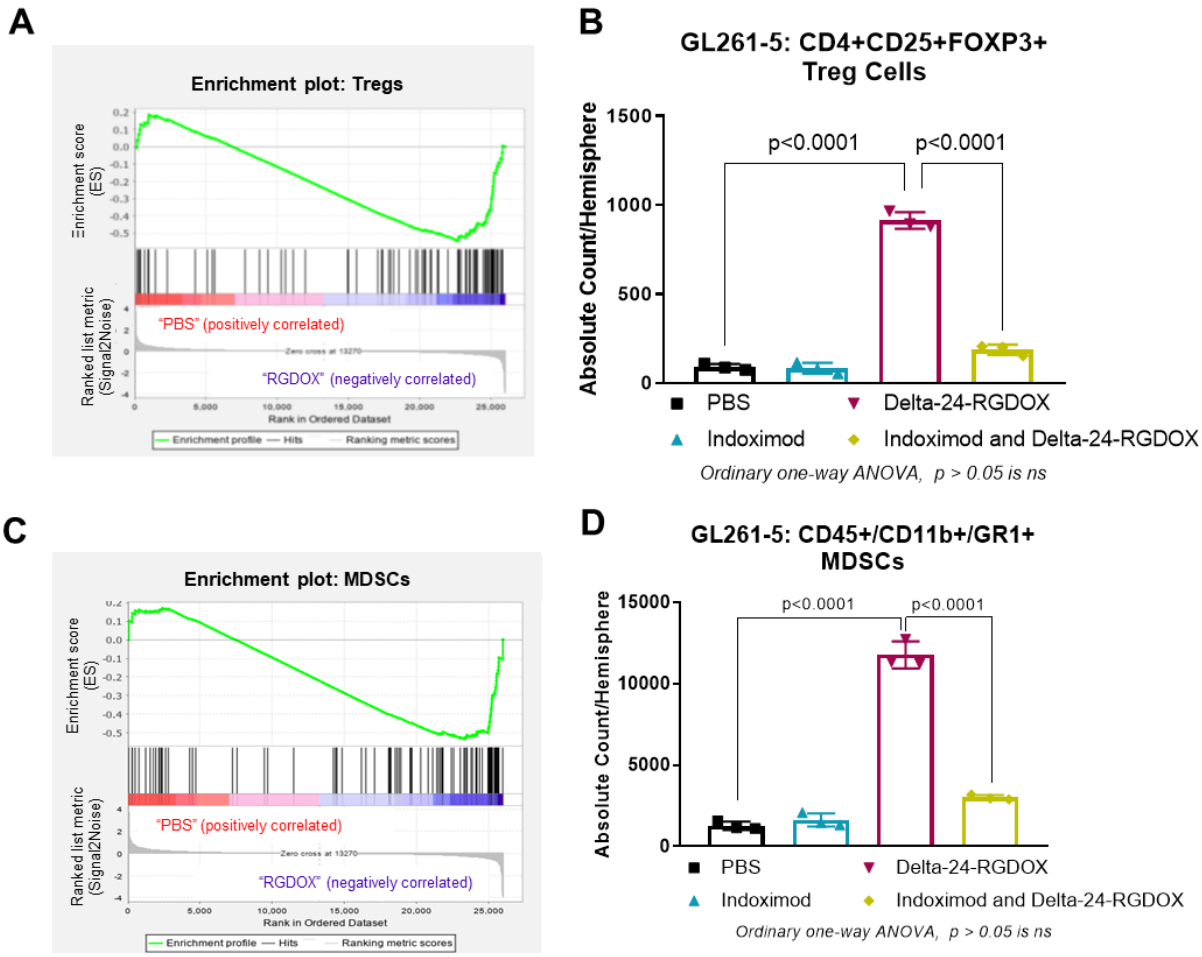

Figure 28: **Delta-24-RGDOX induces regulatory T cells and myeloid derived suppressor cells within the glioma microenvironment, which can be suppressed with the addition of an IDO inhibitor.**

Mice were bolted on day -7, implanted with the $5x10^4$ GL261-5 cells on day 0, injected with Delta-24-RGDOX ($5x10^7$ pfu/mouse in 5µL) or PBS on days 7, 9, and 11, and/or treated with 275 mg/kg per mouse of Indoximod on days 7-24. On day 12, RNA from the brain tumors were submitted to gene sequencing enrichment analysis to determine enrichment of the (A) Treg or (C) MDSC gene sets in PBS or Delta-24-RGDOX treated brain tumors. Mice were sacrificed on day 24, and brains were processed into single cells and enriched for immune cells using a percoll gradient. Immune cells were stained for CD45, CD3, CD4, CD8, CD25, FOXP3, CD11b, and GR1, then analyzed by flow cytometry. Column graphs show absolute count of cells per hemisphere of tumor tolerant populations, B) regulatory T cells or D) myeloid derived suppressor cells.

Conclusions

We developed the next generation of Delta-24-RGD by adding the OX40L to the backbone of the virus to enhance the immune responses via co-stimulation of the OX40 receptor of activated T cells. Our previously published studies show that treatment of murine glioma with Delta-24-RGDOX increases both immune-activating and immune-suppressing properties within the tumor microenvironment, including more infiltration of $CD8^+$ T cells or higher expression of PD-L1 on glioma cells compared to PBS or Delta-24-RGD treatment (91). In the current study, we also showed that Delta-24-RGDOX can contribute to immunosuppressive properties, as indicated by elicitation of IDO or AhR expression and activation (***Chapter 4***). The enhanced survival of glioma bearing mice treated with combined Delta-24-RGDOX and IDO inhibitor treatment compared to Delta-24-RGDOX alone, as discussed in ***Chapter 7***, also suggests a level of immunosuppression generated by Delta-24-RGDOX that allows immune evasion of antitumor responses.

To determine how the combination treatment of Delta-24-RGDOX and IDO inhibitors remodels the immune landscape of the glioma microenvironment, we studied the infiltration of different immune populations, including $CD4^+$ T cells, $CD8^+$ T cells, Tregs, and MDSCs, in brain tumors of mice treated with PBS, IDO inhibitor alone, Delta-24-RGDOX alone, or combined Delta-24-RGDOX and IDO inhibitor. Based on these studies, we can make the following conclusions:

1) The infiltration of $CD3^+$, $CD4^+$, and $CD8^+$ T cells by Delta-24-RGDOX can be enhanced with IDO inhibitors in two immunocompetent murine glioma models, GSC-005 and GL261-5. Furthermore, we were able to show this phenomenon using both Trp-mimetics (Indoximod) and direct IDO enzyme inhibitors (BGB-7204).

2) The use of IDO inhibitors alone provides minimal immunological responses, which corresponds to its similar survival pattern of PBS-treated mice.
3) In all cell populations studied, including that of $CD3^+$ T cells, $CD4^+$ T cells, $CD8^+$ T cells, Treg, or MDSCs, there was minimal and similar absolute count/hemisphere in the PBS- and IDO inhibitor-treated mice.
4) Delta-24-RGDOX treatment increased the absolute count per hemisphere of $CD3^+$ T cells, $CD4^+$ T cells, $CD8^+$ T cells, Treg, or MDSCs, indicating the transformation of these non-immunogenic murine brain tumors into more immunogenic tumors.
5) The combined Delta-24-RGDOX and IDO inhibitor treatment decreased the absolute count/hemisphere of the immunosuppressive Treg and MDSC populations in comparison to Delt-24-RGDOX single treatment.

Overall, our studies indicates that Delta-24-RGDOX enhances infiltration of both immune-activating and immune-suppressive populations; in comparison, the addition of IDO inhibition to Delta-24-RGDOX increases the immune activating populations and decreases the immune suppressive populations. This reshaping of the tumor microenvironment should favor the identification and destruction of the infected tumor by the immune system of the host.

Chapter 10: The combination of IDO inhibitors and Delta-24-RGDOX increases T-cell activation against tumor and viral antigen, which is negatively regulated by kynurenine.

Rationale and Expectations

Our pre-clinical studies have shown that in comparison to Delta-24-RGD, Delta-24-RGDOX enhances the survival of glioma mice, which was accompanied by an increase in functional T cell responses by both brain infiltrating lymphocytes and splenocytes (91). Still, as discussed in this dissertation, Delta-24-RGDOX can also produce immunosuppression, as supported by 1) the elicitation of IDO activation in both the GL261-5 and GSC-005 murine glioma models and 2) the increased infiltration of immunosuppressive immune populations, Tregs and MDSCs.

The activation of the IDO-Kyn-AhR pathway (***Figure 29A***) results in apoptosis and anergy of T effector cells and activation of Tregs (27, 29). The amalgamation of these observations and our results obtained from our current studies led us to our hypothesis that combined Delta-24-RGDOX and IDO inhibitor treatment would increase T cell functions against viral and tumor antigens compared to the single agent treatments. Thus, to confirm our hypothesis we conducted *ex vivo/in vivo* co-culture experiments, where target parental cancer cells (mock infected or Delta-24-RGDOX infected) were cultured with splenocytes from the differently treated glioblastoma-bearing treated mice. Using the supernatants from these co-cultures, we performed ELISAs to detect levels of different T-cell activation cytokines, including IFNγ and IL-2. To determine T-cell function in the context of IDO activation, we also tested the secretion of IFNγ and IL-2 of these co-cultures in the presence of Kyn. Additionally, we used cells that overexpress IDO in some cases to determine the effect of constitutive IDO overexpression on T-cell function.

Based on our previous studies and supporting data, we expected the following:

1) Compared to splenocytes from PBS treated glioma bearing mice, splenocytes from Delta-24-RGDOX treated mice will yield higher levels of IFNγ and IL-2 when co-cultured with mock or virally infected target cells.
2) The levels of IFNγ and IL-2 will be even higher in co-cultures of splenocytes from mice treated with combined Delta-24-RGDOX and IDO inhibitor treatment.
3) The levels of IFNγ and IL-2 will decrease in cultures that contained Kyn or targets that constitutively overexpress IDO.

Results

Combined IDO inhibition and Delta-24-RGDOX increases T-cell activation against tumor and viral antigen.

To study the functional modifications of T cells in response to treatment, the activity of the systemic lymphocyte population was assessed by detecting the secretion of the Th1 cytokines, IFNγ and IL-2, by splenocytes from GL261-5-bearing mice treated with PBS, Delta-24-RGDOX, Indoximod, or combined Delta-24-RGDOX and Indoximod stimulated with tumor and/or viral antigens. Specifically, as outlined in ***Figure 29B***, C57BL/6 mice were implanted with 5×10^4 GL261-5 cells and underwent indicated treatment at specified times; mice were then sacrificed on day 24 to permit analysis of T-cell function. The splenocytes from these differently treated mice were cultured in the presence of different groups of target cells including mock infected GL261-5 cells or Delta-24-RGDOX-infected GL261-5 cells. It was noteworthy that among splenocytes cultured with mock-infected GL261-5 cells, secretion of IFNγ and IL-2 was enhanced in splenocytes derived from mice previously infected with Delta-24-RGDOX compared to mice previously treated with PBS or Indoximod alone ($p < 0.05$, both groups), as seen in ***Figure 29C***. Activation, via IFNγ and IL-2 secretion, is further enhanced against the tumor antigens (Mock GL261-5 Target Cells) in splenocytes from mice previously treated with the combination of Delta-24-RGDOX and Indoximod compared to Delta-24-RGDOX alone (***Figure 29C***, IFNγ, $p = 0.0157$; IL-2 $p = 0.0333$). Similarly, the highest amount of secretion of IFNγ and IL-2 against the Delta-24-RGDOX infected target cells comes from the splenocytes from mice were treated with combined Delta-24-RGDOX and Indoximod (***Figure 29D***). These results suggested that splenocytes not only are activated against viral antigens but also recognize tumor antigens.

We performed a similar experiment as described above to study the T-cell function at 15 days in the same GL261-5 model to study this effect over time. In splenocytes cultured with mock-infected GL261-5 target cells, the trends in IFNγ secretion on day 15 were similar to those on day 24 (***Figure 30B***), where we saw highest amount of IFNγ secretion in splenocytes that came from combination-treated mice when cultured with mock infected GL261-5 cells. Interestingly, as seen in ***Figure 30C***, when the splenocytes were cultured with Delta-24-RGDOX infected GL261-5 cells, levels of IFNγ secretion were higher on day 15 than on day 24 by nearly 10-fold in the splenocytes from Delta-24-RGDOX-treated or combination-treated mice. Moreover, on day 15, the levels of IFNγ secretion were similar in splenocytes from Delta-24-RGDOX-treated and combination-treated mice; notably, the secretion values in these splenocytes were about 50 times as high as the values in splenocytes from control and Indoximod-treated mice. This could indicate an early robust anti-viral immune effect and perhaps the conversion to a relatively less immune-activating environment generated by clearance of the virus and complete tumor eradication by day 24. Overall, these functional studies showed that lymphocytes from the combination treated mice recognized not only viral antigens but also tumoral antigens, suggesting the triggering of anti-tumoral immunity.

We next performed experiments using the GSC-005 C57BL/6 murine glioma model. As outlined in ***Figure 31B***, C57BL/6 mice were implanted with 5×10^4 GSC-005 cells and underwent indicated treatment at specified times; mice were then sacrificed on day 24 to permit analysis of T-cell function. As seen in ***Figure 31***, on day 24, splenocytes from the combination-treated mice secreted highest levels of IFNγ compared to splenocytes from all other groups when stimulated GSC-005 cells that were treated with a mock infection (***Figure 31C***, $p = 0.0003$) or treated with BGB-7204 and infected with Delta-24-RGDOX (***Figure 31E***, $p = 0.0003$). These data complement the data seen with the GL261-5 model and suggests the enhanced T-cell function in

splenocytes of mice that were treated with combined IDO inhibitor and Delta-24-RGDOX treatment compared to either treatment alone.

Kyn or constitutive IDO expression negatively regulates T-cell activation against tumor and viral antigen.

Because kynurenine has been reported to be involved with immunosuppression, we then wanted to dissect the role of kynurenine on T-cell activation using this same assay. To test this theory, we performed similar functional co-culture assays with kynurenine added to the cultures. Specifically, in a separate animal experiment, C57BL/6 mice were bolted on day -7, implanted with $5x10^4$ GSC-005 cells on day 0, and split into two groups that included PBS or Delta-24-RGDOX ($1x10^8$ pfu/mouse on days 7, 10, and 13). On day 15, mice were sacrificed, and splenocytes were then stimulated with pre-fixed uninfected (Mock) (***Figure 32A/B left***) or Delta-24-RGD infected (***Figure 32A/B right***) GL261 (***Figure 32A***) or GL261-IDO-OE cells (***Figure 32B***); an additional group that also contained kynurenine within the media was added. As expected, as seen in ***Figure 32A***, the secretion of IL-2 was increased in splenocytes that came from Delta-24-RGD infected mice compared to PBS treated mice when cultured with either the mock infected or Delta-24-RGD infected GL261 cells (p=0.0039, p=0.0490, respectively), indicating the T cell activation against both tumor and viral antigen generated by Delta-24-RGD. Interestingly, when kynurenine was added to the cultures containing Delta-24-RGD treated splenocytes, the secretion of IL-2 was significantly reduced, suggesting the anti-tumor effect generated by kynurenine (mock GL261 target, p=0.0381; Delta-24-RGD infected GL261 target, p=0.0446). When these same experiments were done using the GL261-IDO-OE target cells, as seen in ***Figure 32B***, the secretion of IL-2 of splenocytes from Delta-24-RGD infected mice when

cultured with the mock GL261-IDO-OE or Delta-24-RGD infected GL261-IDO-OE was either unchanged or diminished, respectively, compared to splenocytes from PBS treated mice. Furthermore, the IL-2 secretion of co-cultures containing either mock infected GL261-IDO-OE or Delta-24-RGD infected GL261-IDO-OE target cells with Delta-24-RGD treated splenocytes were significantly decreased when kynurenine was added to the cultures (mock target, $p = 0.0355$, Delta-24-RGD target, $p = 0.0271$), reinforcing the claim that the anti-tumor immune effect can be generated by kynurenine. Of note, the magnitude of IL-2 levels is decreased in the co-cultures that involved GL261-IDO-OE compared to WT GL261 co-cultures, suggesting the negative regulation of T-cell activation by constitutive IDO overexpression. Overall, these experiments elucidate the complex relationship between IDO, Kyn, and viral infection on the immune response against tumor and viral antigens in these murine glioma models.

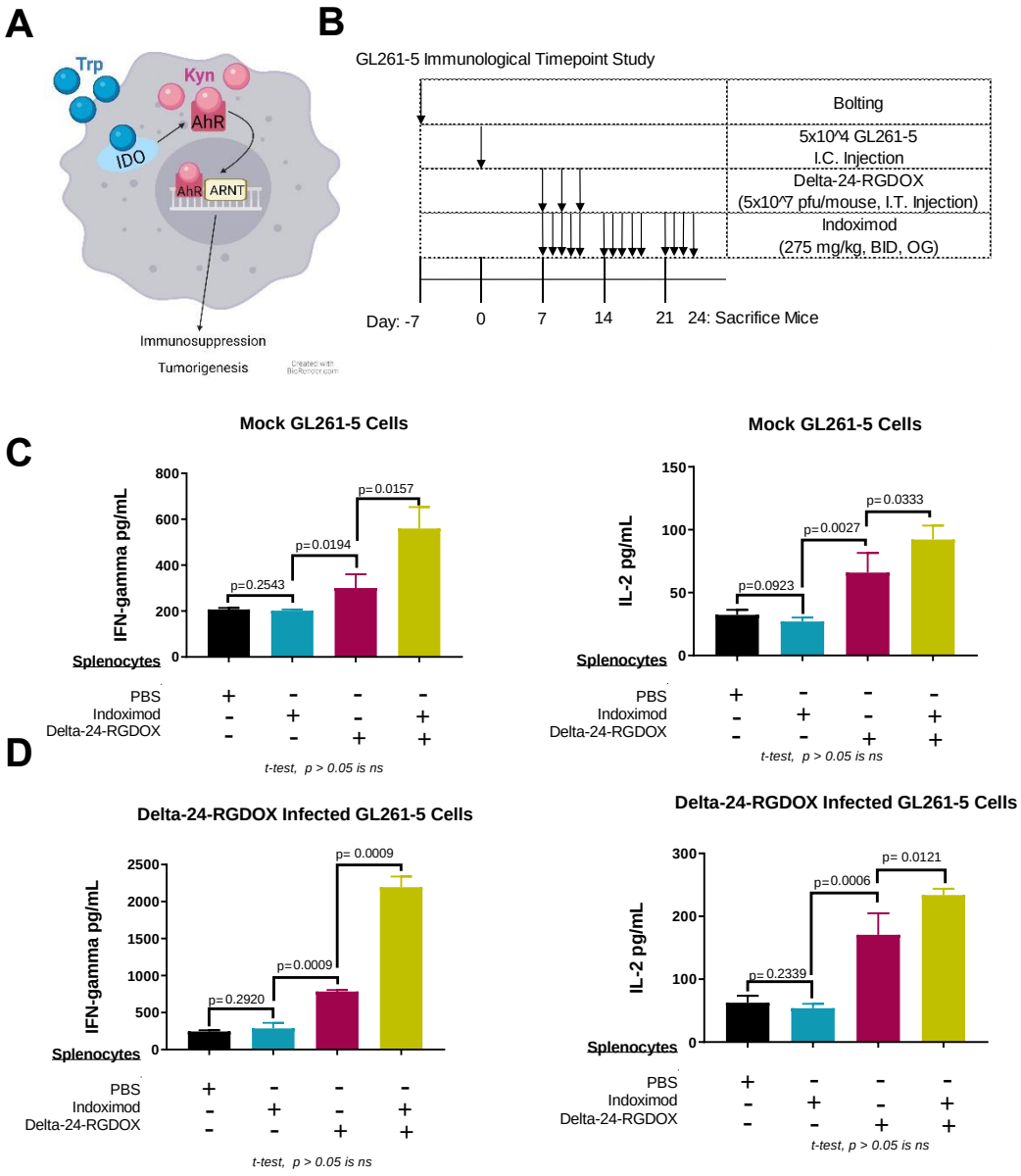

Figure 29: **Indoximod combined with Delta-24-RGDOX treatment increases T-cell activation against glioma and viral antigen.**

Panel (A) shows a schematic of the IDO-Kyn-AhR circuit. Panel (B) shows the schematic of experimental timeline, where mice were bolted on day -7, implanted with the $5x10^4$ GL261-5 cells on day 0, injected with Delta-24-RGDOX ($5x10^7$ pfu/mouse in 5µL) or PBS on days 7, 9, and 11, and/or treated with 275 mg/kg per mouse of Indoximod on days 7-24. Mice were sacrificed on day 24, and splenocytes were isolated from these GL261-5 bearing mice that were treated with PBS, Indoximod, Delta-24-RGDOX, or combined Indoximod and Delta-24-RGDOX and stimulated with prefixed GL261-5 cells that were (C) uninfected (mock infection) or (D) infected with Delta-24-RGDOX. Forty-eight hours later, the concentration of IFNγ (C/D left) or IL-2 (C/D right) in the co-culture supernatant was assessed by ELISA. Column graphs show mean pg/mL (n=3). I.C., intracranial. I.T., intratumoral. OG, oral gavage. BID, *bis in die*, twice daily.

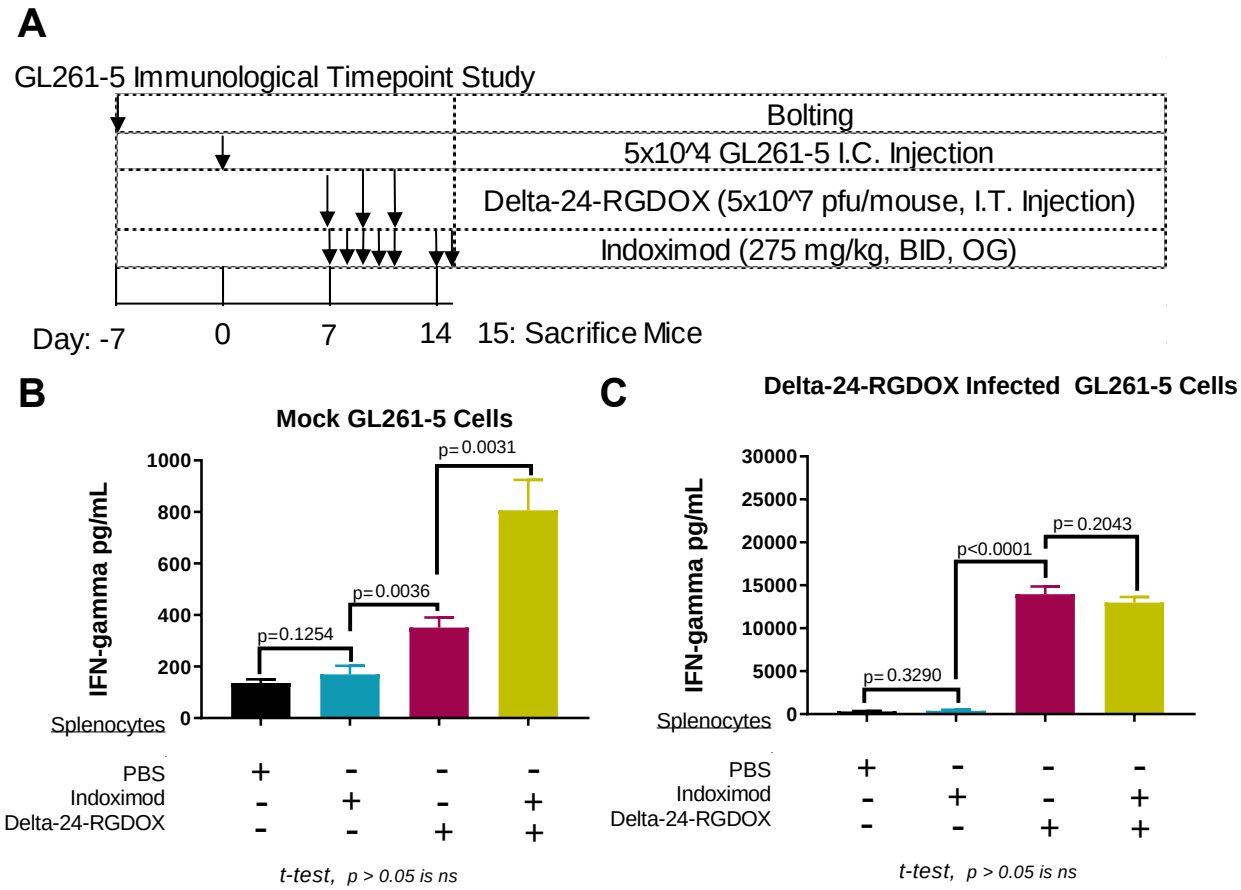

Figure 30: **Indoximod combined with Delta-24-RGDOX treatment increases T-cell activation against glioma antigen at an early timepoint.**

Mice were bolted on day -7, implanted with the $5x10^4$ GL261-5 cells on day 0, injected with Delta-24-RGDOX ($5x10^7$ pfu/mouse in 5µL) or PBS on days 7, 9, and 11, and/or treated with 275 mg/kg per mouse of Indoximod on days 7-24. Mice were sacrificed on day 15, and splenocytes were isolated from these GL261-5 bearing mice treated with PBS, Indoximod, Delta-24-RGDOX, or combined Indoximod and Delta-24-RGDOX and stimulated with prefixed GL261-5 cells that were (B) uninfected (mock infection) or (C) infected with Delta-24-RGDOX. Forty-eight hours later, the concentration of IFNγ in the co-culture supernatant was assessed by ELISA. Column graphs show mean pg/mL IFNγ (n=3). I.C., intracranial. I.T., intratumoral. OG, oral gavage. BID, *bis in die*, twice daily.

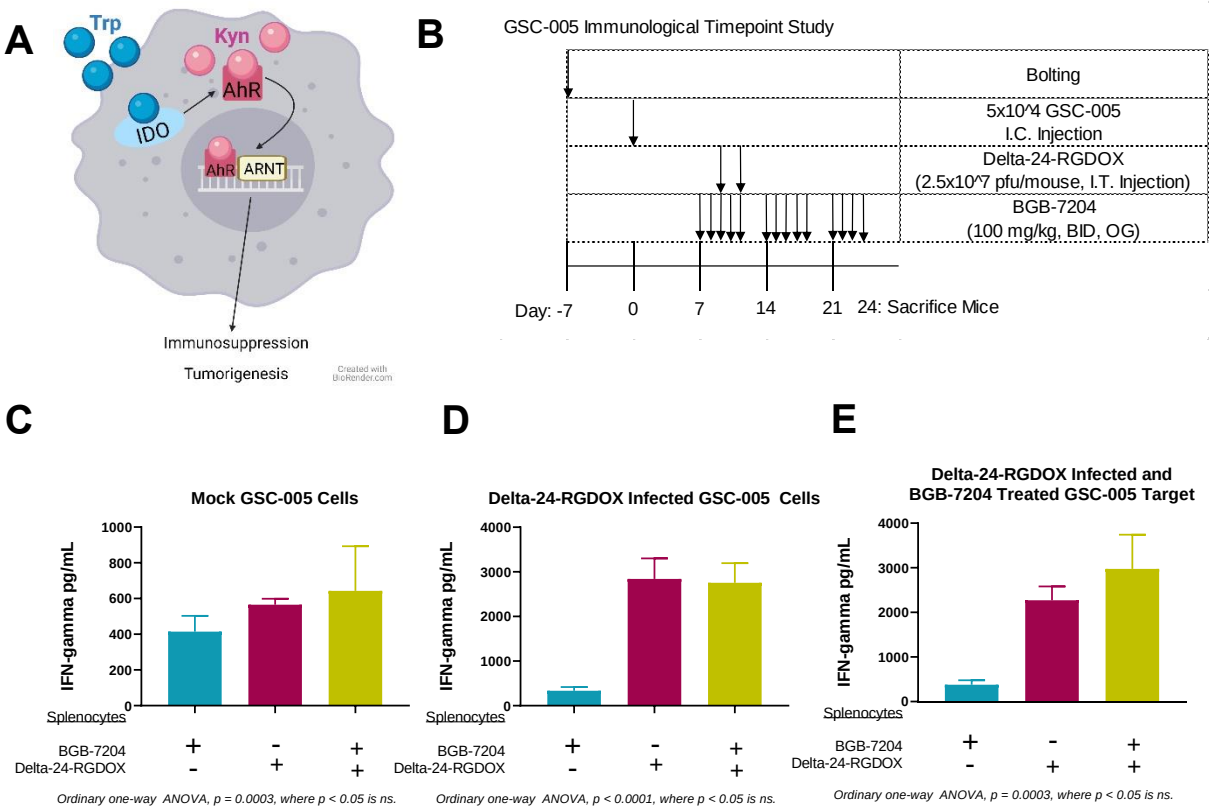

Figure 31: **BGB-7204 combined with Delta-24-RGDOX increases T-cell activation against glioma and viral antigen.**

Panel (A) shows a schematic of the IDO-Kyn-AhR circuit. Panel (B) shows the schematic of experimental timeline, where mice were bolted on day -7, followed by injection of $5x10^4$ GSC-005 cells on day 0. On day 7, mice were split up into three treatment groups including BGB-7204 alone, Delta-24-RGDOX alone, or combined BGB-7204 and Delta-24-RGDOX. Mice received Delta-24-RGDOX ($2.5x10^7$ pfu/mouse) on days 9 and 11. BGB-7204 treatment started on day 7 at a dose of 100 mg/kg twice daily and lasted until day 24, when we sacrificed the mice. Splenocytes from the differently treated mice were stimulated with pre-fixed GSC-005 cells that were (C) mock infected, (D) infected with Delta-24-RGDOX, or (E) treated with BGB-7204 and infected with Delta-24-RGDOX. Forty-eight hours later, the concentration of IFNγ in the co-culture supernatant was assessed by ELISA (R&D Systems). The column graphs show of mean pg/mL of IFNγ (n=3). I.C., intracranial. I.T., intratumoral. OG, oral gavage. BID, *bis in die*, twice daily.

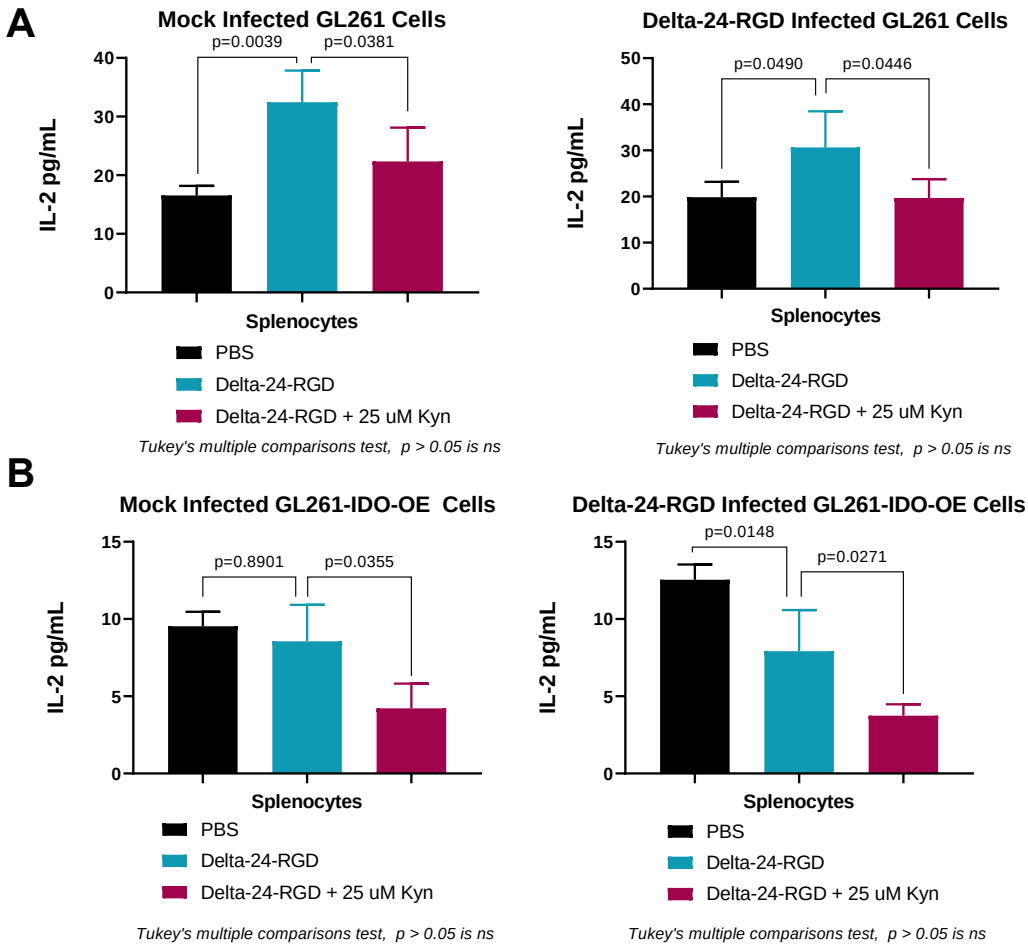

Figure 32: **Kyn or constitutive IDO expression negatively regulates T-cell activation against glioma and viral antigen.**

C57BL/6 mice were bolted on day -7, implanted with $5x10^4$ GSC-005 cells on day 0, and split into two groups that included PBS or Delta-24-RGDOX ($1x10^8$ pfu/mouse on days 7, 10, and 13). On day 15, mice were sacrificed, and splenocytes were then stimulated with pre-fixed (A and B left) uninfected (Mock) or (A and B right) Delta-24-RGDOX infected A) GL261 or B) GL261-IDO-OE cells; an additional group that also contained 25 µM kynurenine was added. Forty-eight hours later, the concentration of IL-2 in the co-culture supernatant was assessed by ELISA (R&D Systems). All column graphs show mean pg/mL of IL-2 (n=3).

Conclusions

The results of this dissertation thus far have strengthened our rationale to combine IDO inhibitors with Delta-24-RGDOX for the treatment of murine glioma. We have demonstrated that Delta-24-RGDOX induces IDO expression and activation and increases T cell infiltration within the glioma, which associated with a substantial survival effect in glioma bearing mice. The addition of an IDO inhibitor to Delta-24-RGDOX further enhances T cell infiltration, decreases immune tolerant populations, and provides even greater survival benefit in glioma bearing mice.

To further strengthen the rationale of our proposed therapy, we performed functional studies to determine how combined IDO inhibitor and Delta-24-RGDOX treatment in glioma bearing mice modulates T cell activation against both viral and glioma antigens. We further determined the effects of Kyn and constitutive IDO expression on the function of these T cells. Based off these studies, we can make the following conclusions:

1) Increased T cell function against tumor and viral antigens, via elevated IFNγ and IL-2 levels, from splenocytes of Delta-24-RGDOX treated glioma bearing mice was reproducible (91).
2) T cell function against both viral and tumor antigens was enhanced in splenocytes from mice treated with combined Delta-24-RGDOX and IDO inhibitor treatment.
3) The presence of Kyn and/or constitutive IDO expression diminished the oncolytic virus-induced T-cell function recognize viral and glioma antigen.

Overall, these functional studies combined with results describes in this dissertation strongly validate the central hypothesis of this study, which stated that therapy of Delta-24-RGDOX combined with an IDO inhibitor will stimulate a cytotoxic immune response and inhibit the suppressive immune response against the tumor cells providing a potential effective novel treatment for glioblastoma.

Chapter 11: List of Conclusions

1. Delta-24-RGDOX reshapes the murine brain tumor microenvironment.
2. Delta-24-RGDOX increases the predicted diversity and percentage of immune populations.
3. Delta-24-RGDOX increases both immune-activating and immune-suppressing pathways.
4. Delta-24-RGDOX induces expression of genes from the IDO pathway.
5. IFNγ induces IDO expression in human glioma, murine glioma, and other cancer cells.
6. Delta-24-RGDOX activates the AhR pathway in human cancer cells.
7. Delta-24-RGDOX induces Ahr expression and translocation into the nucleus in human cancer cells.
8. Delta-24-RGD or Delta-24-RGDOX induces IDO expression *in vitro* in murine glioblastoma models.
9. Delta-24-RGD or Delta-24-RGDOX induces IDO expression and activation *in vivo* of murine models of cancer.
10. Inhibition of IDO *in vitro,* does not alter viral infection, viral replication, or viral-induced cytopathic ability of Delta-24-RGDOX.
11. There is a greater therapeutic effect of Delta-24-RGDOX compared to PBS in IDO-KO mice bearing glioma.
12. Glioblastoma-bearing IDO-KO mice live longer than WT mice when treated with Delta-24-RGDOX.
13. Delta-24-RGDOX combined with Trp-Mimetic, 1MT or Indoximod, leads to a more robust decrease in tumor mass, provides a survival advantage, and induces anti-tumor

immunity compared to single agents in the treatment of murine brain tumors compared to Delta-24-RGDOX treatment alone.

14. Delta-24-RGDOX combined with direct IDO enzyme inhibitor, BGB-7204, results in greater reduction of tumor size compared to single agents in murine glioblastoma compared to Delta-24-RGDOX treatment alone.
15. The therapeutic efficacy of Delta-24-RGDOX or combined Delta-24-RGDOX and IDO inhibitor treatment in murine glioblastoma requires $CD4^+$ T cell activity.
16. Delta-24-RGDOX increases the immunogenicity of murine glioblastoma indicated by enhanced infiltration of both immune-activating and immune-suppressive populations.
17. The combination of Delta-24-RGDOX with IDO inhibitors increases the frequency of intratumoral T cells in murine glioblastoma compared to Delta-24-RGDOX treatment alone.
18. The combination of Delta-24-RGDOX with IDO inhibitors decreases the frequency of immune tolerant populations, including Tregs and MDSCs, within the murine glioblastoma microenvironment compared to Delta-24-RGDOX treatment alone.
19. The use of IDO inhibitors alone in the treatment of murine glioblastoma provides minimal immunological responses and is associated with poor survival.
20. Combined IDO inhibition and Delta-24-RGDOX increases T-cell activation against tumor and viral antigen in the setting of murine glioblastoma.
21. Kyn or constitutive IDO expression negatively regulates T-cell activation against tumor and viral antigen in the setting of murine glioblastoma.
22. ***The use of IDO inhibitors with armed oncolytic adenoviruses provides a potential and effective treatment for glioblastoma.***

Chapter 12: Discussion

Encouraging results from a phase III clinical trial led to the recent US Food and Drug Administration approval of the modified type 1 herpes simplex virus, Talimogene laherparepvec (T-VEC), for treatment of advanced melanoma (182) leading to a resurgence of interest in oncolytic viruses as a cancer therapy. There is particular interest of oncolytic adenoviruses in the treatment of glioma because of the convenience of administering the virus intratumorally during surgery. Currently, eight different families of viruses are being tested for the treatment of glioma. Overall, these studies have shown us that the treatment of oncolytic viruses results in minimal toxicity, increases immunogenicity, and can lead to long term survival in 6-25% of patients with recurrent glioma (90, 97-106, 108, 109, 122, 183). Of these studies, the predecessor of Delta-24-RGDOX, Delta-24-RGD, resulted in 20% of patients surviving past three years. Exploratory objectives of this study showed anti-tumor responses via the elicitation of an immune response, as indicated by infiltration of T-bet^{+} CD8^{+} T cells and the pseudoprogression of a tumor post treatment before complete regression; this could imply initial generation of inflammation by the virus before the subsequent anti-tumor immune response (90). These observations support the emerging paradigm that oncolytic viruses are a type of immunotherapy. These clinical studies also reveal that single agent therapy of oncolytic viruses will most likely not result in maximal therapeutic benefits. Hence, we decided to combine Dellta-24-RGDOX with IDO inhibitors for the treatment of glioblastoma based on observations that 1) IDO is commonly upregulated after viral infection (58, 66, 166, 170, 184, 185) and 2) IDO causes immunosuppression conducive to tumor growth (28, 32, 186-188).

Our previous studies show that Delta-24-RGDOX elicits a more potent anti-tumor immune and immune memory response compared to Delta-24-RGD, leading to more survival of glioma bearing mice (91). The enhanced immune effect, as evidenced by increased infiltration,

activation, and memory of lymphocytes within the tumor microenvironment is provided by activation of the OX40 pathway of the effector T cell via Delta-24-RGDOX induced OX40L expression on cancer cells (91). These data supported the start of a phase I clinical trial testing Delta-24-RGDOX on patients with recurrent glioblastoma in Spain (NCT03714334). Despite these directed anti-tumor immune responses by Delta-24-RGDOX, maximal therapeutic benefits were never achieved, signifying the presence of a sustained negative regulation of immune activation against the tumor. Interestingly, the RNA sequencing results revealed that in the GL261-5 murine glioblastoma model, Delta-24-RGDOX reshaped the tumor microenvironment producing the upregulation of genes involved in both immune activating and immune suppressive pathways. Of significance, Delta-24-RGDOX treated brain tumors showed enrichment of the IDO pathway and its related cell targets, Tregs and MDSCs. Furthermore, the RNA sequencing analyses revealed elicitation of common immune checkpoint proteins including CTLA-4 and PD-1. This result validated our previous studies showed that the combination of Delta-24-RGDOX and anti-PD-L1 provided a greater survival benefit compared to Delta-24-RGDOX alone in the GL261-5 murine glioblastoma model (91). Collectively, these data support the ongoing clinical trial testing the treatment of patients of recurrent glioblastoma with Delta-24-RGD and pembrolizumab (anti-PD-1) (NCT02798406). The RNA sequencing analyses also validated our quantitative PCR studies that showed this phenomenon of negative immune regulation elicited by Delta-24-RGDOX infection, where IDO expression increased in the GL261-5 murine glioblastoma model and the unrelated 4T1.2 murine breast cancer model in response to the viral infection.

Activation of IDO by Delta-24-RGDOX was also evident in the GL261-5 and GSC-005 murine glioblastoma models. Furthermore, even when we remove the immune component, Delta-24-RGDOX can still increase the expression of IDO and AhR in cancer cells *in vitro,* indicating

an IFNγ-independent mechanism of IDO induction by Delta-24-RGDOX; correspondingly, we observed the activation and translocation of AhR from the cytoplasm to the nucleus in these virally infected tumor cells. Importantly, IDO and AhR overexpression is implicated in brain malignancies (23, 189). These data provided the rationale supporting the combination of Delta-24-RGDOX and IDO inhibitors for the treatment of murine glioma.

Thus, to increase the anti-tumor immune effect of Delta-24-RGDOX, we tested the addition of IDO inhibitors in two immunocompetent murine glioma models, GL261-5 and GSC-005. We demonstrated the survival advantage or complete tumor eradication by the combination treatment of IDO inhibitor and Delta-24-RGDOX over single-agent treatments in both models. We reproduced these results in the highly aggressive B16 murine melanoma intracranial tumor model. These data are consistent with our additional survival data in the GSC-005 model, where we observed long term survival of IDO-KO mice compared to WT mice following intratumoral administration of Delta-24-RGDOX; importantly, this result exhibits the on-target effect of IDO inhibition and its enhanced therapeutic effect when combined with Delta-24-RGDOX. However, we must note here that the survival curve of the combination of IDO inhibitor and Delta-24-RGDOX we observed in the GL261-5 model was not similar to the survival curve of the GL261-5 bearing IDO-KO mice treated with Delta-24-RGDOX. Here, there are a couple considerations to make: first, the viral dose in the IDO-KO experiment was lower, and second, we used Indoximod to test the therapeutic efficacy of its combination with Detla-24-RGDOX. Indoximod is not considered a direct enzyme inhibitor; instead, it provides a Trp sufficiency signal to reverse stress kinase signals that can inhibit mTORC signaling in surrounding T effector cells (27). Further studies testing direct IDO inhibitors in the GL261-5 model will be required to determine the therapeutic efficacy of direct IDO inhibitors in the context of direct IDO enzyme inhibitors. Notably, we still see viral-induced cytopathic ability of Delta-24-RGDOX in cases of IDO

inhibition, such as with the IDO inhibition *in vitro* by BGB-7204 or in the extreme case of IDO inhibition in GSC-005 or GL261-5 bearing IDO-KO mice. Overall, these results indicate that combined IDO inhibition and oncolytic adenoviral treatment presents no unwanted drug interactions and highlight the potential therapeutic effects that can be seen in patients if treated with this drug combination.

Our studies displayed that Delta-24-RGDOX transformed the murine glioblastoma from a non-immunogenic to an immunogenic tumor, as indicated by an influx of $CD3^+$ T cells and other immune cells evident by our histopathological analysis and flow cytometry assays. This conversion of immunogenicity by Delta-24-RGDOX increased the amounts of both activating and immunosuppressive immune populations, which provided a target for the Indoximod or BGB-7204 to work as intended. Furthermore, we showed that both Delta-24-RGD and Delta-24-RGDOX could induce IDO expression and activation in the tumor cells, most likely through an IFN-dependent mechanism, and thus increasing the likelihood of response to the IDO inhibitor. Related to our study, Ladomersky et al. recently reported a durable survival benefit in the GL261 immunocompetent murine glioma model with the triple combination of CNS-penetrating IDO1 enzyme inhibitor, BGB-5777 (39) or BGB-7204 (57), anti-PD1 mAb, and radiotherapy; in that study, the radiotherapy generated an immunogenic tumor, allowing the targets of the IDO enzyme inhibitor and the anti-PD1 mAb to be exposed. These and our results are consistent with the concept described by Sharma and Allison (41) that if a non-immunogenic tumor becomes immunogenic, it should become more responsive to immunotherapy.

To our knowledge, our study is the first to report the efficacy of combining IDO inhibitors and an armed oncolytic adenovirus in a murine glioblastoma model. In agreement with our study, Berrong et al. recently reported an enhanced survival effect with addition of Trp-mimetic, Indoximod, to the combination of an anti-OX40 agonist and a vaccine against HPV16 E7 in an

HPV16-E6-E7/HRAS–driven lung epithelial cancer model (190). This result validates our studies, which shows that IDO inhibition enhances the anti-cancer effects of OX40 activation. This study also supports that this anti-cancer effect generated by the therapeutic strategy of combined IDO inhibition and OX40 pathway activation is not limited to the treatment of glioma. In contrast with the use of cancer vaccines, the use of oncolytic viruses does not require previous knowledge about the tumor antigen load since the oncolytic virus can infect and lyse all RB-deficient cells to release tumor-associated antigens into the tumor microenvironment. Consistent with the effects of their triple combination, we observed both a reduction in regulatory T cells and an increase in $CD8^+$ T cells in the tumors of mice treated with Delta-24-RGDOX and Indoximod/BGB-7204. Furthermore, Berrong et al. showed an increase in tumor-antigen-specific $CD8^+$ T cells, which is consistent with our co-culture experiments in which we found increased IFNγ and IL-2 responses against both viral and tumor antigens in splenocytes from brain tumor–bearing mice treated with combined Delta-24-RGDOX and Indoximod/ BGB-7204. This result also suggests the generation of a tumor-specific immune memory, as these splenocytes were presented with the same cancer antigens after being extracted from the mouse in an *ex vivo* setting. This finding, along with our discovery of 100% survival in re-challenged GL261-5-bearing mice previously treated with combined Delta-24-RGDOX and Indoximod, strongly indicates the presence of a tumor-specific immune memory generated by the combination treatment. These results emphasize the importance of the host immune system for the development of therapeutic efficacy and memory against tumor antigen. Similarly, the results from our $CD4^+$ T cell depletion survival experiment in the GL261-5 model revealed the requirement of the $CD4^+$ T cell population on the therapeutic efficacy of the combined Delta-24-RGDOX and IDO inhibitor treatment.

Our studies also demonstrate the antitumor immunosuppression generated via the IDO-Kyn circuitry in the context of oncolytic adenoviral infection. That is, the presence of Kyn was

able to decrease the T-cell activation against both tumor and viral antigen that was generated by the oncolytic virus. Consistently, T-cell activation generated by the oncolytic virus was reduced in the presence of targets that constitutively overexpress IDO compared to IDO-WT targets. This result led to the speculation that that the IDO-Kyn pathway aids in negative regulation of anti-tumor immunity during virotherapy, and it can be reversed with the use of IDO inhibitors.

The murine glioblastoma models utilized in this study do not express IDO. Thus, the effects of the IDO inhibitor are presumably due to changes of the host immune tumor microenvironment. The literature shows that IDO can be expressed by dendritic cells and macrophages (147), but we did not identify the source of IDO in our model; doing so, through the use of CyTOF or RNA sequencing of the brain tumors of differently treated mice, might elucidate how our virus can alter IDO expression in different immune cell populations to produce more immunosuppression within the tumor microenvironment. Still, our studies show that Delta-24-RGDOX or IFNγ can increase the expression of IDO *in vitro* in different murine and human glioma cells. Additionally, the infection of Delta-24-RGDOX in human cancer cells increased AhR activity and its translocation into the nucleus, suggesting that activation of IDO, whose catabolite, Kyn, is an agonist for AhR. AhR has been reported to cause immunosuppression in glioblastoma via activation of Tregs (32, 33), induction of either apoptosis or dysfunction of effector $CD8^+$ T-cells, or activation of immunosuppressive macrophages and other population of immune cells causing immunosuppression (46). This activation of IDO and AhR in the tumor microenvironment cooperate to suppress tumor-specific immune responses, promoting glioma immune evasion and tumor progression (32, 33). Importantly in our study, in addition to the Delta-24-RGDOX induced AhR expression and activity *in vitro*, the *in vivo* brain tumors from the virus-infected groups expressed and activated more IDO compared to control-treated mice, indicating that the tumor microenvironment of this model contained an active IDO that could be

involved in the subsequent activation of the Kyn-AhR cascade. Consistent with the negligible levels of IDO or Kyn in PBS treated brain tumors, Treg and MDSC populations were nearly undetectable in these samples of the GL261-5 model. Upon treatment with Delta-24-RGDOX, the brain tumors displayed increases in the Treg and MDSC populations. This result was validated by our RNA sequencing analyses that showed enrichment of the Treg and MDSC gene sets in Delta-24-RGDOX murine brain tumors. When IDO inhibitors were combined with Delta-24-RGDOX, the Treg and MDSC populations were diminished. These data are consistent with the new paradigm of viro-immunotherapy, which supports the theory of oncolytic viruses transforming immune-excluded tumors to more immunogenic one. Moreover, the subsequent decrease of the Treg and MDSC populations when an IDO inhibitor is added to Delta-24-RGDOX underline the ability of these inhibitors to decrease immunosuppressive populations.

In conclusion, we have shown for the first time that combined treatment with Delta-24-RGDOX and IDO inhibitors produces long-term survival in a murine glioblastoma model without any observable toxic effects. We further shown that this effect may be mediated by an increase in cytotoxic T-cell activity, a decrease in immunosuppressive immune populations, and subsequent generation of anti-glioma immune memory. This highly translatable study strongly suggests that the use of IDO inhibitors with armed oncolytic adenoviruses will be a promising treatment for patients with glioblastoma and other solid tumors.

Chapter 13: Future Directions

The studies of this dissertation have shown that the modified oncolytic adenovirus armed with OX40L, or Delta-24-RGDOX, can induce the expression and activation of the IDO pathway upon infection of murine glioblastoma, a result that validated observations made from RNA sequencing analyses. Further RNA sequencing analyses demonstrated that Delta-24-RGDOX elicited expression of both Th2 and Th1 responses, which could explain the modest survival of glioma bearing mice (191). We demonstrated that combined Delta-24-RGDOX and IDO inhibitor treatment increases survival and aids in complete tumor regression of glioma bearing mice. This antitumor effect was most likely due to enhanced anti-tumor and decreased immune suppressive responses, most likely through a skewed Th1 response provided by the IDO inhibitor when added to Delta-24-RGDOX (27, 39, 52, 190). This was evidenced by more infiltration of $CD3^+$, $CD4^+$, and $CD8^+$ T cells compared to the single treatment of Delta-24-RGDOX. Exploration of the systemic splenocytes revealed that the combined Delta-24-RGDOX and IDO inhibitor treatment led to enhanced T cell responses against tumor and viral antigens compared to Delta-24-RGDOX alone, and that Kyn was able to reverse these T cell responses. Furthermore, the treatment of these mice with Delta-24-RGDOX increased immune tolerant populations, Tregs and MDSCs, and were decreased in the tumor microenvironment when an IDO inhibitor was added. This current model is summarized in ***Figure 33.***

Although these studies provide a significant rationale to combine IDO inhibitors with armed oncolytic adenoviruses in the clinic, there is still much to be discovered regarding the basic interactions of OX40, IDO, and AhR. There are few reports studying pathways of this tumor necrosis superfamily and its direct effects on IDO and AhR signaling and vice versa (190, 192). Studied separately, the consensus of IDO and AhR signaling in glioblastoma, is that it aids in a tumor tolerant microenvironment (26, 189). Elucidation of the detailed biological underpinnings

of OX40, IDO, and AhR signalling within the glioma microenvironment would yield valuable insights into potential druggable targets that could be applied to the treatment of glioma. Furthermore, our studies focused only on the use of IDO inhibitors. Very few AhR antagonists are being studied pre-clinically and clinically (189, 193). We propose that additional studies using AhR inhibitors will clarify which arm of the IDO-Kyn-AhR cascade causes more immunosuppression within the tumor, which will provide a strong basis for the translation of IDO or AhR inhibitors in combination with armed oncolytic adenoviruses into the clinic. We also expect that new IDO and AhR inhibitors will arrive to the clinical arena soon and that their addition to virotherapy might result in the improvement of the prognosis of patients with brain tumors and other solid tumors.

Three clinical trials are determining the safety profile of combining Indoximod with chemotherapy and/or radiation in adult and pediatric patients with recurrent glioma (NCT02052648, NCT04049669, NCT02502708) are currently underway. Similarly, we propose to translate the combination of Delta-24-RGDOX and Indoximod into a phase I clinical trial to first determine the safety profile of the drug combination in patients with recurrent glioblastoma. We predict that this combined therapy of Indoximod and Delta-24-RGDOX will improve the survival of patients with recurrent glioblastoma.

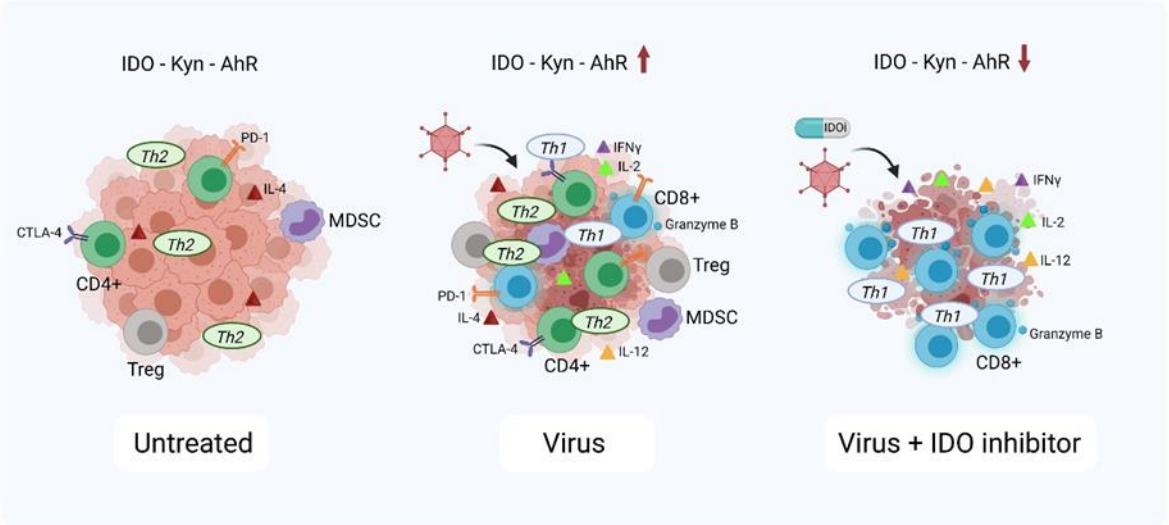

Figure 33: **The immunological effects of Delta-24-RGDOX combined with IDO inhibitors within the glioma microenvironment.**

The microenvironment of gliomas is characterized by a paucity of T cells skewed towards the Th2 phenotype. This Th2 phenotype promotes IL-4 function and recruitment of MDSCs, Tregs, or anergic PD-1^+ or CTLA-4^+ T cells. Infection of gliomas with oncolytic viruses, such as Delta-24-RGDOX, results in the induction of a Th1 phenotype with an increase of the production of IL-12 or IFNγ. However, the viral infection activates both the IFNγ-driven IDO-Kyn-AhR cascade and the maintenance of immune suppression via activation of MDSCs and Tregs. The addition of IDO inhibitors to virotherapy results in an imbalance of the signaling with a predominance of Th1 and $CD8^+$ cytotoxic T cells leading to the eradication of the tumor. Figure created with BioRender.com.

Acknowledgements of Scientific Support

We would like to acknowledge members of the Brain Tumor Center Animal Core of the University of Texas MD Anderson Cancer Center for their participation in the animal experiments discussed in this work, including Verlene Henry, Caroline Carillo, and Tiara Collier. We would also like to give special thanks to Joy Gumin for assisting in animal studies. We also Sanjay K. Singh, PhD, for his contribution in the RNA sequencing analyses. We thank Rahul Deshpande, PhD and William Russel, PhD of the Mass Spectrometry Proteomics Center at The University of Texas Medical Branch. We thank Xin Ru "Cheryl" Jiang for her help in preparing ***Figure 1***. This work was supported by the National Cancer Institute of the National Institutes of Health Ruth L. Kirschstein National Research Service Award (NRSA) Individual Predoctoral Fellowship (Parent F31; 5F31CA228207-03) and the American Legion Auxiliary Fellowship in Cancer Research.

References Cited

1. Louis DN, Perry A, Reifenberger G, von Deimling A, Figarella-Branger D, Cavenee WK, Ohgaki H, Wiestler OD, Kleihues P, Ellison DW. 2016. The 2016 World Health Organization Classification of Tumors of the Central Nervous System: a summary. *Acta Neuropathol* 131: 803-20
2. Ostrom QT, Gittleman H, Truitt G, Boscia A, Kruchko C, Barnholtz-Sloan JS. 2018. CBTRUS Statistical Report: Primary Brain and Other Central Nervous System Tumors Diagnosed in the United States in 2011-2015. *Neuro Oncol* 20: iv1-iv86
3. Fernandes C, Costa A, Osorio L, Lago RC, Linhares P, Carvalho B, Caeiro C. 2017. Current Standards of Care in Glioblastoma Therapy. In *Glioblastoma*, ed. S De Vleeschouwer. Brisbane (AU)
4. Roy S, Lahiri D, Maji T, Biswas J. 2015. Recurrent Glioblastoma: Where we stand. *South Asian J Cancer* 4: 163-73
5. Taal W, Oosterkamp HM, Walenkamp AM, Dubbink HJ, Beerepoot LV, Hanse MC, Buter J, Honkoop AH, Boerman D, de Vos FY, Dinjens WN, Enting RH, Taphoorn MJ, van den Berkmortel FW, Jansen RL, Brandsma D, Bromberg JE, van Heuvel I, Vernhout RM, van der Holt B, van den Bent MJ. 2014. Single-agent bevacizumab or lomustine versus a combination of bevacizumab plus lomustine in patients with recurrent glioblastoma (BELOB trial): a randomised controlled phase 2 trial. *Lancet Oncol* 15: 943-53
6. Brem H, Piantadosi S, Burger PC, Walker M, Selker R, Vick NA, Black K, Sisti M, Brem S, Mohr G, et al. 1995. Placebo-controlled trial of safety and efficacy of intraoperative

controlled delivery by biodegradable polymers of chemotherapy for recurrent gliomas. The Polymer-brain Tumor Treatment Group. *Lancet* 345: 1008-12

7. Stupp R, Taillibert S, Kanner A, Read W, Steinberg D, Lhermitte B, Toms S, Idbaih A, Ahluwalia MS, Fink K, Di Meco F, Lieberman F, Zhu JJ, Stragliotto G, Tran D, Brem S, Hottinger A, Kirson ED, Lavy-Shahaf G, Weinberg U, Kim CY, Paek SH, Nicholas G, Bruna J, Hirte H, Weller M, Palti Y, Hegi ME, Ram Z. 2017. Effect of Tumor-Treating Fields Plus Maintenance Temozolomide vs Maintenance Temozolomide Alone on Survival in Patients With Glioblastoma: A Randomized Clinical Trial. *JAMA* 318: 2306-16

8. Wing K, Sakaguchi S. 2010. Regulatory T cells exert checks and balances on self tolerance and autoimmunity. *Nat Immunol* 11: 7-13

9. Alterman RL, Stanley ER. 1994. Colony stimulating factor-1 expression in human glioma. *Mol Chem Neuropathol* 21: 177-88

10. Pyonteck SM, Akkari L, Schuhmacher AJ, Bowman RL, Sevenich L, Quail DF, Olson OC, Quick ML, Huse JT, Teijeiro V, Setty M, Leslie CS, Oei Y, Pedraza A, Zhang J, Brennan CW, Sutton JC, Holland EC, Daniel D, Joyce JA. 2013. CSF-1R inhibition alters macrophage polarization and blocks glioma progression. *Nat Med* 19: 1264-72

11. Kohanbash G, McKaveney K, Sakaki M, Ueda R, Mintz AH, Amankulor N, Fujita M, Ohlfest JR, Okada H. 2013. GM-CSF promotes the immunosuppressive activity of glioma-infiltrating myeloid cells through interleukin-4 receptor-alpha. *Cancer Res* 73: 6413-23

12. Gabrilovich DI, Chen HL, Girgis KR, Cunningham HT, Meny GM, Nadaf S, Kavanaugh D, Carbone DP. 1996. Production of vascular endothelial growth factor by human tumors inhibits the functional maturation of dendritic cells. *Nat Med* 2: 1096-103

13. Roth P, Aulwurm S, Gekel I, Beier D, Sperry RG, Mittelbronn M, Meyermann R, Beaman KD, Weller M, Wischhusen J. 2006. Regeneration and tolerance factor: a novel mediator of glioblastoma-associated immunosuppression. *Cancer Res* 66: 3852-8

14. Seidel JA, Otsuka A, Kabashima K. 2018. Anti-PD-1 and Anti-CTLA-4 Therapies in Cancer: Mechanisms of Action, Efficacy, and Limitations. *Front Oncol* 8: 86

15. Thompson CB, Allison JP. 1997. The emerging role of CTLA-4 as an immune attenuator. *Immunity* 7: 445-50

16. Wintterle S, Schreiner B, Mitsdoerffer M, Schneider D, Chen L, Meyermann R, Weller M, Wiendl H. 2003. Expression of the B7-related molecule B7-H1 by glioma cells: a potential mechanism of immune paralysis. *Cancer Res* 63: 7462-7

17. Crane CA, Ahn BJ, Han SJ, Parsa AT. 2012. Soluble factors secreted by glioblastoma cell lines facilitate recruitment, survival, and expansion of regulatory T cells: implications for immunotherapy. *Neuro Oncol* 14: 584-95

18. Uyttenhove C, Pilotte L, Theate I, Stroobant V, Colau D, Parmentier N, Boon T, Van den Eynde BJ. 2003. Evidence for a tumoral immune resistance mechanism based on tryptophan degradation by indoleamine 2,3-dioxygenase. *Nat Med* 9: 1269-74

19. Abou-Ghazal M, Yang DS, Qiao W, Reina-Ortiz C, Wei J, Kong LY, Fuller GN, Hiraoka N, Priebe W, Sawaya R, Heimberger AB. 2008. The incidence, correlation with tumor-infiltrating inflammation, and prognosis of phosphorylated STAT3 expression in human gliomas. *Clin Cancer Res* 14: 8228-35

20. Wei Q, Huang XL, Lin JY, Fei YJ, Liu ZX, Zhang XA. 2011. Adeno associated viral vector-delivered and hypoxia response element-regulated CD151 expression in ischemic rat heart. *Acta Pharmacol Sin* 32: 201-8

21. Zagzag D, Lukyanov Y, Lan L, Ali MA, Esencay M, Mendez O, Yee H, Voura EB, Newcomb EW. 2006. Hypoxia-inducible factor 1 and VEGF upregulate CXCR4 in glioblastoma: implications for angiogenesis and glioma cell invasion. *Lab Invest* 86: 1221-32

22. Munn DH, Zhou M, Attwood JT, Bondarev I, Conway SJ, Marshall B, Brown C, Mellor AL. 1998. Prevention of allogeneic fetal rejection by tryptophan catabolism. *Science* 281: 1191-3

23. Wainwright DA, Balyasnikova IV, Chang AL, Ahmed AU, Moon KS, Auffinger B, Tobias AL, Han Y, Lesniak MS. 2012. IDO expression in brain tumors increases the recruitment of regulatory T cells and negatively impacts survival. *Clin Cancer Res* 18: 6110-21

24. Platten M, von Knebel Doeberitz N, Oezen I, Wick W, Ochs K. 2014. Cancer Immunotherapy by Targeting IDO1/TDO and Their Downstream Effectors. *Front Immunol* 5: 673

25. Pantouris G, Serys M, Yuasa HJ, Ball HJ, Mowat CG. 2014. Human indoleamine 2,3-dioxygenase-2 has substrate specificity and inhibition characteristics distinct from those of indoleamine 2,3-dioxygenase-1. *Amino Acids* 46: 2155-63

26. Zhai L, Ladomersky E, Lenzen A, Nguyen B, Patel R, Lauing KL, Wu M, Wainwright DA. 2018. IDO1 in cancer: a Gemini of immune checkpoints. *Cell Mol Immunol* 15: 447-57

27. Prendergast GC, Mondal A, Dey S, Laury-Kleintop LD, Muller AJ. 2018. Inflammatory Reprogramming with IDO1 Inhibitors: Turning Immunologically Unresponsive 'Cold' Tumors 'Hot'. *Trends Cancer* 4: 38-58

28. Zhai L, Lauing KL, Chang AL, Dey M, Qian J, Cheng Y, Lesniak MS, Wainwright DA. 2015. The role of IDO in brain tumor immunotherapy. *J Neurooncol* 123: 395-403

29. Murray IA, Patterson AD, Perdew GH. 2014. Aryl hydrocarbon receptor ligands in cancer: friend and foe. *Nat Rev Cancer* 14: 801-14

30. Labadie BW, Bao R, Luke JJ. 2019. Reimagining IDO Pathway Inhibition in Cancer Immunotherapy via Downstream Focus on the Tryptophan-Kynurenine-Aryl Hydrocarbon Axis. *Clin Cancer Res* 25: 1462-71

31. Gabriely G, Wheeler MA, Takenaka MC, Quintana FJ. 2017. Role of AHR and HIF-1alpha in Glioblastoma Metabolism. *Trends Endocrinol Metab* 28: 428-36

32. Mezrich JD, Fechner JH, Zhang X, Johnson BP, Burlingham WJ, Bradfield CA. 2010. An interaction between kynurenine and the aryl hydrocarbon receptor can generate regulatory T cells. *J Immunol* 185: 3190-8

33. Quintana FJ, Basso AS, Iglesias AH, Korn T, Farez MF, Bettelli E, Caccamo M, Oukka M, Weiner HL. 2008. Control of T(reg) and T(H)17 cell differentiation by the aryl hydrocarbon receptor. *Nature* 453: 65-71

34. Harding HP, Zhang Y, Zeng H, Novoa I, Lu PD, Calfon M, Sadri N, Yun C, Popko B, Paules R, Stojdl DF, Bell JC, Hettmann T, Leiden JM, Ron D. 2003. An integrated stress response regulates amino acid metabolism and resistance to oxidative stress. *Mol Cell* 11: 619-33

35. Opitz CA, Wick W, Steinman L, Platten M. 2007. Tryptophan degradation in autoimmune diseases. *Cell Mol Life Sci* 64: 2542-63

36. Thevenot PT, Sierra RA, Raber PL, Al-Khami AA, Trillo-Tinoco J, Zarreii P, Ochoa AC, Cui Y, Del Valle L, Rodriguez PC. 2014. The stress-response sensor chop regulates the

function and accumulation of myeloid-derived suppressor cells in tumors. *Immunity* 41: 389-401

37. Smith C, Chang MY, Parker KH, Beury DW, DuHadaway JB, Flick HE, Boulden J, Sutanto-Ward E, Soler AP, Laury-Kleintop LD, Mandik-Nayak L, Metz R, Ostrand-Rosenberg S, Prendergast GC, Muller AJ. 2012. IDO is a nodal pathogenic driver of lung cancer and metastasis development. *Cancer Discov* 2: 722-35

38. Mita MM, Mita A, Rowinsky EK. 2003. The molecular target of rapamycin (mTOR) as a therapeutic target against cancer. *Cancer Biol Ther* 2: S169-77

39. Ladomersky E, Zhai L, Lenzen A, Lauing KL, Qian J, Scholtens DM, Gritsina G, Sun X, Liu Y, Yu F, Gong W, Liu Y, Jiang B, Tang T, Patel R, Platanias LC, James CD, Stupp R, Lukas RV, Binder DC, Wainwright DA. 2018. IDO1 Inhibition Synergizes with Radiation and PD-1 Blockade to Durably Increase Survival Against Advanced Glioblastoma. *Clin Cancer Res* 24: 2559-73

40. Zhai L, Ladomersky E, Dostal CR, Lauing KL, Swoap K, Billingham LK, Gritsina G, Wu M, McCusker RH, Binder DC, Wainwright DA. 2017. Non-tumor cell IDO1 predominantly contributes to enzyme activity and response to CTLA-4/PD-L1 inhibition in mouse glioblastoma. *Brain Behav Immun* 62: 24-9

41. Sharma P, Allison JP. 2015. The future of immune checkpoint therapy. *Science* 348: 56-61

42. Gutierrez-Vazquez C, Quintana FJ. 2018. Regulation of the Immune Response by the Aryl Hydrocarbon Receptor. *Immunity* 48: 19-33

43. Moorthy B, Chu C, Carlin DJ. 2015. Polycyclic aromatic hydrocarbons: from metabolism to lung cancer. *Toxicol Sci* 145: 5-15

44. Barnett JA, Urbauer DL, Murray GI, Fuller GN, Heimberger AB. 2007. Cytochrome P450 1B1 expression in glial cell tumors: an immunotherapeutic target. *Clin Cancer Res* 13: 3559-67

45. Schnekenburger M, Peng L, Puga A. 2007. HDAC1 bound to the Cyp1a1 promoter blocks histone acetylation associated with Ah receptor-mediated trans-activation. *Biochim Biophys Acta* 1769: 569-78

46. Takenaka MC, Gabriely G, Rothhammer V, Mascanfroni ID, Wheeler MA, Chao CC, Gutierrez-Vazquez C, Kenison J, Tjon EC, Barroso A, Vandeventer T, de Lima KA, Rothweiler S, Mayo L, Ghannam S, Zandee S, Healy L, Sherr D, Farez MF, Prat A, Antel J, Reardon DA, Zhang H, Robson SC, Getz G, Weiner HL, Quintana FJ. 2019. Control of tumor-associated macrophages and T cells in glioblastoma via AHR and CD39. *Nat Neurosci* 22: 729-40

47. Theate I, van Baren N, Pilotte L, Moulin P, Larrieu P, Renauld JC, Herve C, Gutierrez-Roelens I, Marbaix E, Sempoux C, Van den Eynde BJ. 2015. Extensive profiling of the expression of the indoleamine 2,3-dioxygenase 1 protein in normal and tumoral human tissues. *Cancer Immunol Res* 3: 161-72

48. Blair AB, Kleponis J, Thomas DL, 2nd, Muth ST, Murphy AG, Kim V, Zheng L. 2019. IDO1 inhibition potentiates vaccine-induced immunity against pancreatic adenocarcinoma. *J Clin Invest* 129: 1742-55

49. Spranger S, Koblish HK, Horton B, Scherle PA, Newton R, Gajewski TF. 2014. Mechanism of tumor rejection with doublets of CTLA-4, PD-1/PD-L1, or IDO blockade involves restored IL-2 production and proliferation of CD8(+) T cells directly within the tumor microenvironment. *J Immunother Cancer* 2: 3

50. Holmgaard RB, Zamarin D, Munn DH, Wolchok JD, Allison JP. 2013. Indoleamine 2,3-dioxygenase is a critical resistance mechanism in antitumor T cell immunotherapy targeting CTLA-4. *J Exp Med* 210: 1389-402

51. Muller AJ, DuHadaway JB, Donover PS, Sutanto-Ward E, Prendergast GC. 2005. Inhibition of indoleamine 2,3-dioxygenase, an immunoregulatory target of the cancer suppression gene Bin1, potentiates cancer chemotherapy. *Nat Med* 11: 312-9

52. Wainwright DA, Chang AL, Dey M, Balyasnikova IV, Kim CK, Tobias A, Cheng Y, Kim JW, Qiao J, Zhang L, Han Y, Lesniak MS. 2014. Durable therapeutic efficacy utilizing combinatorial blockade against IDO, CTLA-4, and PD-L1 in mice with brain tumors. *Clin Cancer Res* 20: 5290-301

53. Platten M, Nollen EAA, Rohrig UF, Fallarino F, Opitz CA. 2019. Tryptophan metabolism as a common therapeutic target in cancer, neurodegeneration and beyond. *Nat Rev Drug Discov* 18: 379-401

54. Metz R, Rust S, Duhadaway JB, Mautino MR, Munn DH, Vahanian NN, Link CJ, Prendergast GC. 2012. IDO inhibits a tryptophan sufficiency signal that stimulates mTOR: A novel IDO effector pathway targeted by D-1-methyl-tryptophan. *Oncoimmunology* 1: 1460-8

55. Mitchell TC, Hamid O, Smith DC, Bauer TM, Wasser JS, Olszanski AJ, Luke JJ, Balmanoukian AS, Schmidt EV, Zhao Y, Gong X, Maleski J, Leopold L, Gajewski TF. 2018. Epacadostat Plus Pembrolizumab in Patients With Advanced Solid Tumors: Phase I Results From a Multicenter, Open-Label Phase I/II Trial (ECHO-202/KEYNOTE-037). *J Clin Oncol* 36: 3223-30

56. Long GV, Dummer R, Hamid O, Gajewski T, Caglevic C, Dalle S, Arance A, Carlino MS, Grob J-J, Kim TM, Demidov LV, Robert C, Larkin JMG, Anderson J, Maleski JE, Jones

MM, Diede SJ, Mitchell TC. 2018. Epacadostat (E) plus pembrolizumab (P) versus pembrolizumab alone in patients (pts) with unresectable or metastatic melanoma: Results of the phase 3 ECHO-301/KEYNOTE-252 study. *Journal of Clinical Oncology* 36: 108-

57. Ladomersky E, Zhai L, Lauing KL, Bell A, Xu J, Kocherginsky M, Zhang B, Wu JD, Podojil JR, Platanias LC, Mochizuki AY, Prins RM, Kumthekar P, Raizer JJ, Dixit K, Lukas RV, Horbinski C, Wei M, Zhou C, Pawelec G, Campisi J, Grohmann U, Prendergast GC, Munn DH, Wainwright DA. 2020. Advanced Age Increases Immunosuppression in the Brain and Decreases Immunotherapeutic Efficacy in Subjects with Glioblastoma. *Clin Cancer Res* 26: 5232-45

58. Schmidt SV, Schultze JL. 2014. New Insights into IDO Biology in Bacterial and Viral Infections. *Front Immunol* 5: 384

59. Schroecksnadel K, Zangerle R, Bellmann-Weiler R, Garimorth K, Weiss G, Fuchs D. 2007. Indoleamine-2, 3-dioxygenase and other interferon-gamma-mediated pathways in patients with human immunodeficiency virus infection. *Curr Drug Metab* 8: 225-36

60. Boasso A, Herbeuval JP, Hardy AW, Anderson SA, Dolan MJ, Fuchs D, Shearer GM. 2007. HIV inhibits CD4+ T-cell proliferation by inducing indoleamine 2,3-dioxygenase in plasmacytoid dendritic cells. *Blood* 109: 3351-9

61. Boasso A, Hardy AW, Anderson SA, Dolan MJ, Shearer GM. 2008. HIV-induced type I interferon and tryptophan catabolism drive T cell dysfunction despite phenotypic activation. *PLoS One* 3: e2961

62. Favre D, Mold J, Hunt PW, Kanwar B, Loke P, Seu L, Barbour JD, Lowe MM, Jayawardene A, Aweeka F, Huang Y, Douek DC, Brenchley JM, Martin JN, Hecht FM, Deeks SG, McCune JM. 2010. Tryptophan catabolism by indoleamine 2,3-dioxygenase 1 alters the balance of TH17 to regulatory T cells in HIV disease. *Sci Transl Med* 2: 32ra6

63. Yoshida R, Urade Y, Tokuda M, Hayaishi O. 1979. Induction of indoleamine 2,3-dioxygenase in mouse lung during virus infection. *Proc Natl Acad Sci U S A* 76: 4084-6

64. Huang L, Li L, Klonowski KD, Tompkins SM, Tripp RA, Mellor AL. 2013. Induction and role of indoleamine 2,3 dioxygenase in mouse models of influenza a virus infection. *PLoS One* 8: e66546

65. Fox JM, Sage LK, Huang L, Barber J, Klonowski KD, Mellor AL, Tompkins SM, Tripp RA. 2013. Inhibition of indoleamine 2,3-dioxygenase enhances the T-cell response to influenza virus infection. *J Gen Virol* 94: 1451-61

66. Sage LK, Fox JM, Mellor AL, Tompkins SM, Tripp RA. 2014. Indoleamine 2,3-dioxygenase (IDO) activity during the primary immune response to influenza infection modifies the memory T cell response to influenza challenge. *Viral Immunol* 27: 112-23

67. Larrea E, Riezu-Boj JI, Gil-Guerrero L, Casares N, Aldabe R, Sarobe P, Civeira MP, Heeney JL, Rollier C, Verstrepen B, Wakita T, Borras-Cuesta F, Lasarte JJ, Prieto J. 2007. Upregulation of indoleamine 2,3-dioxygenase in hepatitis C virus infection. *J Virol* 81: 3662-6

68. Higashitani K, Kanto T, Kuroda S, Yoshio S, Matsubara T, Kakita N, Oze T, Miyazaki M, Sakakibara M, Hiramatsu N, Mita E, Imai Y, Kasahara A, Okuno A, Takikawa O, Hayashi N, Takehara T. 2013. Association of enhanced activity of indoleamine 2,3-dioxygenase in dendritic cells with the induction of regulatory T cells in chronic hepatitis C infection. *J Gastroenterol* 48: 660-70

69. Zhu J, Huang X, Yang Y. 2007. Innate immune response to adenoviral vectors is mediated by both Toll-like receptor-dependent and -independent pathways. *J Virol* 81: 3170-80

70. Nociari M, Ocheretina O, Schoggins JW, Falck-Pedersen E. 2007. Sensing infection by adenovirus: Toll-like receptor-independent viral DNA recognition signals activation of the interferon regulatory factor 3 master regulator. *J Virol* 81: 4145-57

71. Pitkaranta A, Hovi T. 1993. Induction of interferon in human leukocyte cultures by natural pathogenic respiratory viruses. *J Interferon Res* 13: 423-6

72. Reich N, Pine R, Levy D, Darnell JE, Jr. 1988. Transcription of interferon-stimulated genes is induced by adenovirus particles but is suppressed by E1A gene products. *J Virol* 62: 114-9

73. Scheler M, Wenzel J, Tuting T, Takikawa O, Bieber T, von Bubnoff D. 2007. Indoleamine 2,3-dioxygenase (IDO): the antagonist of type I interferon-driven skin inflammation? *Am J Pathol* 171: 1936-43

74. Doerfler W. 1996. Adenoviruses. In *Medical Microbiology*, ed. th, S Baron. Galveston (TX)

75. Smith JG, Wiethoff CM, Stewart PL, Nemerow GR. 2010. Adenovirus. *Curr Top Microbiol Immunol* 343: 195-224

76. White E. 2001. Regulation of the cell cycle and apoptosis by the oncogenes of adenovirus. *Oncogene* 20: 7836-46

77. Ahi YS, Mittal SK. 2016. Components of Adenovirus Genome Packaging. *Front Microbiol* 7: 1503

78. Ying B, Wold WS. 2003. Adenovirus ADP protein (E3-11.6K), which is required for efficient cell lysis and virus release, interacts with human MAD2B. *Virology* 313: 224-34

79. Brennan CW, Verhaak RG, McKenna A, Campos B, Noushmehr H, Salama SR, Zheng S, Chakravarty D, Sanborn JZ, Berman SH, Beroukhim R, Bernard B, Wu CJ, Genovese G, Shmulevich I, Barnholtz-Sloan J, Zou L, Vegesna R, Shukla SA, Ciriello G, Yung WK,

Zhang W, Sougnez C, Mikkelsen T, Aldape K, Bigner DD, Van Meir EG, Prados M, Sloan A, Black KL, Eschbacher J, Finocchiaro G, Friedman W, Andrews DW, Guha A, Iacocca M, O'Neill BP, Foltz G, Myers J, Weisenberger DJ, Penny R, Kucherlapati R, Perou CM, Hayes DN, Gibbs R, Marra M, Mills GB, Lander E, Spellman P, Wilson R, Sander C, Weinstein J, Meyerson M, Gabriel S, Laird PW, Haussler D, Getz G, Chin L, Network TR. 2013. The somatic genomic landscape of glioblastoma. *Cell* 155: 462-77

80. Fueyo J, Gomez-Manzano C, Alemany R, Lee PS, McDonnell TJ, Mitlianga P, Shi YX, Levin VA, Yung WK, Kyritsis AP. 2000. A mutant oncolytic adenovirus targeting the Rb pathway produces anti-glioma effect in vivo. *Oncogene* 19: 2-12

81. Nevins JR. 1992. E2F: a link between the Rb tumor suppressor protein and viral oncoproteins. *Science* 258: 424-9

82. Chintala SK, Fueyo J, Gomez-Manzano C, Venkaiah B, Bjerkvig R, Yung WK, Sawaya R, Kyritsis AP, Rao JS. 1997. Adenovirus-mediated p16/CDKN2 gene transfer suppresses glioma invasion in vitro. *Oncogene* 15: 2049-57

83. Bergelson JM, Cunningham JA, Droguett G, Kurt-Jones EA, Krithivas A, Hong JS, Horwitz MS, Crowell RL, Finberg RW. 1997. Isolation of a common receptor for Coxsackie B viruses and adenoviruses 2 and 5. *Science* 275: 1320-3

84. Fueyo J, Alemany R, Gomez-Manzano C, Fuller GN, Khan A, Conrad CA, Liu TJ, Jiang H, Lemoine MG, Suzuki K, Sawaya R, Curiel DT, Yung WK, Lang FF. 2003. Preclinical characterization of the antiglioma activity of a tropism-enhanced adenovirus targeted to the retinoblastoma pathway. *J Natl Cancer Inst* 95: 652-60

85. Pasqualini R, Koivunen E, Ruoslahti E. 1997. Alpha v integrins as receptors for tumor targeting by circulating ligands. *Nat Biotechnol* 15: 542-6

86. Bello L, Francolini M, Marthyn P, Zhang J, Carroll RS, Nikas DC, Strasser JF, Villani R, Cheresh DA, Black PM. 2001. Alpha(v)beta3 and alpha(v)beta5 integrin expression in glioma periphery. *Neurosurgery* 49: 380-9; discussion 90

87. Jiang H, Gomez-Manzano C, Aoki H, Alonso MM, Kondo S, McCormick F, Xu J, Kondo Y, Bekele BN, Colman H, Lang FF, Fueyo J. 2007. Examination of the therapeutic potential of Delta-24-RGD in brain tumor stem cells: role of autophagic cell death. *J Natl Cancer Inst* 99: 1410-4

88. Ito H, Aoki H, Kuhnel F, Kondo Y, Kubicka S, Wirth T, Iwado E, Iwamaru A, Fujiwara K, Hess KR, Lang FF, Sawaya R, Kondo S. 2006. Autophagic cell death of malignant glioma cells induced by a conditionally replicating adenovirus. *J Natl Cancer Inst* 98: 625-36

89. Jiang H, Fueyo J. 2014. Healing after death: antitumor immunity induced by oncolytic adenoviral therapy. *Oncoimmunology* 3: e947872

90. Lang FF, Conrad C, Gomez-Manzano C, Yung WKA, Sawaya R, Weinberg JS, Prabhu SS, Rao G, Fuller GN, Aldape KD, Gumin J, Vence LM, Wistuba I, Rodriguez-Canales J, Villalobos PA, Dirven CMF, Tejada S, Valle RD, Alonso MM, Ewald B, Peterkin JJ, Tufaro F, Fueyo J. 2018. Phase I Study of DNX-2401 (Delta-24-RGD) Oncolytic Adenovirus: Replication and Immunotherapeutic Effects in Recurrent Malignant Glioma. *J Clin Oncol*: JCO2017758219

91. Jiang H, Rivera-Molina Y, Gomez-Manzano C, Clise-Dwyer K, Bover L, Vence LM, Yuan Y, Lang FF, Toniatti C, Hossain MB, Fueyo J. 2017. Oncolytic Adenovirus and Tumor-Targeting Immune Modulatory Therapy Improve Autologous Cancer Vaccination. *Cancer Res* 77: 3894-907

92. Croft M. 2009. The role of TNF superfamily members in T-cell function and diseases. *Nat Rev Immunol* 9: 271-85

93. Croft M, Benedict CA, Ware CF. 2013. Clinical targeting of the TNF and TNFR superfamilies. *Nat Rev Drug Discov* 12: 147-68

94. Jiang H, Shin DH, Nguyen TT, Fueyo J, Fan X, Henry V, Carrillo CC, Yi Y, Alonso MM, Collier TL, Yuan Y, Lang FF, Gomez-Manzano C. 2019. Localized Treatment with Oncolytic Adenovirus Delta-24-RGDOX Induces Systemic Immunity against Disseminated Subcutaneous and Intracranial Melanomas. *Clin Cancer Res* 25: 6801-14

95. Lang F, Conrad C, Gomez-Manzano C, Turafo F, Yung W, Sawaya R, Weinberg J, Prahbu S, Fuller G, Aldape K, Fueyo J. 2014. First-in-human phase I clinical trial of oncolytic Delta-24-RGD (DNX-2401) with biological endpoints: implications for viro-immunotherapy. *Neuro-Oncology* 16

96. Cloughesy TF, Landolfi J, Hogan DJ, Bloomfield S, Carter B, Chen CC, Elder JB, Kalkanis SN, Kesari S, Lai A, Lee IY, Liau LM, Mikkelsen T, Nghiemphu PL, Piccioni D, Walbert T, Chu A, Das A, Diago OR, Gammon D, Gruber HE, Hanna M, Jolly DJ, Kasahara N, McCarthy D, Mitchell L, Ostertag D, Robbins JM, Rodriguez-Aguirre M, Vogelbaum MA. 2016. Phase 1 trial of vocimagene amiretrorepvec and 5-fluorocytosine for recurrent high-grade glioma. *Sci Transl Med* 8: 341ra75

97. Desjardins A, Gromeier M, Herndon JE, 2nd, Beaubier N, Bolognesi DP, Friedman AH, Friedman HS, McSherry F, Muscat AM, Nair S, Peters KB, Randazzo D, Sampson JH, Vlahovic G, Harrison WT, McLendon RE, Ashley D, Bigner DD. 2018. Recurrent Glioblastoma Treated with Recombinant Poliovirus. *N Engl J Med* 379: 150-61

98. Markert JM, Razdan SN, Kuo HC, Cantor A, Knoll A, Karrasch M, Nabors LB, Markiewicz M, Agee BS, Coleman JM, Lakeman AD, Palmer CA, Parker JN, Whitley

RJ, Weichselbaum RR, Fiveash JB, Gillespie GY. 2014. A phase 1 trial of oncolytic HSV-1, G207, given in combination with radiation for recurrent GBM demonstrates safety and radiographic responses. *Mol Ther* 22: 1048-55

99. Harrow S, Papanastassiou V, Harland J, Mabbs R, Petty R, Fraser M, Hadley D, Patterson J, Brown SM, Rampling R. 2004. HSV1716 injection into the brain adjacent to tumour following surgical resection of high-grade glioma: safety data and long-term survival. *Gene Ther* 11: 1648-58

100. Markert JM, Liechty PG, Wang W, Gaston S, Braz E, Karrasch M, Nabors LB, Markiewicz M, Lakeman AD, Palmer CA, Parker JN, Whitley RJ, Gillespie GY. 2009. Phase Ib trial of mutant herpes simplex virus G207 inoculated pre-and post-tumor resection for recurrent GBM. *Mol Ther* 17: 199-207

101. Rampling R, Cruickshank G, Papanastassiou V, Nicoll J, Hadley D, Brennan D, Petty R, MacLean A, Harland J, McKie E, Mabbs R, Brown M. 2000. Toxicity evaluation of replication-competent herpes simplex virus (ICP 34.5 null mutant 1716) in patients with recurrent malignant glioma. *Gene Ther* 7: 859-66

102. Forsyth P, Roldan G, George D, Wallace C, Palmer CA, Morris D, Cairncross G, Matthews MV, Markert J, Gillespie Y, Coffey M, Thompson B, Hamilton M. 2008. A phase I trial of intratumoral administration of reovirus in patients with histologically confirmed recurrent malignant gliomas. *Mol Ther* 16: 627-32

103. Kicielinski KP, Chiocca EA, Yu JS, Gill GM, Coffey M, Markert JM. 2014. Phase 1 clinical trial of intratumoral reovirus infusion for the treatment of recurrent malignant gliomas in adults. *Mol Ther* 22: 1056-62

104. Samson A, Scott KJ, Taggart D, West EJ, Wilson E, Nuovo GJ, Thomson S, Corns R, Mathew RK, Fuller MJ, Kottke TJ, Thompson JM, Ilett EJ, Cockle JV, van Hille P,

Sivakumar G, Polson ES, Turnbull SJ, Appleton ES, Migneco G, Rose AS, Coffey MC, Beirne DA, Collinson FJ, Ralph C, Alan Anthoney D, Twelves CJ, Furness AJ, Quezada SA, Wurdak H, Errington-Mais F, Pandha H, Harrington KJ, Selby PJ, Vile RG, Griffin SD, Stead LF, Short SC, Melcher AA. 2018. Intravenous delivery of oncolytic reovirus to brain tumor patients immunologically primes for subsequent checkpoint blockade. *Sci Transl Med* 10

105. Csatary LK, Gosztonyi G, Szeberenyi J, Fabian Z, Liszka V, Bodey B, Csatary CM. 2004. MTH-68/H oncolytic viral treatment in human high-grade gliomas. *J Neurooncol* 67: 83-93

106. Freeman AI, Zakay-Rones Z, Gomori JM, Linetsky E, Rasooly L, Greenbaum E, Rozenman-Yair S, Panet A, Libson E, Irving CS, Galun E, Siegal T. 2006. Phase I/II trial of intravenous NDV-HUJ oncolytic virus in recurrent glioblastoma multiforme. *Mol Ther* 13: 221-8

107. Schirrmacher V. 2015. Signaling through RIG-I and type I interferon receptor: Immune activation by Newcastle disease virus in man versus immune evasion by Ebola virus (Review). *Int J Mol Med* 36: 3-10

108. Steiner HH, Bonsanto MM, Beckhove P, Brysch M, Geletneky K, Ahmadi R, Schuele-Freyer R, Kremer P, Ranaie G, Matejic D, Bauer H, Kiessling M, Kunze S, Schirrmacher V, Herold-Mende C. 2004. Antitumor vaccination of patients with glioblastoma multiforme: a pilot study to assess feasibility, safety, and clinical benefit. *J Clin Oncol* 22: 4272-81

109. Geletneky K, Huesing J, Rommelaere J, Schlehofer JR, Leuchs B, Dahm M, Krebs O, von Knebel Doeberitz M, Huber B, Hajda J. 2012. Phase I/IIa study of intratumoral/intracerebral or intravenous/intracerebral administration of Parvovirus H-1

(ParvOryx) in patients with progressive primary or recurrent glioblastoma multiforme: ParvOryx01 protocol. *BMC Cancer* 12: 99

110. Harrington K, Freeman DJ, Kelly B, Harper J, Soria JC. 2019. Optimizing oncolytic virotherapy in cancer treatment. *Nat Rev Drug Discov* 18: 689-706

111. Gordon YJ, Gilden DM, Becker Y. 1983. HSV-1 thymidine kinase promotes virulence and latency in the mouse. *Invest Ophthalmol Vis Sci* 24: 599-602

112. He B, Gross M, Roizman B. 1997. The gamma(1)34.5 protein of herpes simplex virus 1 complexes with protein phosphatase 1alpha to dephosphorylate the alpha subunit of the eukaryotic translation initiation factor 2 and preclude the shutoff of protein synthesis by double-stranded RNA-activated protein kinase. *Proc Natl Acad Sci U S A* 94: 843-8

113. Orvedahl A, Alexander D, Talloczy Z, Sun Q, Wei Y, Zhang W, Burns D, Leib DA, Levine B. 2007. HSV-1 ICP34.5 confers neurovirulence by targeting the Beclin 1 autophagy protein. *Cell Host Microbe* 1: 23-35

114. MacLean AR, ul-Fareed M, Robertson L, Harland J, Brown SM. 1991. Herpes simplex virus type 1 deletion variants 1714 and 1716 pinpoint neurovirulence-related sequences in Glasgow strain 17+ between immediate early gene 1 and the 'a' sequence. *J Gen Virol* 72 (Pt 3): 631-9

115. McKie EA, Brown SM, MacLean AR, Graham DI. 1998. Histopathological responses in the CNS following inoculation with a non-neurovirulent mutant (1716) of herpes simplex virus type 1 (HSV 1): relevance for gene and cancer therapy. *Neuropathol Appl Neurobiol* 24: 367-72

116. McKie EA, MacLean AR, Lewis AD, Cruickshank G, Rampling R, Barnett SC, Kennedy PG, Brown SM. 1996. Selective in vitro replication of herpes simplex virus type 1 (HSV-

1) ICP34.5 null mutants in primary human CNS tumours--evaluation of a potentially effective clinical therapy. *Br J Cancer* 74: 745-52

117. Goldstein DJ, Weller SK. 1988. Factor(s) present in herpes simplex virus type 1-infected cells can compensate for the loss of the large subunit of the viral ribonucleotide reductase: characterization of an ICP6 deletion mutant. *Virology* 166: 41-51

118. Mineta T, Rabkin SD, Martuza RL. 1994. Treatment of malignant gliomas using ganciclovir-hypersensitive, ribonucleotide reductase-deficient herpes simplex viral mutant. *Cancer Res* 54: 3963-6

119. Aghi M, Visted T, Depinho RA, Chiocca EA. 2008. Oncolytic herpes virus with defective ICP6 specifically replicates in quiescent cells with homozygous genetic mutations in p16. *Oncogene* 27: 4249-54

120. Papanastassiou V, Rampling R, Fraser M, Petty R, Hadley D, Nicoll J, Harland J, Mabbs R, Brown M. 2002. The potential for efficacy of the modified (ICP 34.5(-)) herpes simplex virus HSV1716 following intratumoural injection into human malignant glioma: a proof of principle study. *Gene Ther* 9: 398-406

121. Markert JM, Medlock MD, Rabkin SD, Gillespie GY, Todo T, Hunter WD, Palmer CA, Feigenbaum F, Tornatore C, Tufaro F, Martuza RL. 2000. Conditionally replicating herpes simplex virus mutant, G207 for the treatment of malignant glioma: results of a phase I trial. *Gene Ther* 7: 867-74

122. Friedman GK, Johnston JM, Bag AK, Bernstock JD, Li R, Aban I, Kachurak K, Nan L, Kang KD, Totsch S, Schlappi C, Martin AM, Pastakia D, McNall-Knapp R, Farouk Sait S, Khakoo Y, Karajannis MA, Woodling K, Palmer JD, Osorio DS, Leonard J, Abdelbaki MS, Madan-Swain A, Atkinson TP, Whitley RJ, Fiveash JB, Markert JM, Gillespie GY.

2021. Oncolytic HSV-1 G207 Immunovirotherapy for Pediatric High-Grade Gliomas. *N Engl J Med*

123. Kambara H, Okano H, Chiocca EA, Saeki Y. 2005. An oncolytic HSV-1 mutant expressing ICP34.5 under control of a nestin promoter increases survival of animals even when symptomatic from a brain tumor. *Cancer Res* 65: 2832-9

124. Todo T, Martuza RL, Rabkin SD, Johnson PA. 2001. Oncolytic herpes simplex virus vector with enhanced MHC class I presentation and tumor cell killing. *Proc Natl Acad Sci U S A* 98: 6396-401

125. Roth JC, Cassady KA, Cody JJ, Parker JN, Price KH, Coleman JM, Peggins JO, Noker PE, Powers N, Grimes S, Carroll SL, Gillespie GY, Whitley R, Markert J. 2014. Evaluation of the Safety and Biodistribution of M032, an Attenuated HSV-1 Virus Expressing hIL-12, After Intracerebral Administration to Aotus Non-Human Primates. *Hum Gene Ther Clin Dev*

126. Strong JE, Coffey MC, Tang D, Sabinin P, Lee PW. 1998. The molecular basis of viral oncolysis: usurpation of the Ras signaling pathway by reovirus. *EMBO J* 17: 3351-62

127. Wilcox ME, Yang W, Senger D, Rewcastle NB, Morris DG, Brasher PM, Shi ZQ, Johnston RN, Nishikawa S, Lee PW, Forsyth PA. 2001. Reovirus as an oncolytic agent against experimental human malignant gliomas. *J Natl Cancer Inst* 93: 903-12

128. Ganar K, Das M, Sinha S, Kumar S. 2014. Newcastle disease virus: current status and our understanding. *Virus Res* 184: 71-81

129. Krishnamurthy S, Takimoto T, Scroggs RA, Portner A. 2006. Differentially regulated interferon response determines the outcome of Newcastle disease virus infection in normal and tumor cell lines. *J Virol* 80: 5145-55

130. Lai YJ, Tsai JC, Tseng YT, Wu MS, Liu WS, Lam HI, Yu JH, Nozell SE, Benveniste EN. 2017. Small G protein Rac GTPases regulate the maintenance of glioblastoma stem-like cells in vitro and in vivo. *Oncotarget* 8: 18031-49

131. Puhlmann J, Puehler F, Mumberg D, Boukamp P, Beier R. 2010. Rac1 is required for oncolytic NDV replication in human cancer cells and establishes a link between tumorigenesis and sensitivity to oncolytic virus. *Oncogene* 29: 2205-16

132. Garcia-Romero N, Palacin-Aliana I, Esteban-Rubio S, Madurga R, Rius-Rocabert S, Carrion-Navarro J, Presa J, Cuadrado-Castano S, Sanchez-Gomez P, Garcia-Sastre A, Nistal-Villan E, Ayuso-Sacido A. 2020. Newcastle Disease Virus (NDV) Oncolytic Activity in Human Glioma Tumors Is Dependent on CDKN2A-Type I IFN Gene Cluster Codeletion. *Cells* 9

133. Zulkifli MM, Ibrahim R, Ali AM, Aini I, Jaafar H, Hilda SS, Alitheen NB, Abdullah JM. 2009. Newcastle diseases virus strain V4UPM displayed oncolytic ability against experimental human malignant glioma. *Neurol Res* 31: 3-10

134. Kazimirsky G, Jiang W, Slavin S, Ziv-Av A, Brodie C. 2016. Mesenchymal stem cells enhance the oncolytic effect of Newcastle disease virus in glioma cells and glioma stem cells via the secretion of TRAIL. *Stem Cell Res Ther* 7: 149

135. Koks CA, Garg AD, Ehrhardt M, Riva M, Vandenberk L, Boon L, De Vleeschouwer S, Agostinis P, Graf N, Van Gool SW. 2015. Newcastle disease virotherapy induces long-term survival and tumor-specific immune memory in orthotopic glioma through the induction of immunogenic cell death. *Int J Cancer* 136: E313-25

136. Bai Y, Chen Y, Hong X, Liu X, Su X, Li S, Dong X, Zhao G, Li Y. 2018. Newcastle disease virus enhances the growth-inhibiting and proapoptotic effects of temozolomide on glioblastoma cells in vitro and in vivo. *Sci Rep* 8: 11470

137. Gromeier M, Alexander L, Wimmer E. 1996. Internal ribosomal entry site substitution eliminates neurovirulence in intergeneric poliovirus recombinants. *Proc Natl Acad Sci U S A* 93: 2370-5

138. Merrill MK, Bernhardt G, Sampson JH, Wikstrand CJ, Bigner DD, Gromeier M. 2004. Poliovirus receptor CD155-targeted oncolysis of glioma. *Neuro Oncol* 6: 208-17

139. Dobrikova EY, Broadt T, Poiley-Nelson J, Yang X, Soman G, Giardina S, Harris R, Gromeier M. 2008. Recombinant oncolytic poliovirus eliminates glioma in vivo without genetic adaptation to a pathogenic phenotype. *Mol Ther* 16: 1865-72

140. Gromeier M, Lachmann S, Rosenfeld MR, Gutin PH, Wimmer E. 2000. Intergeneric poliovirus recombinants for the treatment of malignant glioma. *Proc Natl Acad Sci U S A* 97: 6803-8

141. Russell SJ, Peng KW, Bell JC. 2012. Oncolytic virotherapy. *Nat Biotechnol* 30: 658-70

142. Russell SJ, Peng KW. 2007. Viruses as anticancer drugs. *Trends Pharmacol Sci* 28: 326-33

143. Jiang H, Gomez-Manzano C, Rivera-Molina Y, Lang FF, Conrad CA, Fueyo J. 2015. Oncolytic adenovirus research evolution: from cell-cycle checkpoints to immune checkpoints. *Curr Opin Virol* 13: 33-9

144. Sanmamed MF, Pastor F, Rodriguez A, Perez-Gracia JL, Rodriguez-Ruiz ME, Jure-Kunkel M, Melero I. 2015. Agonists of Co-stimulation in Cancer Immunotherapy Directed Against CD137, OX40, GITR, CD27, CD28, and ICOS. *Semin Oncol* 42: 640-55

145. Pardoll DM. 2012. The blockade of immune checkpoints in cancer immunotherapy. *Nat Rev Cancer* 12: 252-64

146. Munn DH, Sharma MD, Baban B, Harding HP, Zhang Y, Ron D, Mellor AL. 2005. GCN2 kinase in T cells mediates proliferative arrest and anergy induction in response to indoleamine 2,3-dioxygenase. *Immunity* 22: 633-42

147. Munn DH, Shafizadeh E, Attwood JT, Bondarev I, Pashine A, Mellor AL. 1999. Inhibition of T cell proliferation by macrophage tryptophan catabolism. *J Exp Med* 189: 1363-72

148. Mellor AL, Munn DH. 1999. Tryptophan catabolism and T-cell tolerance: immunosuppression by starvation? *Immunol Today* 20: 469-73

149. Terness P, Bauer TM, Rose L, Dufter C, Watzlik A, Simon H, Opelz G. 2002. Inhibition of allogeneic T cell proliferation by indoleamine 2,3-dioxygenase-expressing dendritic cells: mediation of suppression by tryptophan metabolites. *J Exp Med* 196: 447-57

150. Fallarino F, Grohmann U, Vacca C, Bianchi R, Orabona C, Spreca A, Fioretti MC, Puccetti P. 2002. T cell apoptosis by tryptophan catabolism. *Cell Death Differ* 9: 1069-77

151. Frumento G, Rotondo R, Tonetti M, Damonte G, Benatti U, Ferrara GB. 2002. Tryptophan-derived catabolites are responsible for inhibition of T and natural killer cell proliferation induced by indoleamine 2,3-dioxygenase. *J Exp Med* 196: 459-68

152. Yoshida R, Imanishi J, Oku T, Kishida T, Hayaishi O. 1981. Induction of pulmonary indoleamine 2,3-dioxygenase by interferon. *Proc Natl Acad Sci U S A* 78: 129-32

153. Bolger AM, Lohse M, Usadel B. 2014. Trimmomatic: a flexible trimmer for Illumina sequence data. *Bioinformatics* 30: 2114-20

154. Dobin A, Davis CA, Schlesinger F, Drenkow J, Zaleski C, Jha S, Batut P, Chaisson M, Gingeras TR. 2013. STAR: ultrafast universal RNA-seq aligner. *Bioinformatics* 29: 15-21

155. Liao Y, Smyth GK, Shi W. 2013. The Subread aligner: fast, accurate and scalable read mapping by seed-and-vote. *Nucleic Acids Res* 41: e108

156. Blankenberg D, Von Kuster G, Bouvier E, Baker D, Afgan E, Stoler N, Galaxy T, Taylor J, Nekrutenko A. 2014. Dissemination of scientific software with Galaxy ToolShed. *Genome Biol* 15: 403

157. Love MI, Huber W, Anders S. 2014. Moderated estimation of fold change and dispersion for RNA-seq data with DESeq2. *Genome Biol* 15: 550

158. Chen Z, Quan L, Huang A, Zhao Q, Yuan Y, Yuan X, Shen Q, Shang J, Ben Y, Qin FX, Wu A. 2018. seq-ImmuCC: Cell-Centric View of Tissue Transcriptome Measuring Cellular Compositions of Immune Microenvironment From Mouse RNA-Seq Data. *Front Immunol* 9: 1286

159. Alshetaiwi H, Pervolarakis N, McIntyre LL, Ma D, Nguyen Q, Rath JA, Nee K, Hernandez G, Evans K, Torosian L, Silva A, Walsh C, Kessenbrock K. 2020. Defining the emergence of myeloid-derived suppressor cells in breast cancer using single-cell transcriptomics. *Sci Immunol* 5

160. Mellor AL, Lemos H, Huang L. 2017. Indoleamine 2,3-Dioxygenase and Tolerance: Where Are We Now? *Front Immunol* 8: 1360

161. Katze MG, He Y, Gale M, Jr. 2002. Viruses and interferon: a fight for supremacy. *Nat Rev Immunol* 2: 675-87

162. Kurokawa C, Iankov ID, Anderson SK, Aderca I, Leontovich AA, Maurer MJ, Oberg AL, Schroeder MA, Giannini C, Greiner SM, Becker MA, Thompson EA, Haluska P, Jentoft ME, Parney IF, Weroha SJ, Jen J, Sarkaria JN, Galanis E. 2018. Constitutive Interferon Pathway Activation in Tumors as an Efficacy Determinant Following Oncolytic Virotherapy. *J Natl Cancer Inst* 110: 1123-32

163. Arumuggam N, Bhowmick NA, Rupasinghe HP. 2015. A Review: Phytochemicals Targeting JAK/STAT Signaling and IDO Expression in Cancer. *Phytother Res* 29: 805-17

164. Rothhammer V, Quintana FJ. 2019. The aryl hydrocarbon receptor: an environmental sensor integrating immune responses in health and disease. *Nat Rev Immunol* 19: 184-97

165. Munn DH, Mellor AL. 2013. Indoleamine 2,3 dioxygenase and metabolic control of immune responses. *Trends Immunol* 34: 137-43

166. Adams O, Besken K, Oberdorfer C, MacKenzie CR, Takikawa O, Daubener W. 2004. Role of indoleamine-2,3-dioxygenase in alpha/beta and gamma interferon-mediated antiviral effects against herpes simplex virus infections. *J Virol* 78: 2632-6

167. Bodaghi B, Goureau O, Zipeto D, Laurent L, Virelizier JL, Michelson S. 1999. Role of IFN-gamma-induced indoleamine 2,3 dioxygenase and inducible nitric oxide synthase in the replication of human cytomegalovirus in retinal pigment epithelial cells. *J Immunol* 162: 957-64

168. Obojes K, Andres O, Kim KS, Daubener W, Schneider-Schaulies J. 2005. Indoleamine 2,3-dioxygenase mediates cell type-specific anti-measles virus activity of gamma interferon. *J Virol* 79: 7768-76

169. Terajima M, Leporati AM. 2005. Role of Indoleamine 2,3-Dioxygenase in Antiviral Activity of Interferon-gamma Against Vaccinia Virus. *Viral Immunol* 18: 722-9

170. Raniga K, Liang C. 2018. Interferons: Reprogramming the Metabolic Network against Viral Infection. *Viruses* 10

171. Arenas-Huertero F, Zaragoza-Ojeda M, Sanchez-Alarcon J, Milic M, Segvic Klaric M, Montiel-Gonzalez JM, Valencia-Quintana R. 2019. Involvement of Ahr Pathway in Toxicity of Aflatoxins and Other Mycotoxins. *Front Microbiol* 10: 2347

172. Fueyo J, Gomez-Manzano C, Yung WK, Kyritsis AP. 1998. The functional role of tumor suppressor genes in gliomas: clues for future therapeutic strategies. *Neurology* 51: 1250-5

173. Shiina M, Lacher MD, Christian C, Korn WM. 2009. RNA interference-mediated knockdown of p21(WAF1) enhances anti-tumor cell activity of oncolytic adenoviruses. *Cancer Gene Ther* 16: 810-9

174. Rivera-Molina Y, Jiang H, Fueyo J, Nguyen T, Shin DH, Youssef G, Fan X, Gumin J, Alonso MM, Phadnis S, Lang FF, Gomez-Manzano C. 2019. GITRL-armed Delta-24-RGD oncolytic adenovirus prolongs survival and induces anti-glioma immune memory. *Neurooncol Adv* 1: vdz009

175. Lang FF, Conrad C, Gomez-Manzano C, Yung WKA, Sawaya R, Weinberg JS, Prabhu SS, Rao G, Fuller GN, Aldape KD, Gumin J, Vence LM, Wistuba I, Rodriguez-Canales J, Villalobos PA, Dirven CMF, Tejada S, Valle RD, Alonso MM, Ewald B, Peterkin JJ, Tufaro F, Fueyo J. 2018. Phase I Study of DNX-2401 (Delta-24-RGD) Oncolytic Adenovirus: Replication and Immunotherapeutic Effects in Recurrent Malignant Glioma. *J Clin Oncol* 36: 1419-27

176. Gajdasik DW, Gaspal F, Halford EE, Fiancette R, Dutton EE, Willis C, Ruckert T, Romagnani C, Gerard A, Bevington SL, MacDonald AS, Botto M, Vyse T, Withers DR. 2020. Th1 responses in vivo require cell-specific provision of OX40L dictated by environmental cues. *Nat Commun* 11: 3421

177. Croft M. 2010. Control of immunity by the TNFR-related molecule OX40 (CD134). *Annu Rev Immunol* 28: 57-78

178. Veldhoen M, Hirota K, Westendorf AM, Buer J, Dumoutier L, Renauld JC, Stockinger B. 2008. The aryl hydrocarbon receptor links TH17-cell-mediated autoimmunity to environmental toxins. *Nature* 453: 106-9

179. Zou W. 2006. Regulatory T cells, tumour immunity and immunotherapy. *Nat Rev Immunol* 6: 295-307

180. Longhi MS, Moss A, Bai A, Wu Y, Huang H, Cheifetz A, Quintana FJ, Robson SC. 2014. Characterization of human CD39+ Th17 cells with suppressor activity and modulation in inflammatory bowel disease. *PLoS One* 9: e87956

181. Neavin DR, Liu D, Ray B, Weinshilboum RM. 2018. The Role of the Aryl Hydrocarbon Receptor (AHR) in Immune and Inflammatory Diseases. *Int J Mol Sci* 19

182. Andtbacka RH, Kaufman HL, Collichio F, Amatruda T, Senzer N, Chesney J, Delman KA, Spitler LE, Puzanov I, Agarwala SS, Milhem M, Cranmer L, Curti B, Lewis K, Ross M, Guthrie T, Linette GP, Daniels GA, Harrington K, Middleton MR, Miller WH, Jr., Zager JS, Ye Y, Yao B, Li A, Doleman S, VanderWalde A, Gansert J, Coffin RS. 2015. Talimogene Laherparepvec Improves Durable Response Rate in Patients With Advanced Melanoma. *J Clin Oncol* 33: 2780-8

183. Chiocca EA, Abbed KM, Tatter S, Louis DN, Hochberg FH, Barker F, Kracher J, Grossman SA, Fisher JD, Carson K, Rosenblum M, Mikkelsen T, Olson J, Markert J, Rosenfeld S, Nabors LB, Brem S, Phuphanich S, Freeman S, Kaplan R, Zwiebel J. 2004. A phase I open-label, dose-escalation, multi-institutional trial of injection with an E1B-Attenuated adenovirus, ONYX-015, into the peritumoral region of recurrent malignant gliomas, in the adjuvant setting. *Mol Ther* 10: 958-66

184. Routy JP, Routy B, Graziani GM, Mehraj V. 2016. The Kynurenine Pathway Is a Double-Edged Sword in Immune-Privileged Sites and in Cancer: Implications for Immunotherapy. *Int J Tryptophan Res* 9: 67-77

185. Yamada T, Horimoto H, Kameyama T, Hayakawa S, Yamato H, Dazai M, Takada A, Kida H, Bott D, Zhou AC, Hutin D, Watts TH, Asaka M, Matthews J, Takaoka A. 2016. Constitutive aryl hydrocarbon receptor signaling constrains type I interferon-mediated antiviral innate defense. *Nat Immunol* 17: 687-94

186. Curti A, Pandolfi S, Valzasina B, Aluigi M, Isidori A, Ferri E, Salvestrini V, Bonanno G, Rutella S, Durelli I, Horenstein AL, Fiore F, Massaia M, Colombo MP, Baccarani M, Lemoli RM. 2007. Modulation of tryptophan catabolism by human leukemic cells results in the conversion of CD25- into CD25+ T regulatory cells. *Blood* 109: 2871-7

187. Holmgaard RB, Zamarin D, Li Y, Gasmi B, Munn DH, Allison JP, Merghoub T, Wolchok JD. 2015. Tumor-Expressed IDO Recruits and Activates MDSCs in a Treg-Dependent Manner. *Cell Rep* 13: 412-24

188. Levina V, Su Y, Gorelik E. 2012. Immunological and nonimmunological effects of indoleamine 2,3-dioxygenase on breast tumor growth and spontaneous metastasis formation. *Clin Dev Immunol* 2012: 173029

189. Perepechaeva ML, Grishanova AY. 2020. The Role of Aryl Hydrocarbon Receptor (AhR) in Brain Tumors. *Int J Mol Sci* 21

190. Berrong Z, Mkrtichyan M, Ahmad S, Webb M, Mohamed E, Okoev G, Matevosyan A, Shrimali R, Abu Eid R, Hammond S, Janik JE, Khleif SN. 2018. Antigen-Specific Antitumor Responses Induced by OX40 Agonist Are Enhanced by the IDO Inhibitor Indoximod. *Cancer Immunol Res* 6: 201-8

191. Disis ML. 2010. Immune regulation of cancer. *J Clin Oncol* 28: 4531-8

192. Campesato LF, Budhu S, Tchaicha J, Weng CH, Gigoux M, Cohen IJ, Redmond D, Mangarin L, Pourpe S, Liu C, Zappasodi R, Zamarin D, Cavanaugh J, Castro AC, Manfredi MG, McGovern K, Merghoub T, Wolchok JD. 2020. Blockade of the AHR restricts a Treg-macrophage suppressive axis induced by L-Kynurenine. *Nat Commun* 11: 4011

193. Safe S, Cheng Y, Jin UH. 2017. The Aryl Hydrocarbon Receptor (AhR) as a Drug Target for Cancer Chemotherapy. *Curr Opin Toxicol* 2: 24-9

Vita

Teresa Tuệ-Minh Nguyen was born in Denver, Colorado in 1992 to her parents Thuy Lan Nguyen and Tai Nguyen. She grew up with three older sisters and one younger sister, Judy, Marie, Catherine, and Bernadette. Teresa graduated, *cum laude,* and received her Bachelor of Science degree in Biology at the University of Colorado Denver in 2013. During her undergraduate studies, Teresa worked as a research assistant in the lab of Dr. Marileila Varella-Garcia, where she learned how to identify oncogenic drivers using fluorescence *in situ* hybridization. She then moved on to work in the lab of Dr. Lynn Heasley, where she studied the resistance mechanisms to EGFR tyrosine kinase inhibitors in EGFR-positive head and neck cancers. After graduating from college, Teresa joined the lab of Dr. Raphael Nemenoff to work as a professional research assistant focusing on the 5-lipoxygenase driven immune responses of murine lung cancer. In 2015, Teresa entered the Graduate School of Biomedical Sciences at the University of Texas MD Anderson Cancer Center to pursue her goal of becoming a professor focusing on cancer therapeutics. In 2016, Teresa joined the lab of Dr. Juan Fueyo, where she accomplished her doctoral dissertation on the treatment of and immune effects of combining IDO inhibitors and agonist-armed oncolytic adenoviruses in murine glioblastoma. During this time, Teresa was funded by the American Legion Auxiliary Fellowship in Cancer Research from 2017-2019. She was also supported by the Ruth L. Kirschstein National Research Service Award (NRSA) Individual Predoctoral Fellowship (Parent F31), funded by the National Cancer Institute of the National Institutes of Health (NIH) from 2019-2021. Teresa will return to the lab of Dr. Lynn Heasley to begin a post-doctoral fellowship at the University of Colorado Cancer Center shortly after the defense of her dissertation. Here, she will apply for the T32 training grant funded by the NIH. She will continue working in the field of cancer immunotherapy and focus on studying the immune responses to specific tyrosine kinase inhibitors in specific-oncogenic driven cancers to elucidate synergistic combination therapies with immunotherapies.